LV-2016-031

Landsvirkjun

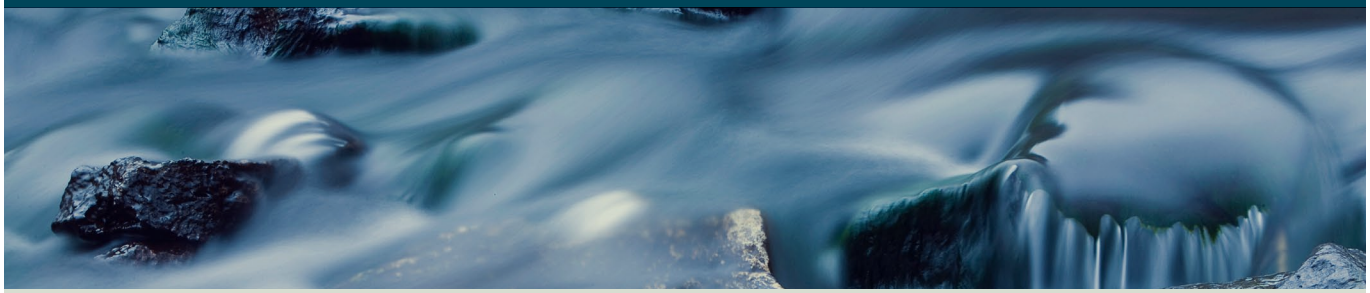

Vatnajökull

Mass balance, meltwater drainage and surface velocity of the glacial year 2014–15

Lykilsíða

Landsvirkjun

Skýrsla LV nr:	LV-2016-031	**Dags:**	Febrúar 2016

Fjöldi síðna: 55 **Upplag:** 3 **Dreifing:**

☐ **Birt á vef LV**
☒ **Opin**
☐ **Takmörkuð til**

Titill: Vatnajökull: Mass balance, meltwater drainage and surface velocity of the glacial year 2014-15

Höfundar/fyrirtæki: Finnur Pálsson, Andri Gunnarsson, Þorsteinn Jónsson, Sveinbjörn Steinþórsson, Hlynur Skagfjörð Pálsson

Verkefnisstjóri: Andri Gunnarsson

Unnið fyrir: Landsvirkjun

Samvinnuaðilar:

Útdráttur: The glacial year of 2014_15 was the first in two decades with positive mass balance for Vatnajökull. The total mass loss over the 24 year survey period is 10,46 mwe (ice volume of ~92,7 km3) since 1991_92 (13.42 mwe (ice volume of 120.28 km3) since 1994_95 the first year of 2 decades of negative balance). The volume loss since 1991_92 amounts to ~3% of total ice volume (~4% since 1994_95). Glacier meltwater runoff (estimated from summer balance only, summer rain and snow that falls and melts during summer is not included) to: Tungnaá was 67% of average, 60 % of average to Kaldakvísl, 47% of average to Jökulsá á Fjöllum, 51% of average to Hálslón, 55% to Jökulsá í Fljótsdal and 56% over average to Jökulsá á Breiðamerkursandi.

Lykilorð: Vatnajökull, glacier, mass balance, meltwater

ISBN nr:

Samþykki verkefnisstjóra Landsvirkjunar

Andri Gunnarsson

Skýrsla nr. LV–2016–031

Landsvirkjun

Vatnajökull

Mass balance, meltwater drainage and surface velocity of the glacial year 2014–15

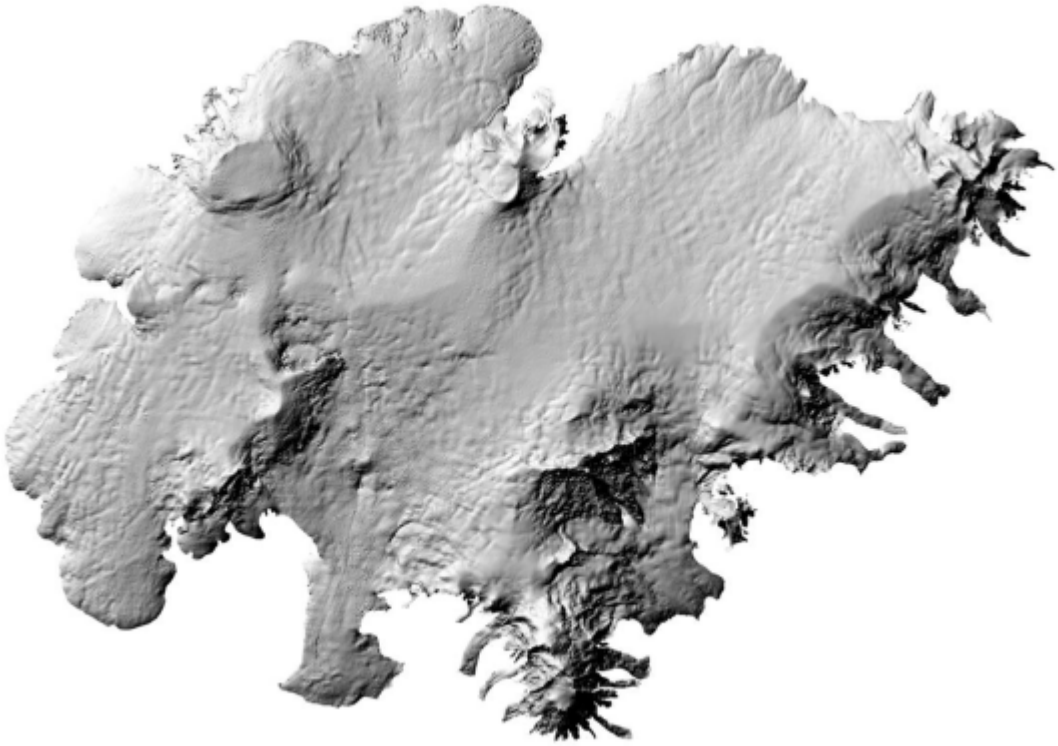

Febrúar 2016

Contents:

Figures:

Tables:

Appendixes:

1. INTRODUCTION

In 1992 (glacial year 1991_1992) a program of mass balance measurements was started for Vatnajökull by the Science Institute University of Iceland (now Institute of Earth Sciences, IES) in collaboration with the National Power Company (NPC). For the first year the program was limited to the western part of the glacier, but then expanded to include the northern outlets as well. In 1996 this study was further expanded to include southern outlets, with support from The European Union (Framework IV - Environment and Climate, TEMBA project 1996-1997). This program was extended 1998–2000 with further support from EU (Framework IV - Environment and Climate, ICEMASS project, 1998-2000). In 2000-2002 NPC and IES continued the program. In 2003-2005 IES participated in a multinational research project, which was financially supported by The European Union (EVK2-CT-2002-00152 SPICE). IES was responsible for obtaining data sets for calibration of models of the mass balance and dynamics of Vatnajökull. This work was also supported by The National Power Company of Iceland and The National Road Authority, and is a continuation of the TEMBA-project of 1996-97 and ICEMASS project 1998-2001.
In 2013-2014 IES and NPC continued a similar program. Mass balance measurements on the southeast outlets Breiðamerkurjökull and Hoffellsjökull is financially supported by the National Road Authority.
The aim of the collaborative work of NPC and IES is to improve our understanding of the mass balance and melt water runoff from glaciers. This work in combination with energy balance measurements by NPC and IES on Vatnajökull will be used for calibration of models of the energy and mass balance of Vatnajökull.

This report describes the field measurements, GPS survey, the mass balance and melt water runoff for the glacial year 2014_15.

2. DIARY

April 4; installation of melt wires, maintenance of AWSs on Breiðamerkurjökull
May 7 - 16: measurements of the winter balance
June 2 - 10: measurements of the winter balance.
September 6; summer balance measurements, maintenance of AWSs on Breiðamerkurjökull
October 22-28: summer balance measurements.

In all expeditions and short visits to the glacier the locations of mass balance stakes were measured with Kinematic GPS (or fast static GPS and a few with DGPS) for surface velocity calculation.

The following members of staff of the Institute of Earth Sciences, University of Iceland, carried out the fieldwork on Vatnajökull: Finnur Pálsson, Þorsteinn Jónsson, Sveinbjörn Steinþórsson also Andri Gunnarsson (National Power Company) and Hlynur Skagfjörð Pálsson (Reykjavík Rescue Team).
Members of the Iceland Glaciological Society assisted in the June fieldwork.

3. MASS BALANCE MEASUREMENTS

The purpose of the mass balance measurements is to describe the temporal and spatial distribution of the components of the mass balance. The mean annual values of the components and their variation from year to year are analyzed and related to meteoro-logical conditions and climatic variability. The results will be used in studies of changes in the glacier volume, estimates of meltwater contribution to glacial rivers, mass balance modeling, evaluation of altitudinal and regional variations of mass balance in response to climatic variations, and to assess the hydrometeorological and dynamic response of the ice cap to climate change.

The mass balance was determined by a stratigraphic method, measuring changes in thickness and density relative to the summer surface. The winter balance was estimated by drilling ice cores through the winter layer in the spring. Ablation was monitored from markers; snow stakes were put up on the glacier and wires were drilled down in the ablation area. The summer balance was measured in the autumn.

3.1 Methods

Measurements of the surface mass balance on a large ice cap like Vatnajökull are impractical in terms of cost with conventional techniques and sampling density that are typically used on small glaciers. The spatial variability of the mass balance may, however, be predictable on the flat large outlets of such an ice cap given data on several profiles extending over the elevation range of the glacier. The precipitation generally increases with elevation and decreases with the distance from the coast, but both the distribution of snowfall and redistribution of snow by drift depend on the prevailing wind direction during the winter. The summer melting depends mainly on the altitude and the albedo of the glacier surface. Therefore, we have used observations along a limited number of flowlines, which span the elevation range of the outlets to assess aerial estimates of surface mass balance. Each profile describes the variation with elevation, but together they also describe the lateral variation of the mass balance. Recently, modern over-snow vehicles and helicopters have allowed fast traverses to ensure successful fieldwork in spite of frequently poor weather conditions. The error for individual point measurement is estimate ~30 cm_{we} for both summer and winter balance. The error for the area integral of mass balance is however considered smaller, since the error for individual survey sites is independent.

The winter mass balance (b_w) is defined as the mass of snow accumulated during the winter months, the summer balance (b_s) is the mass balance during the summer, and the net balance (b_n) is defined as their sum. The specific mass balance is expressed in terms of the equivalent thickness of water. All mass balance components apply to a time interval between given measurement dates, which are not fixed from one year to another. The dates in the autumn are separated by approximately one calendar year, which roughly coincides with the glaciological year defined as October 1st to September 30th. Snow cores are drilled in April-May through the winter layer and profiles of the density are measured. The summer balance is derived in the autumn from measurements of the changes in the snow core density during the summer in the accumulation area and from readings at stakes and wires drilled into the ice in the ablation areas.

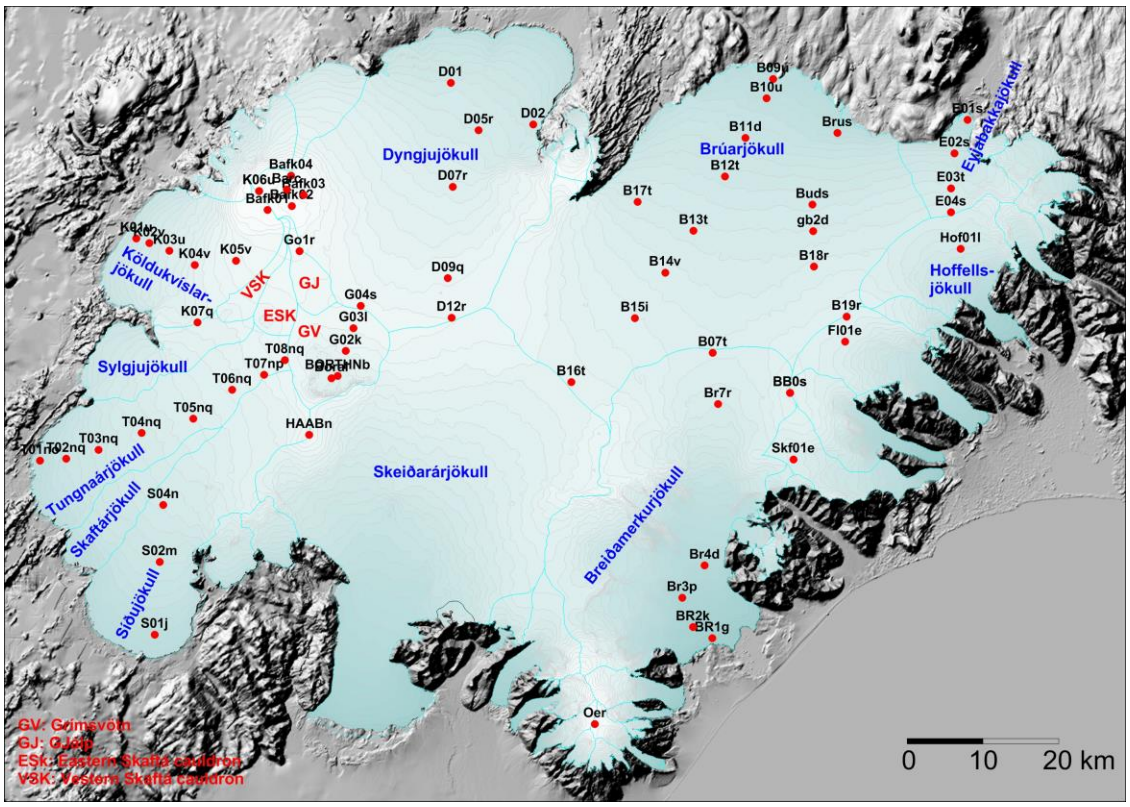

Figure 1. Outlets of Vatnajökull and location of mass balance survey sites 2014_15.

Digital maps are created for winter, summer and net balance for the whole ice cap based on site measurements. The mass balance is calculated over both the ice and water drainage basins. The summer balance over the water basin is an estimate of meltwater contribution to rivers and groundwater storage. This estimate, however, does not include precipitation that falls as rain on the glacier or snow, which falls and melts during the summer. The meltwater contribution is compared with river runoff at stream flow gauges closest to the glacier. For this comparison, we define the glaciological year from the start of October to the end of September and the period draining meltwater from the glacier during the summer from June through September. It would be misleading to include May in the summer period because runoff from the glacier melt in May is delayed due to refreezing during elimination of the cold wave.

3. 2 Results of mass balance measurements.

Mass balance measurements were done at 67 sites in spring 2015 (Fig. 1). The specific mass balance at individual sites is shown in Fig. 2. Most sites are on central flow lines at individual outlets. The specific mass balance along approximate flow lines is given in Fig 3. for the glacier outlets: Síðujökull, Tungnaárjökull, Köldukvíslarjökull, Dyngjujökull, Brúarjökull (west and east), Eyjabakkajökull, Hoffellsjökull and Breiðamerkurjökull.

Digital maps for winter, summer and net balance are shown in Figure 4. Although no balance measurements are available for Skeiðarárjökull, the balance has been estimated by interpolating the balance values from the neighboring outlets, based on our experience from previous years. The mass balance of individual outlet is discussed in the following subsections.

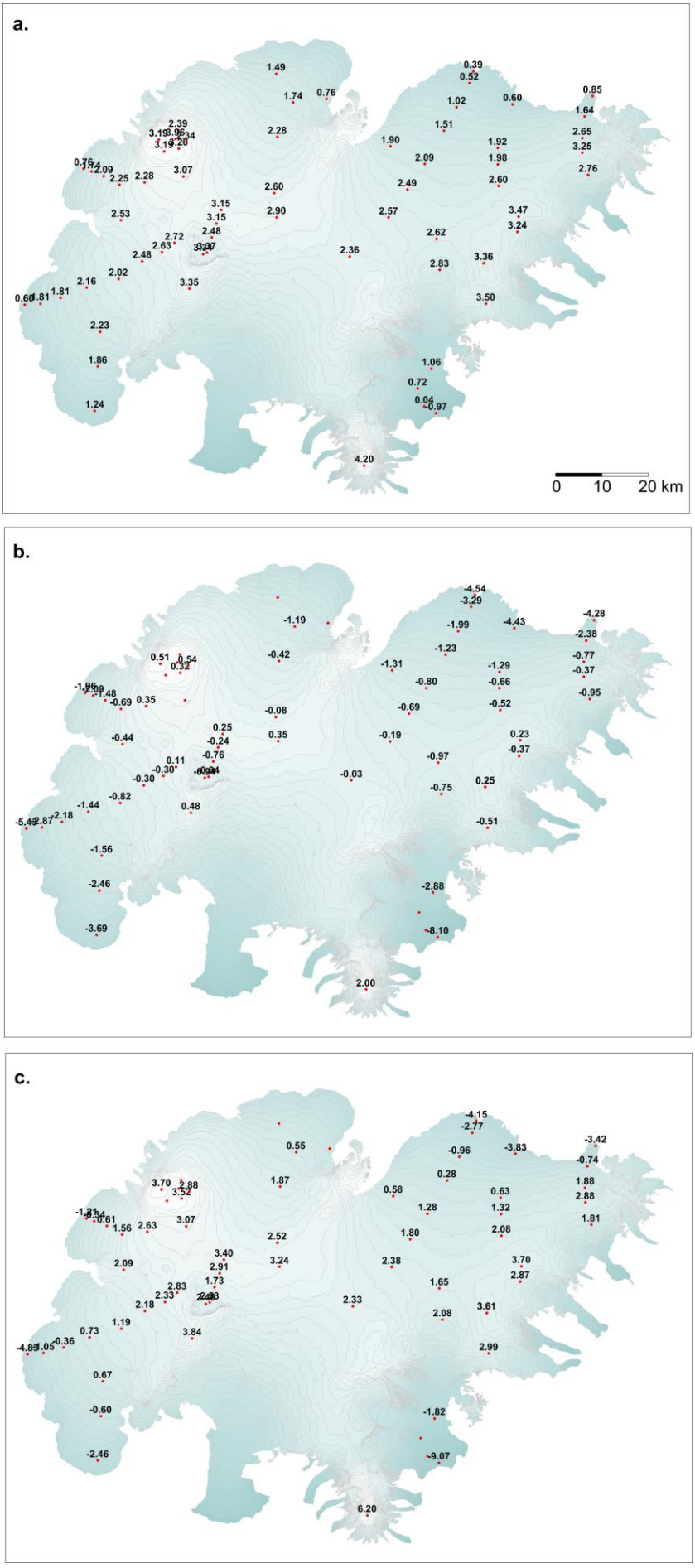

Figure 2. Maps showing point values of specific mass balance in m water equivalent (m_{we}), 2014_15. a. winter, b. summer, c. net balance.

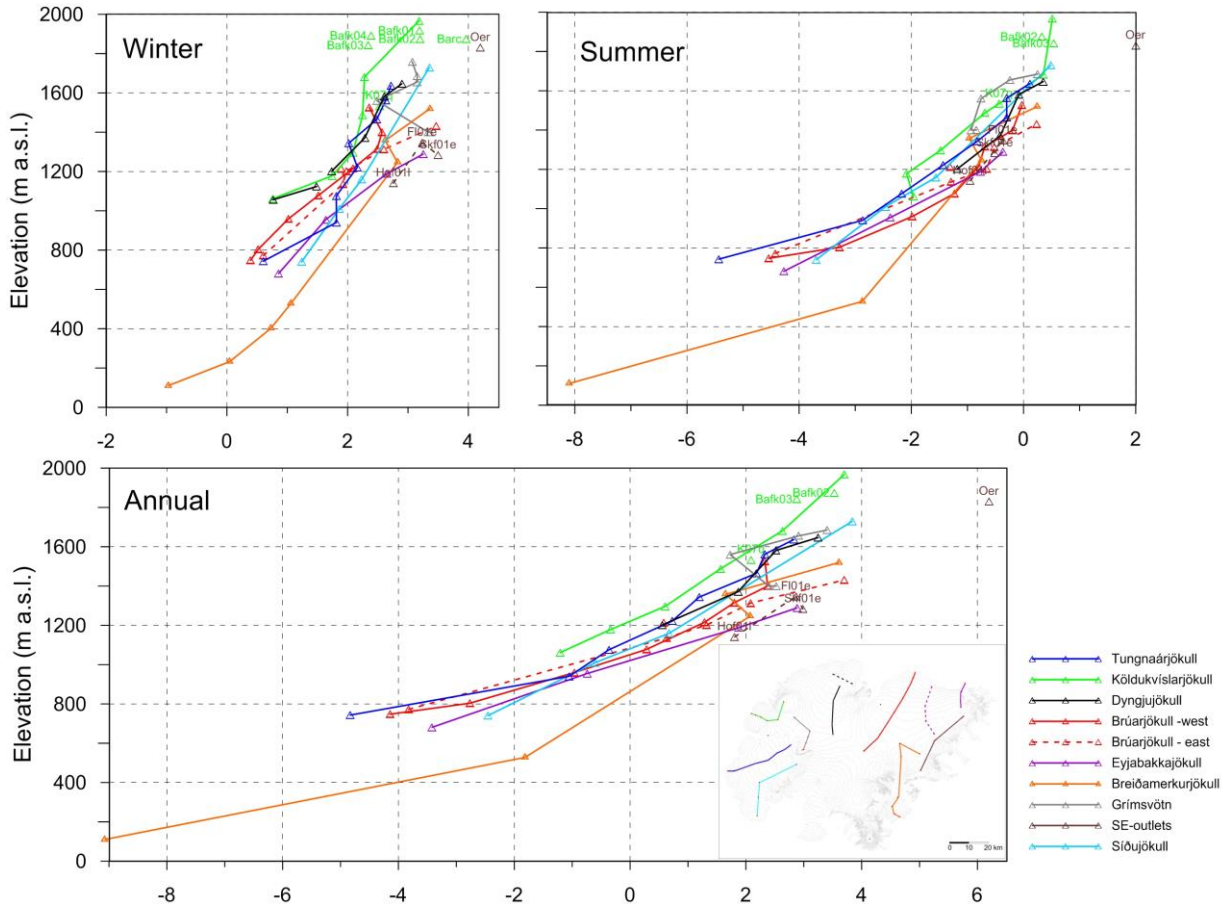

Figure 3a. Specific mass balance (m_{we}), along all mass balance profiles 2014_15.

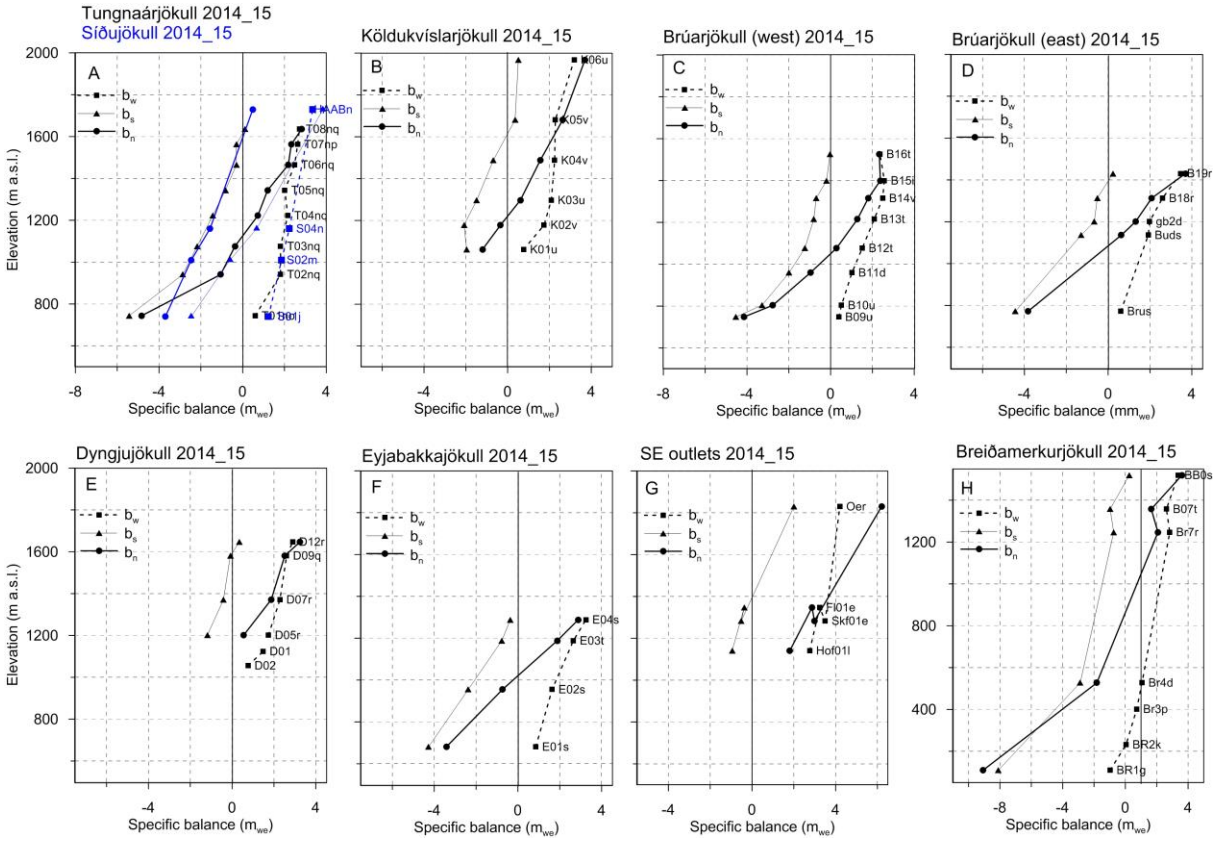

Figure 3b. Specific mass balance (mm$_{we}$) 2014_15 as a function of elevation on central flow lines on Vatnajökull outlets.

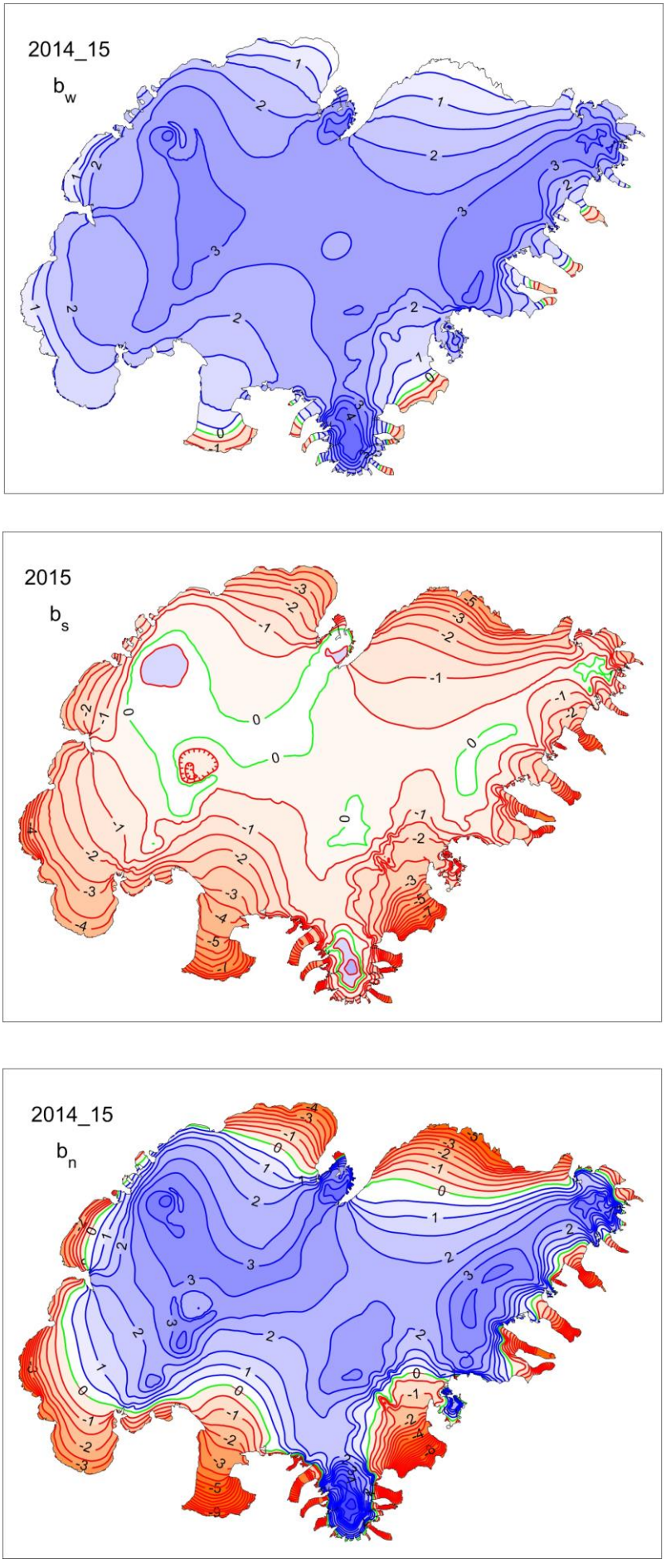

Figure 4. Specific mass balance (m_{we}) maps of Vatnajökull 2014_15. Top: winter, Centre: summer, Bottom: net balance.

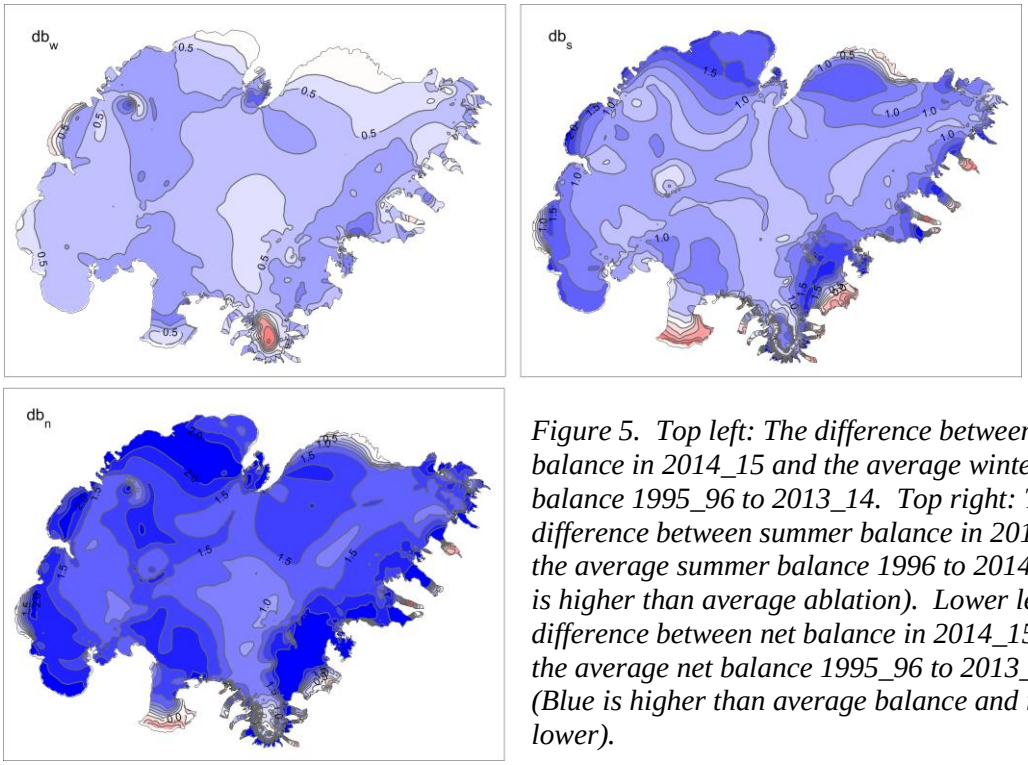

Figure 5. Top left: The difference between winter balance in 2014_15 and the average winter balance 1995_96 to 2013_14. Top right: The difference between summer balance in 2015 and the average summer balance 1996 to 2014. (Red is higher than average ablation). Lower left: The difference between net balance in 2014_15 and the average net balance 1995_96 to 2013_14. (Blue is higher than average balance and red lower).

A DEM of Vatnajökull mostly based on SPOT5 satellite images in 2010, and partly from LiDAR survey 2010, is used for surface area distribution and delineation of ice divides for individual outlets and catchments.

The autumn weather was slightly colder than average the past decade; October rather dry but precipitation in November well over the average in the S and SE. The winter months in Iceland December to March were colder than average, although close to average in the E. Storms were frequent (almost every 3 days) accompanied by unusually high precipitation. In these conditions snow collection is high on SE, E, and N Vatnajökull but high E and NE wind also increased snow accumulation in upper regions of NW Vatnajökull. The spring months were cold and dry, with little change on Vatnajökull, in terms of accumulation or melt.

Figure 5 (top left) shows that the winter accumulation is higher than average all over Vatnajökull. There is much thicker than average snow cover in the upper regions especially on Breiðabunga in the SE (open to SE coastal storms) and the upper regions of Dyngjujökull and Bárðabunga (from high wind from E and NE). This reflects snowfall in SE, E, and NE wind directions.

The summer of 2015 was unusually cold in SE-Iceland, also very wet and cloudy in June and July. Inspection of the MODIS monthly overview of the summer months in Appendix F shows that days with clear skies over Vatnajökull were ~3 in June, 2 in the first half of July, but ~5 days in the latter half of the month (none totally cloud free, most with haze). In august clear sky was more frequent especially in the north, ~4 days, in warm weather (again, none totally cloud free, most with haze).

September was warm and rather dry in the east, ablation was significant until mid October. As indicated in Fig 5, top right, ablation rates were lower than average almost everywhere, far under average during the May-July months. But in the mild, even warm, and windy late August and September partly compensated for the ablation rates were higher than average. The net balance (Fig 5 lower left) was positive in all areas except in the lower ablation areas of S and SE outlets.

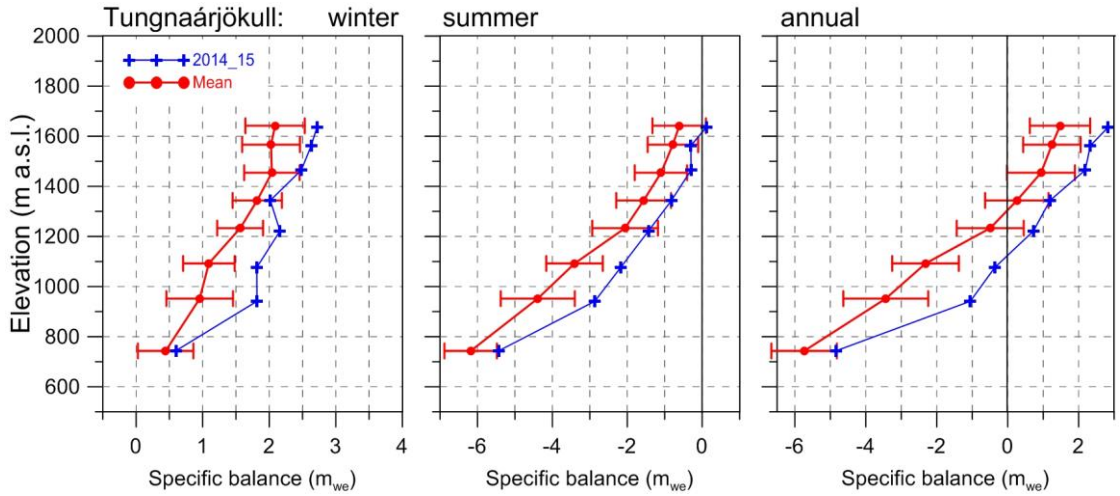

Figure 6. Mass balance at a central flow line of Tungnaárjökull 2014_15, and average mass balance 1991_92 to 2013_14.

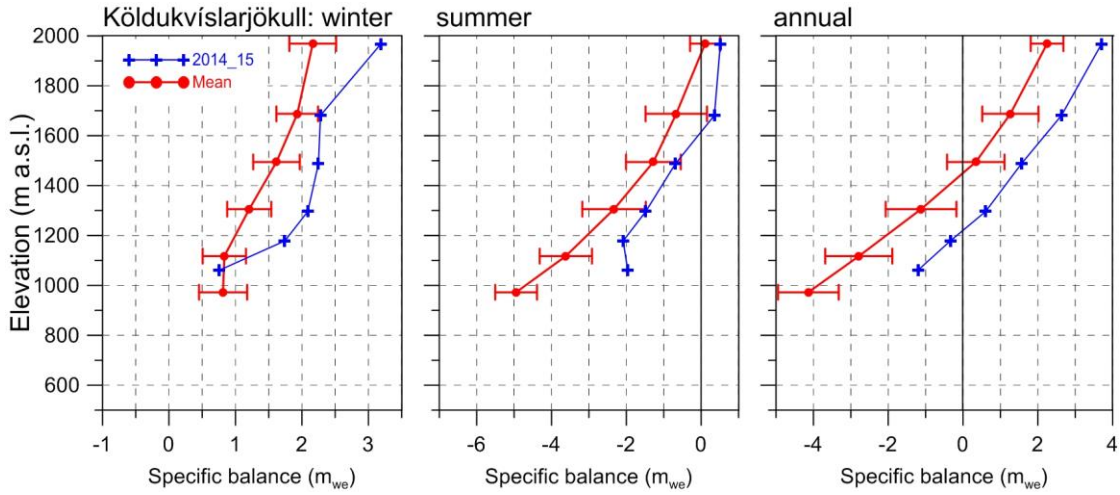

Figure 7. Mass balance at a central flow line of Köldukvíslarjökull 2014_15, and average mass balance 1991_92 to 2013_14.

3.2.1 Tungnaárjökull.

Area = 341 km^2
B_w= 0,67 km^3_{we} ; b_w= 1,96 m_{we}
B_s = -0.60 km^3_{we} ; b_s = -1,77 m_{we}
B_n = 0,07 km^3_{we} ; b_n = 0,19 m_{we}
ELA = 1125 m a.s.l. (at profile)
AAR = 61 %
(The terms are defined at the foot of this page)

Variation of mass balance along a central flow line on Tungnaárjökull is shown in Fig. 6. The winter accumulation was more than ~1 st.dev. higher than average at all survey sites. Total winter balance was 32% over average, even though western Vatnajökull was somewhat shadowed by the topography in the prevailing precipitation direction from SE to NE, Summer melting was over 1st.dev less than average at all survey sites, and accumulation more than the melt at the highest sites. The summer balance was 68% of the average during the survey period. The net balance was positive for the first time in two decades; now +1,25 m_{we} higher than average during the survey.

3.2.2 Köldukvíslarjökull

Area = 298 km^2
B_w = 0,61 km^3_{we} ; b_w = 2,06 m_{we}
B_s = -0,29 km^3_{we}; b_s = -0,99 m_{we}
B_n = 0,32 km^3_{we}; b_n = 1,07 m_{we}
ELA = 1220 m a.s.l. (at profile)
AAR = 74 %

B_w,B_s and B_n are water equivalent volumes of winter, summer and net balance, ELA the equilibrium line altitude, and AAR is the accumulation area ratio.

Variation of mass balance along a central flow line on Köldukvíslarjökull is shown in Fig. 7. Accumulation was far over 1 st. dev. more than average except the lowest survey site, where it was close to average. The winter balance was about 40% higher than average since 1991_92. Summer melting was over 1st.dev less than average at all survey sites, and summer snow accumulation more than the melt at the highest sites. The summer balance was only 50% of the average during the survey period. The net balance was positive for the first time in 20 years; now +1,55 m_{we} higher than average during the survey period.

3.2.3 Dyngjujökull

Area = 1059 km^2
B_w= 2,35km^3_{we} ; b_w= 2,22 m_{we}
B_s = -0,80 km^3_{we} ; b_s = -0,75 m_{we}
B_n = 1,56 km^3_{we} ; b_n = 1,47 m_{we}
ELA = 1130 m a.s.l. (at profile)
AAR = 79 %

Variation of mass balance along a flow line on Dyngjujökull is shown on Fig. 8. Mass balance is not measured at the lowest elevations, but assumed to be correlated (as a function of elevation) to that of Brúarjökull and Köldukvíslarjökull. The winter balance in 2014_15 was more than 1.5 st. dev. over average at all sites except the lowest. Inspection of the winter Modis images shown in appendix F suggest that at the glacier snout snow cover was very thin, In total the winter balance was ~40% over average.
Summer melting was over 1st.dev less than average at all survey sites, and summer snow accumulation more than the melt at the highest site. The summer balance was only 47% of the average during the survey period. The net balance was positive by 1.47 m_{we} , now +1,50 m_{we} higher than average during the survey. The extremely high AAR of 79% reflects this.
Dyngjujökull has often has had mass balance close to zero, and the net balance has been slightly positive in some years of the two decade period of continuous mass loss for Vatnajökull as a whole.

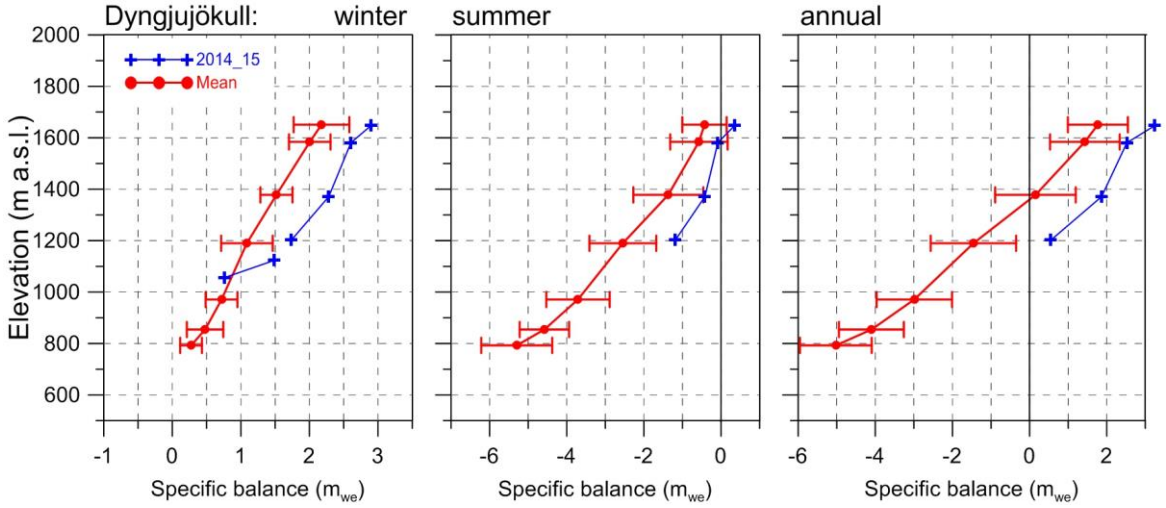

Figure 8. Mass balance at a central flow line on Dyngjujökull 2014_15, and average mass balance 1991_92 to 2013_14 (except 1998_99 – 2003_04 at all but the top elevation).

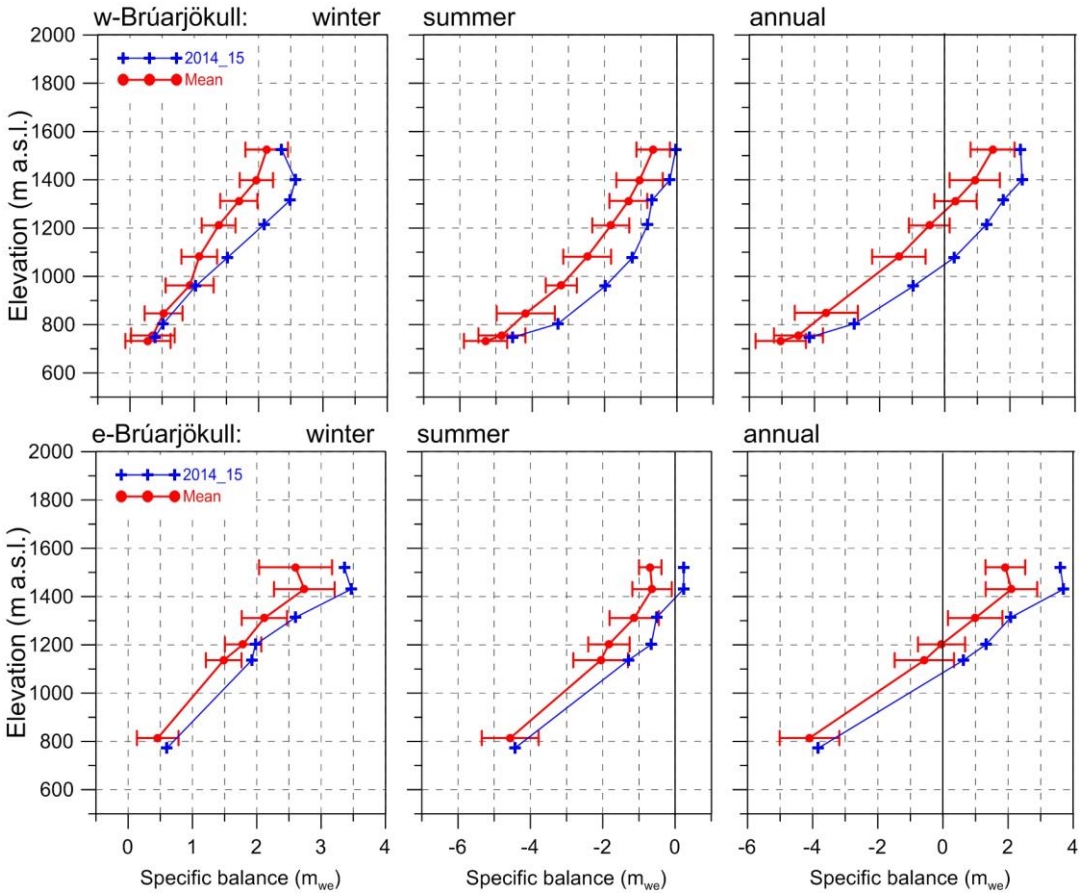

Figure 9. Mass balance at two flow lines on Brúarjökull 2014_15, and average mass balance 1992_93 to 2013_14.

3.2.4 Brúarjökull

Area = 1524 km^2
B_w= 3,18 km^3_{we} ;b_w = 2,09 m_{we}
B_s = -1,59 km^3_{we}; b_s = -1,04 m_{we}
B_n = 1,59 km^3_{we}; b_n = 1,04 m_{we}
ELA = 1210 m a.s.l. (western flow line)
ELA = 1050 m a.s.l. (eastern flow line)
AAR = 77 %

Variation of mass balance along two flow lines on Brúarjökull is shown on Fig. 9. Accumulation was far over 1 st. dev. more than average except the lower survey sites on the western survey line, where it was close to average. The winter balance was about 33% higher than average since 1991_92. Summer melting was over 1st.dev less than average at all survey sites, and summer snow accumulation more than the melt at the highest sites. The summer balance was only 55% of the average during the survey period. The thick snow cover in the ablation zone, delayed ablation in the ablation zone, but this effect was to a large extent compensated by weather favorable to ablation in August and September. The net balance was positive, now by +1,36 m_{we} higher than average during the survey period.
During the survey period, there have been 6 years of positive balance, 17 years with negative balance.

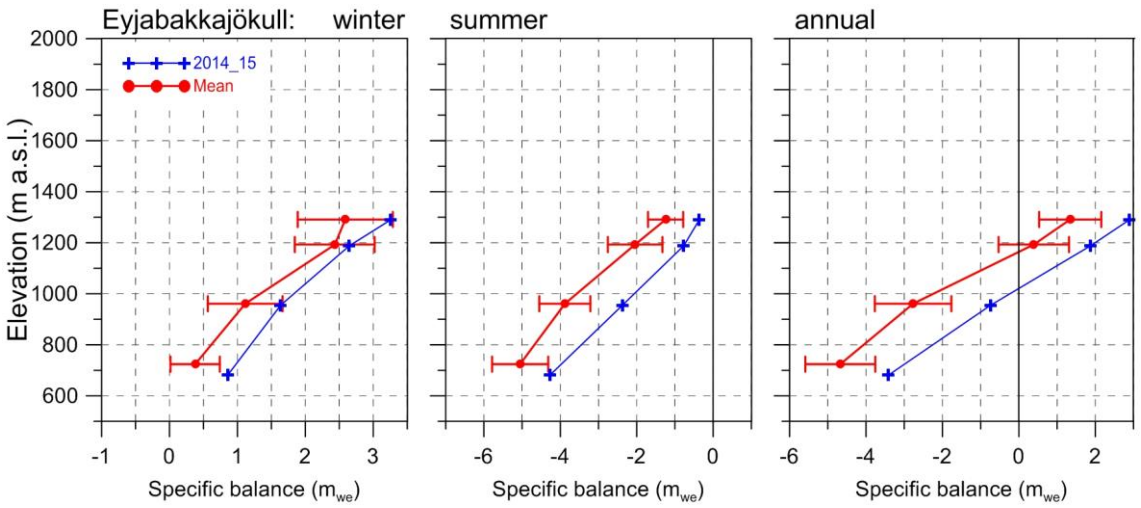

Figure 10. Mass balance at a central flow line of Eyjabakkajökull 2014_15 and average mass balance 1995_96 to 2013_14.

3.2.5 Eyjabakkajökull

Area = 112 km^2
B_w= 0,26 km^3_{we}; b_w = 2,26 m_{we}
B_s = -0,17 km^3_{we}; b_s = -1,53 m_{we}
B_n = 0,08 km^3_{we}; b_n = 0,73 m_{we}
ELA = 1020 m a.s.l. (at profile)
AAR = 65 %

Variation of mass balance along a central flow line on Eyjabakkajökull is shown on Fig. 10. Accumulation was close to 1 st. dev. more than average. The winter balance was about 26% over average since 1991_92. Summer melting was over 1st.dev less than average at all survey sites. The summer balance was only 57% of the average during the survey period. The net balance was positive for the third time during the two decade survey period, now by +1,63 m_{we} higher than average.

3.2.6 Breiðamerkurjökull

Area = 938 km^2
B_w= 2,00 km^3_{we}; b_w = 2,14 m_{we}
B_s = -1,49 km^3_{we}; b_s = -1,59 m_{we}
B_n = 0,51 km^3_{we}; b_n= 0,55 m_{we}
ELA = 870 m a.s.l. (at profile)
AAR = 69 %

Variation of mass balance along a central flow line on Breiðamerkurjökull is shown on Fig. 11.

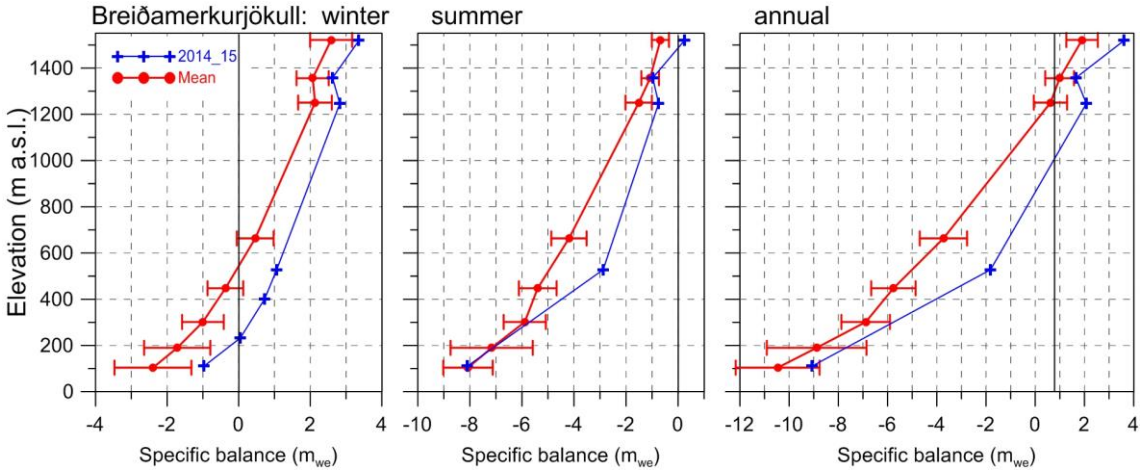

Figure 11. Mass balance at a central flow line of Breiðamerkurjökull 2014_15, and average mass balance 1995_96 to 2013_14.

Accumulation was over 1 st. dev. more than average, close to 2 st.dev. at the centre elevations, and winter ablation similarly less. The winter balance was about 49% close to at the lowest sites, but about 2 st.dev. less than average at the centre where the winter snow cover was by far thicker than average. The summer balance was only 62% of the average during the survey period. The net balance least negative for the 2 decade survey period, only 48% of the average.

3.2.7 Síðujökull

Area = 424 km^2
B_w= 0,86 km^3_{we}; b_w = 2,02 m_{we}
B_s = -0,81 km^3_{we}; b_s = -1,90 m_{we}
B_n = 0,07 km^3_{we}; b_n= 0,12 m_{we}
ELA = 1080 m a.s.l. (at profile)
AAR = 53 %

Variation of mass balance along a central flow line on Síðujökull is shown on Fig. 12.

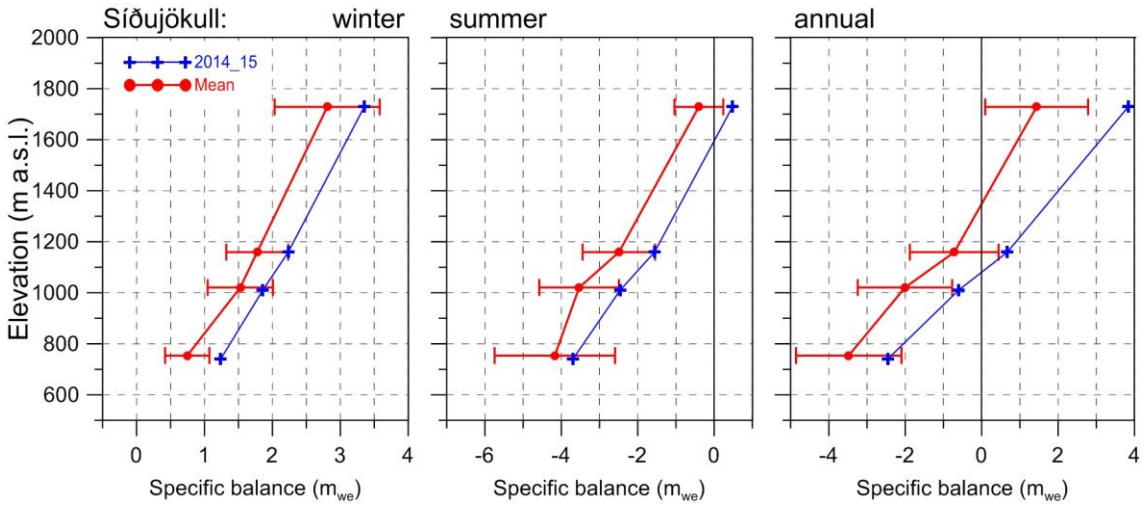

Figure 12. Mass balance at a central flow line of Síðujökull 2014_15, and average mass balance 2004_05 to 2013_14.

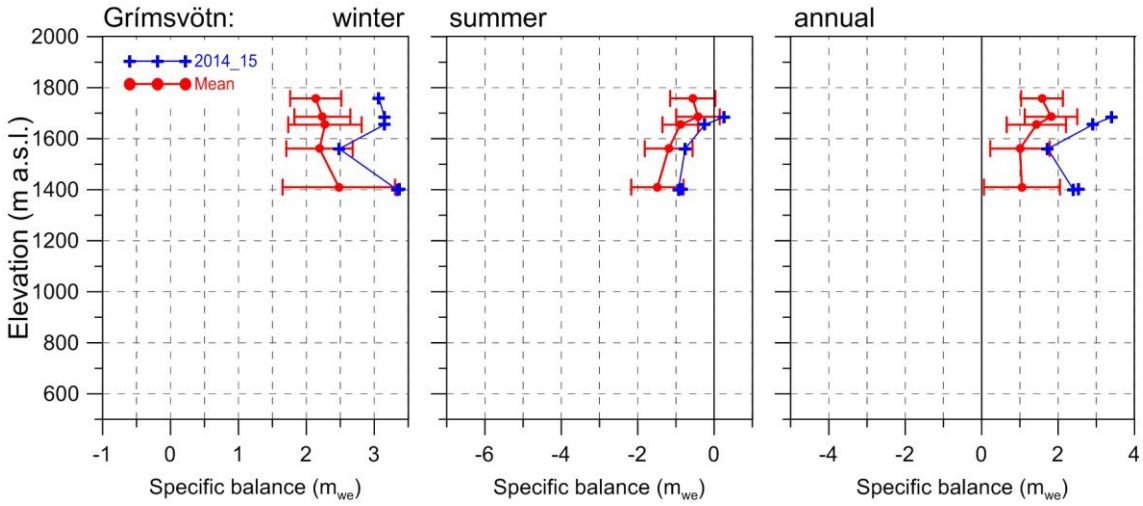

Figure 13. Mass balance at a central flow line towards Grímsvötn 2014_15, and average mass balance 1991_92 to 2013_14.

Snow accumulation was about 1 st. dev higher than average of at all sites. SE wind directions did reach there. The total winter balance was 33% over the average (past decade). Summer melting was over 1st.dev less than average at all survey sites, except the lowest, and summer snow accumulation more than the melt at the highest sites. The summer balance was only 65% of the average during the survey period. The net balance was positive for first time during the 11 year survey period by +1,53 m_{we} higher than average.

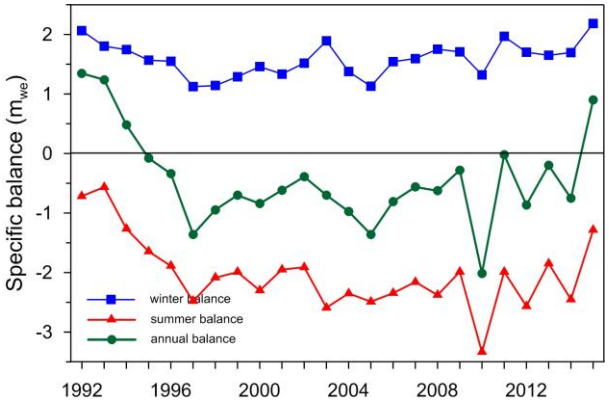

Figure 14. Specific mass balance record for Vatnajökull 1991_92 – 2014_15.

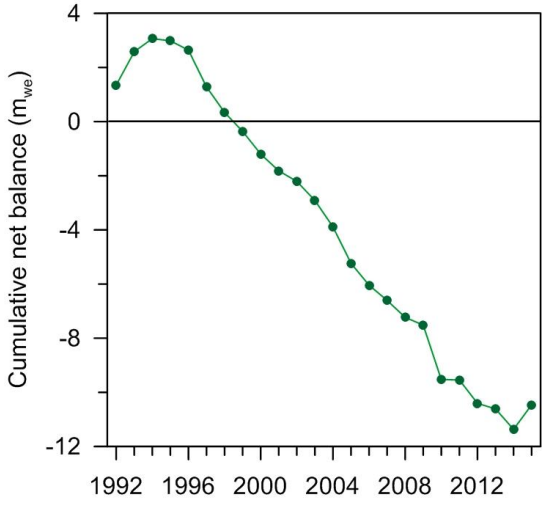

Figure 15. Cumulative specific mass balance of Vatnajökull 1991_92 – 2014_15.

3.2.6 Grímsvötn-Gjálp

Area = 174 km^2
B_w= 0,43 km^3_{we}; b_w = 3,18 m_{we}
B_s = -0,05 km^3_{we}; b_s = -0,36 m_{we}
B_n = 0,38 km^3_{we}; b_n= 2,82 m_{we}

Variation of mass balance close to a central flow line from Bárðarbunga towards Grímsvötn center is shown in Fig. 13. Snow accumulation was about 1 to 2 std. dev. over the average at all survey sites. The winter balance was 39% higher than average. Summer balance ~1 st. dev. less negative than average at the lower survey, but positive (more snowfall than melt during the summer) the summer. The net balance was positive, as almost always, by 54% over the average of the survey period.

3.3 The mass balance record for Vatnajökull.

From the digital maps the total volumes of winter, summer and net balance for Vatnajökull (and selected outlets) have been calculated by integration (appendix D, gives balance values as a function of elevation) and are as follows:

B_w = 17,37 km^3_{we} ; b_w = 2,18 m_{we}
B_s = -10,23 km^3_{we} ; b_s = -1,29 m_{we}
B_n = 7,14 km^3_{we} ; b_n = 0,89 m_{we}
AAR = 73%

Most of the winter was wet windy, with prevailing. The much thicker than average snow cover in the upper regions especially on Breiðabunga in the SE (open to SE coastal storms) and the upper regions of Dyngjujökull and Bárðabunga (from high wind from E and NE). This reflects snowfall in SE, E, and NE wind directions. The total winter balance was 40% higher than average (over the observation period from 1991_92, Fig. 14). The 0 mass

balance turnover for Vatnajökull (current topography) is close to 13,5 km^3_{we} (1,7 m_{we}) and the winter balance 2014_15 29% higher. On Vatnajökull most of the summer was cloudy and wet, August and especially September were more favorable for ablation; this and the unusually thick snow cover lead to low ablation. The total summer balance was less negative than average of the two decade survey period; only 63% of the average during the survey period. Due to a cold summer with repeated snow fall on the glacier surface, the error (under-estimate) in runoff estimation from the summer balance will be even more than average. This error can be estimated from the weather station data collected at 10 sites on Vatnajökull during the summer.

As mentioned above, 0 mass balance turnover for Vatnajökull (current topography) is close to 13,5 km^3_{we} (1,7 m_{we}), the summer balance 2015 was 10,29 km^3_{we} or ~76 % of the zero balance turnover. The net balance was positive for the first time since 1993_94, the mass change +1,38 m_{we} greater than average of the survey period since 1991_92 (-0,49 m); +1,65 m_{we} greater than average of the survey period since 1995_96 (-0,75 m); of the past 20 consecutive years of negative balance. This means that the mass change is equal to the glacier having an extra average winter without a consecutive summer.

The glacial year of 2014_15 was the first in two decades with positive mass balance for Vatnajökull (Fig. 14, Fig. 15). The total mass loss over the 24 year survey period is 10,46 m_{we} (ice volume of ~92,7 km^3) since 1991_92

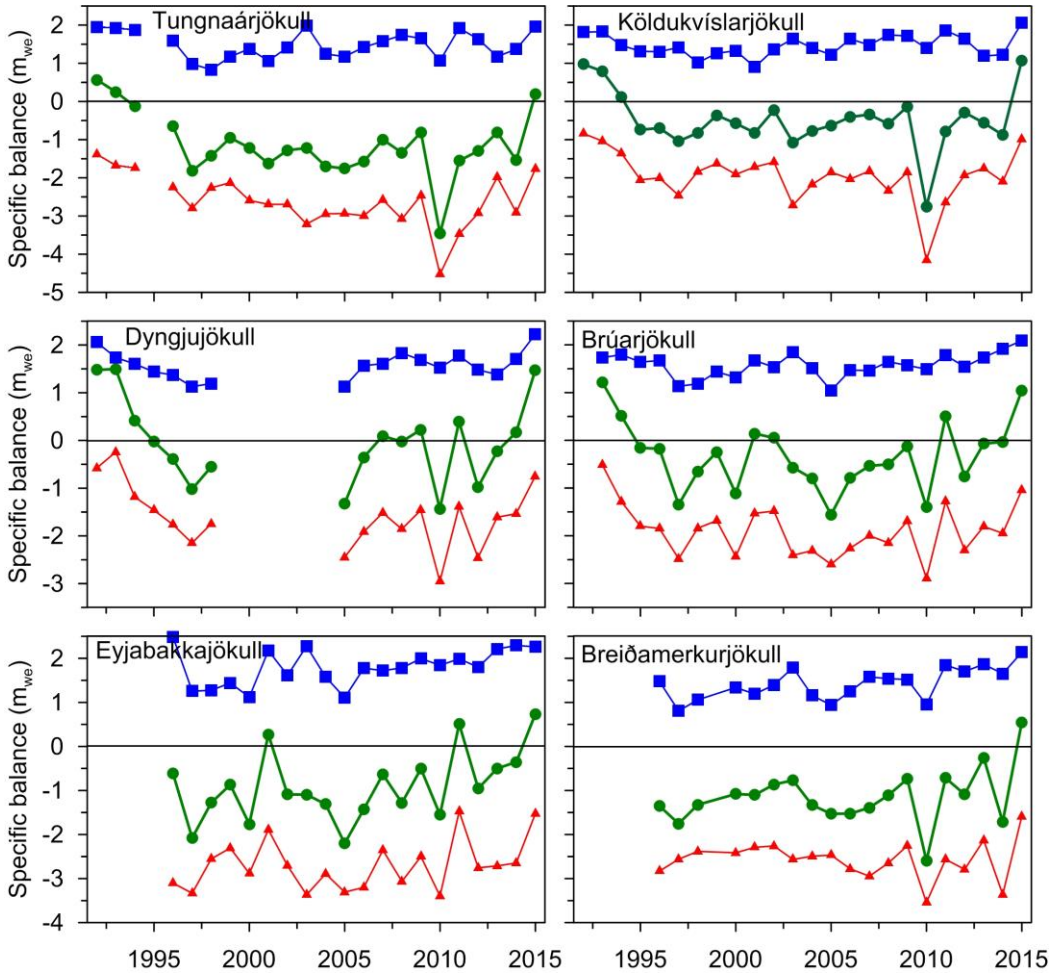

Figure 16. Specific mass balance record for Vatnajökull outlets 1991_92-2014_15.

(13.42 m_{we} (ice volume of 120.28 km^3) since 1994_95 the first year of 2 decades of negative balance).

The temporal variability of mass balance for different outlets is shown in Fig. 16. The greatest variability of the winter balance is for Eyjabakkajökull the eastern most of the studied outlets. This part of the glacier is receives precipitation from all south- and east- and north-easterly wind directions, and thus has high snow accumulation in winters when the paths of the North Atlantic lows are just east of Iceland. This is also the case for the eastern part of Brúarjökull. Breiðamerkurjökull shows lowest variability in mass balance. It is a maritime glacier with climate controlled by the stable sea temperature and humid air mass. The longest winter balance records seem to reveal periodic behavior, with peaks in ~1991_92 and 2002_03 and a low in ~1998. During the period of net mass loss since 1994_95, the northern outlets have had several years of close to zero and positive mass balance.

The cumulative net balance curves for the outlets of Vatnajökull in Fig. 17 show that all outlets have been losing mass since 1994_95. The slope for mass loss is about 0,7 $m_{we}a^{-1}$ for the

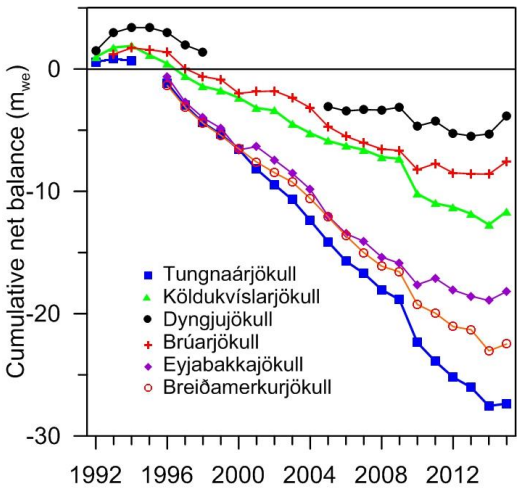

Figure 17. Cumulative specific mass balance for several of Vatnajökull outlets 1991_92 – 2014_15.

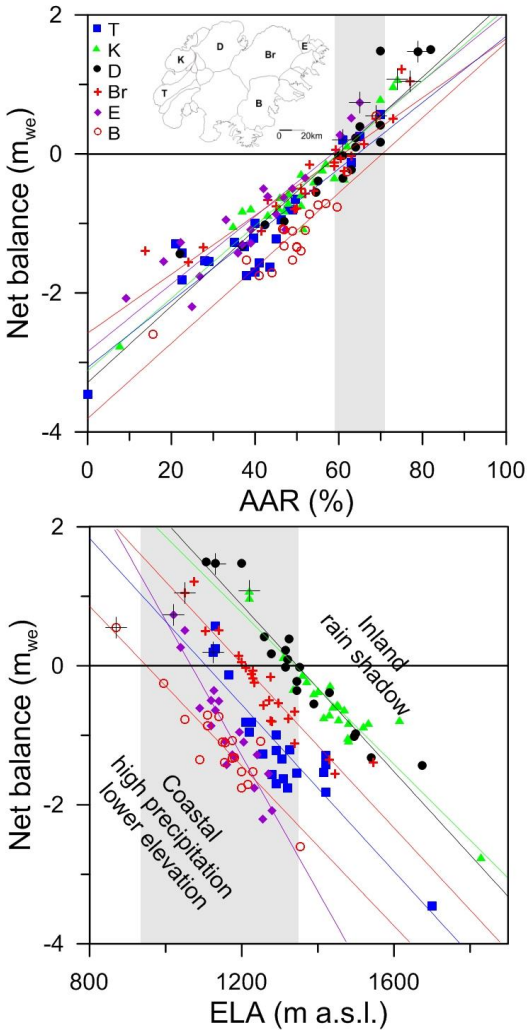

Figure 18. The relation between net annual balance (b_n) and accumulation area ratio (AAR)(upper) and b_n and equilibrium line altitude (ELA), for Vatnajökull outlets during the survey period. (This years points are marked with a black +).

northern outlets but 1,5 $m_{we}a^{-1}$ for the south and western outlets.

In Fig. 18 the relation of the annual net balance to the accumulation area ratio (AAR) and equilibrium line altitude (ELA) is shown for different outlets over the survey period. The b_n-AAR gradient is similar for all outlets, about 0,5 m_{we} for 10% change in AAR. The zero-balance AAR varies for different outlets from about 60-65%, similar for all outlets except for the southern outlet Breiðamerkurjökull.

Breiðamerkurjökull is far from equi-

librium, the ablation area is too large. A large part of the glacier has carved 200-300 m through the former sediment bed, and the surface elevation has lowered accordingly. Breiðamerkurjökull is now retreating at a high rate.

Similarly the zero-balance ELA varies from about 1000-1100 m a.s.l. for the southern outlets to 1400 m a.s.l. for the NW outlets. The b_n-ELA slope is similar for all outlets -0,7 m_{we} per 100 m.

4. SURFACE VELOCITY MEASUREMENTS

The surface velocity of the glacier was calculated from DGPS (accuracy within 1 m), fast static (accuracy about 1 cm) and kinematic GPS (accuracy about 3 cm) positioning of the ablation stakes. All sites were surveyed in spring and autumn (most kinematic, some DGPS), and many also in June (kinematic), August (fast static) and October (kinematic). At a few sites stakes from previous years were found and resurveyed, making it possible to calculate surface velocity over a year or longer time span. The average summer surface velocity is shown on Figure 19.

At sites close to the glacier edge very small horizontal movement is measured. This indicates that the glacier snouts are almost stagnant. In the centre areas of some of the outlets especially close to the equilibrium line, there is an increase in velocity during summer compared to winter. The summer velocity is of the order of two-fold the winter velocity. This suggests that basal sliding is increased in the melting season, and is of the same magnitude as the deformation velocity.

From previous velocity measurements, surging of outlets has been predicted. No signs of a starting surge are seen from this year's survey.

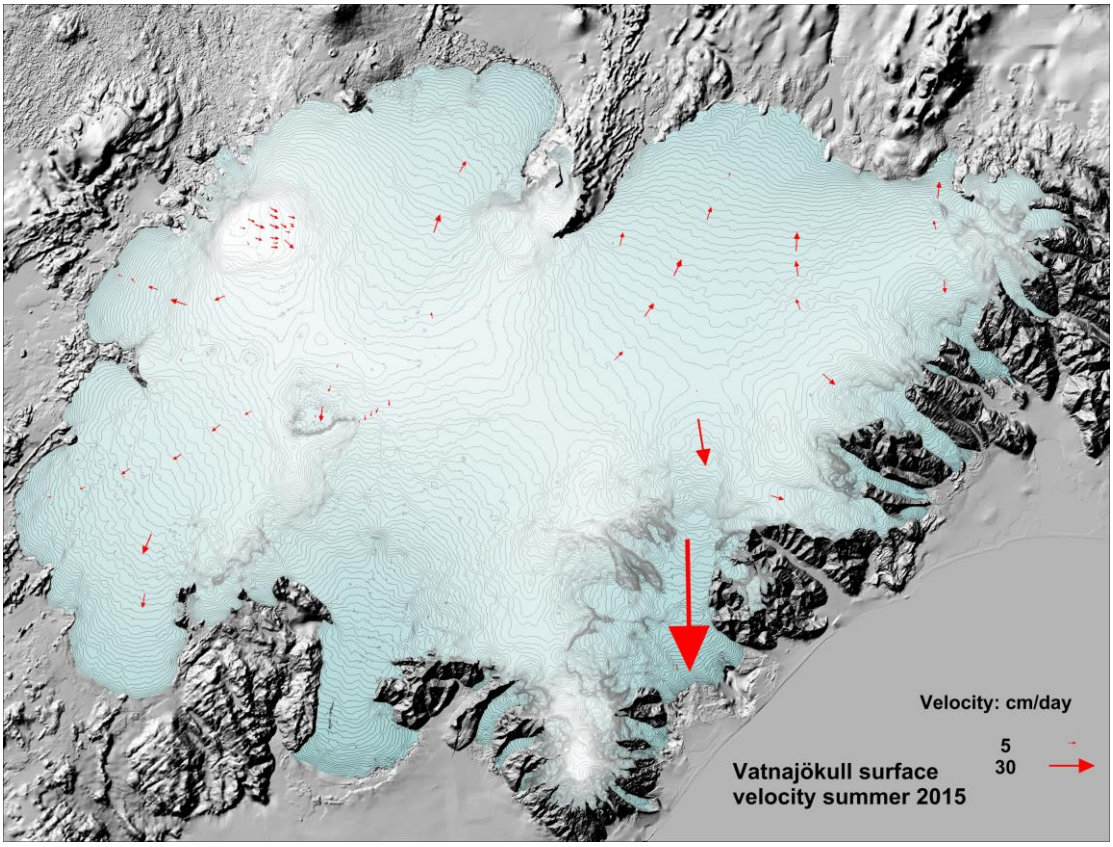

Figure 19. Average surface velocity at survey sites in 2014_15.

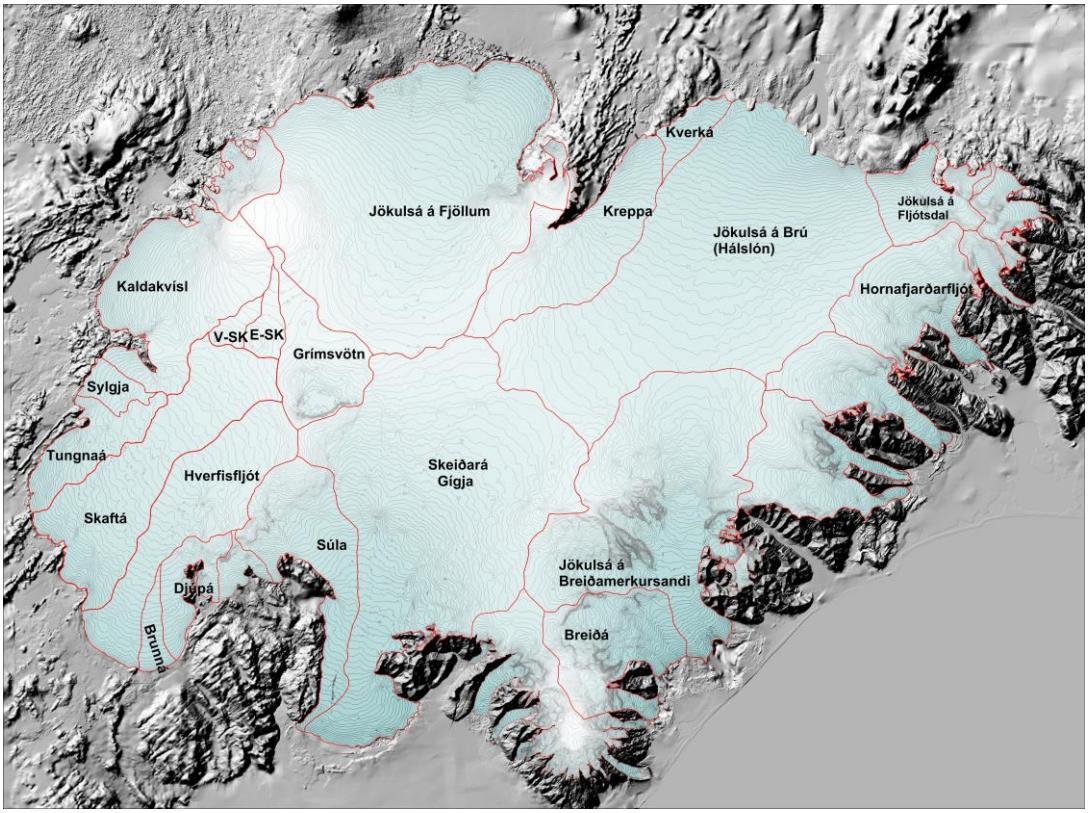

Figure 20. Water divides and drainage basins of selected rivers draining water from Vatnajökull.

5. Melt water runoff.

Water divides and drainage basins for rivers draining water from Vatnajökull have been defined from water pressure potential maps. The potential maps were produced from existing surface (year 2010) and bedrock digital elevation models.

Figure 20 shows the water divides and drainage areas for selected rivers draining melt water from Vatnajökull. The summer balance over the water basin is an estimate of meltwater contribution to rivers and groundwater storage. This estimate, however, does not include precipitation that falls as rain on the glacier, nor snow which falls and melts during the summer. The meltwater contribution can be compared with river runoff at stream flow gauges closest to the glacier. For this comparison, we define the glaciological year from the start of October to the end of September and the period draining meltwater from the glacier during the summer from June through September. It would be misleading to include May in the summer period because runoff from

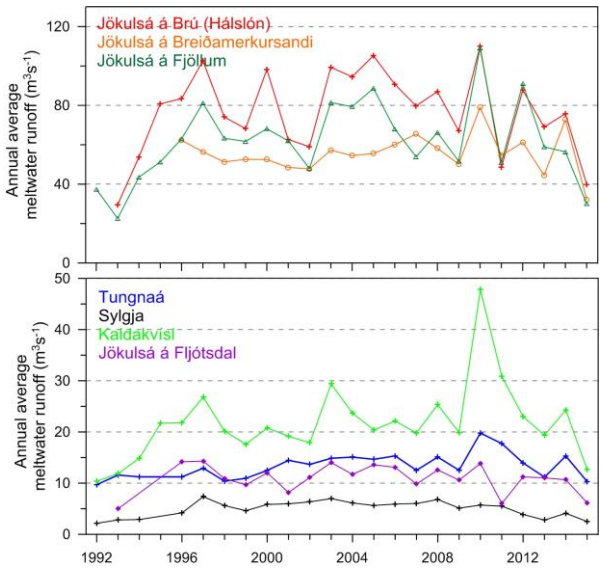

Figure 21. The temporal variation of average annual meltwater runoff to selected river catchments.

Table I. Melt water drainage to selected rivers.

Water Catchment:	Area (km^2)	ΣQ_s ($10^6 m^3$)	Q_s ($m^3 s^{-1}$)	Q_a ($m^3 s^{-1}$)	q_s ($ls^{-1} km^{-2}$)
Vatnajökull	7968,0	10631,0	1008,6	337,1	42,3
Tungnaá	121,8	325,1	30,8	10,3	84,6
Sylgja	39,7	79,3	7,5	2,5	63,3
Kaldakvísl	367,9	398,7	37,8	12,6	34,4
Jokulsa a Fjöllum	1188,3	945,9	89,7	30,0	25,2
Kreppa	291,2	210,4	20,0	6,7	22,9
Kverka	47,0	147,5	14,0	4,7	99,5
Jokulsa a Brú	1214,8	1259,1	119,5	39,9	32,9
Jökulsá á Fljótsdal	130,6	194,5	18,5	6,2	47,2
Jökulsá í Lóni	101,3	147,4	14,0	4,7	46,1
Hornafjarðarfljót	239,1	342,5	32,5	10,9	45,4
Jökulsá á Breiðamerkursandi	739,5	1014,9	96,3	32,2	43,5
Breiðá-Fjallsá	234,6	621,3	58,9	19,7	84,0
Skeiðará-Gígja	1165,2	1634,3	155,0	51,8	44,5
Súla	255,8	584,0	55,4	18,5	72,4
Brunná	35,8	127,3	12,1	4,0	112,8
Djúpá	83,7	226,1	21,4	7,2	85,7
Hverfisfljót	317,7	459,5	43,6	14,6	45,9
Skaftá	394,9	668,2	63,4	21,2	53,7
Grímsvötn	173,3	52,2	5,0	1,7	9,6
Eystri Skaftárketill	39,4	0,5	0,0	0,0	0,4
Vestari Skaftárketill	25,1	0,5	0,0	0,0	0,6
Hólmsá	164,9	245,3	23,3	7,8	47,2
Heinabergsvötn	229,6	370,1	35,1	11,7	51,1
Skjálfandafljót	71,9	38,2	3,6	1,2	16,8

ΣQ_s: total summer melt water; Q_s : average runoff (averaged over summer, 4 months, June – September)
Q_a : average runoff (averaged over a whole year); q_s : average runoff per km^2 (averaged over a whole year)

the glacier melt in May is delayed due to refreezing during elimination of the cold wave and because of the contribution of the spring melt from the highlands to the runoff. Some melting also occurs during winter, especially in the low snouts of the southern outlets.

Average melt water runoff to different rivers is given in Table I, and temporal variation of the average meltwater runoff in Fig. 21. The average specific runoff (q_s) differs from basin to basin from 14 to 112 $ls^{-1}km^{-2}$. This is mainly due to different elevation distributions, for example, the water drainage basins for Tungnaá and Kverká are within the ablation area, while that of Grímsvötn and Skaftárkatlar are high in the accumulation zone.

Due to a cold summer with repeated snow fall on the glacier surface, the error (under-estimate) in runoff estimation from the summer balance will be even more than average.

6. Conclusions

The autumn weather was slightly colder than average the past decade; October rather dry but precipitation in November well over the average in the S and SE. The winter months in Iceland December to March were colder than average, although close to average in the E. Storms were frequent (almost every 3 days) accompanied by unusually high precipitation. Winter accumulation was higher than average all over Vatnajökull. There was much thicker than average snow cover in the upper regions especially on Breiðabunga in the SE (open to SE coastal storms) and the upper regions of Dyngjujökull and Bárðarbunga (from high wind from E and NE). This reflects snowfall in SE, E, and NE wind directions. The spring months were cold and dry, with little change on Vatnajökull, in terms of accumulation or melt.

The summer of 2015 was unusually cold in SE-Iceland, also very wet and cloudy in June and July. In august clear sky was more frequent especially in the north, , in warm weather (again, none totally cloud free, most with haze).

September was warm and rather dry in the east, ablation was significant until mid-October. Ablation rates were lower than average almost everywhere, far under average during the May-July months. But the mild, even warm, and windy late August and September partly compensated this; the ablation rates were higher than average. The net balance was positive in all areas except in the lower ablation areas of S and SE outlets.

The winter balance was 40% higher than average (average since 1991_92). The summer mass balance was only 76% of the average during the survey period. The net balance was positive for the first time since 1993_94, the mass change +1,38 m_{we} greater than average of the survey period since 1991_92 (-0,49 m); +1,65 m_{we} greater than average of the survey period since 1995_96 (-0,75 m); of the past 20 consecutive years of negative balance. This means that the mass change is equal to the glacier having an extra average winter without a consecutive summer.

The glacial year of 2014_15 was the first in two decades with positive mass balance for Vatnajökull (Fig. 14, Fig. 15). The total mass loss over the 24 year survey period is 10,46 m_{we} (ice volume of ~92,7 km^3) since 1991_92 (13.42 m_{we} (ice volume of 120.28 km^3) since 1994_95 the first year of 2 decades of negative balance). The volume loss since 1991_92 amounts to ~3% of total ice volume (~4% since 1994_95).

Glacier meltwater runoff (estimated from summer balance only, summer rain and snow that falls and melts during summer is not included) to: Tungnaá was 67% of average, 60 % of average to Kaldakvísl, 47% of average to Jökulsá á Fjöllum, 51% of average to Hálslón, 55% to Jökulsá í Fljótsdal and 56% over average to Jökulsá á Breiðamerkursandi.

Summary:

B_w : 17,37 km^3_{we}
B_s : -10,23 km^3_{we}
B_n : 7,14 km^3_{we}
AAR = 73%

Specific Values:

b_w= 2,185 m_{we}
b_s= -1,287 m_{we}
b_n= 0,898 m_{we}

Appendix A: Mass balance at measurement sites 2014_15.

b_w: specific winter balance, **b_s**: specific summer balance, **b_n**: specific net balance, **l_a**: new snow in autumn (all in water equivalent).

Site	Position				Elevation	Date	Date	b_w	b_s	b_n	la
	Latitude		Longitude		(m a.s.l.)	in spring	in autumn	(m)	(m)	(m)	(m)
B09u	64	45,040	16	5,474	747,9	20150511	20151024	0,390	-4,539	-4,149	0,035
B10u	64	43,687	16	6,699	803,9	20150511	20151024	0,517	-3,286	-2,769	0,035
B11d	64	40,958	16	10,468	959,8	20150511	20151024	1,021	-1,985	-0,964	0,070
B12t	64	38,276	16	14,132	1077,2	20150511	20151024	1,513	-1,231	0,282	0,070
B13t	64	34,518	16	19,732	1215,5	20150511	20151023	2,087	-0,803	1,284	0,063
B14v	64	31,640	16	24,705	1315,3	20150510	20151023	2,490	-0,690	1,800	0,140
B15i	64	28,487	16	30,016	1399,8	20150510	20151023	2,570	-0,194	2,376	0,140
B16t	64	24,125	16	40,853	1526,2	20150510	20151028	2,360	-0,030	2,330	0,315
B17t	64	36,734	16	28,792	1212,8	20150510	20151023	1,895	-1,312	0,583	0,053
BR1g	64	5,558	16	19,503	110,0	20150415	20151025	-0,972	-8,100	-9,072	0,000
BR2k	64	6,391	16	22,543	232,0	20150415		0,045			
Br3p	64	8,509	16	24,104	401,4	20150415		0,725			
Br4d	64	10,733	16	20,238	527,5	20150415	20150930	1,060	-2,878	-1,818	0,000
Br7r	64	22,147	16	16,939	1246,7	20150513	20151022	2,826	-0,750	2,076	0,116
B07t	64	25,793	16	17,452	1357,7	20150513	20151022	2,620	-0,970	1,650	0,123
BB0s	64	22,718	16	5,051	1519,6	20150513	20151022	3,361	0,245	3,606	0,280
Brus	64	41,000	15	55,223	772,2	20150511	20151023	0,604	-4,429	-3,825	0,021
Buds	64	35,991	15	59,890	1136,2	20150511	20151023	1,920	-1,290	0,630	0,333
gb2d	64	34,109	16	0,026	1201,5	20150512	20151023	1,980	-0,660	1,320	0,070
B18r	64	31,587	16	0,124	1313,0	20150512	20151023	2,599	-0,517	2,082	0,116
B19r	64	27,933	15	55,164	1430,8	20150512	20151022	3,467	0,231	3,698	0,137
BB0s	64	22,718	16	5,051	1519,6	20150513	20151022	3,361	0,245	3,606	0,280
D05r	64	42,235	16	54,662	1201,7	20150510	20151024	1,737	-1,185	0,552	0,060
D07r	64	38,285	16	59,256	1371,4	20150510	20151024	2,283	-0,417	1,866	0,067
D09q	64	31,798	17	0,553	1581,2	20150510	20151024	2,604	-0,084	2,520	0,245
D12r	64	28,984	17	0,140	1646,8	20150509	20151024	2,896	0,348	3,244	0,231
E01s	64	41,455	15	33,503	681,0	20150512	20151023	0,855	-4,275	-3,420	0,035
E02s	64	39,130	15	35,977	955,3	20150512	20151023	1,637	-2,375	-0,738	0,035
E03t	64	36,667	15	36,909	1188,4	20150512	20151023	2,648	-0,770	1,878	0,070
E04s	64	34,952	15	37,106	1288,5	20150512	20151023	3,250	-0,367	2,883	0,123
K01u	64	35,165	17	51,797	1061,3	20150509	20151026	0,758	-1,964	-1,206	0,000
K02v	64	34,817	17	49,685	1178,1	20150509	20151026	1,743	-2,085	-0,342	0,035
K03u	64	34,247	17	46,382	1296,9	20150509	20151026	2,088	-1,482	0,606	0,042
K04v	64	33,209	17	42,251	1487,5	20150509	20151026	2,247	-0,687	1,560	0,231
K05v	64	33,451	17	35,428	1681,1	20150509	20151026	2,280	0,354	2,634	0,284
K06u	64	38,358	17	31,364	1967,5	20150604	20151026	3,185	0,513	3,698	0,385
K07q	64	29,113	17	42,014	1533,7	20150509	20151026	2,526	-0,435	2,091	0,305
S01j	64	7,012	17	49,989	740,4	20150507	20151026	1,238	-3,695	-2,457	0,035
S02m	64	12,164	17	48,966	1009,8	20150507	20151026	1,859	-2,462	-0,603	0,074
S04n	64	16,198	17	48,217	1159,6	20150507	20151026	2,234	-1,562	0,672	0,095
HAABn	64	20,952	17	24,083	1729,3	20150603	20151025	3,353	0,483	3,836	0,875

T01no	64	19,486	18	8,234	743,7	20150507	20151026	0,599	-5,432	-4,833	0,000
T02nq	64	19,600	18	3,968	940,9	20150507	20151026	1,815	-2,868	-1,053	0,035
T03nq	64	20,210	17	58,600	1076,1	20150507	20151027	1,812	-2,177	-0,365	0,109
T04nq	64	21,339	17	51,527	1222,1	20150507	20151027	2,161	-1,435	0,726	0,182
T05nq	64	22,287	17	43,012	1343,5	20150507	20151027	2,016	-0,822	1,194	0,238
T06nq	64	24,281	17	36,538	1465,2	20150508	20151027	2,482	-0,298	2,184	0,354
T07np	64	25,291	17	31,200	1562,6	20150509	20151025	2,630	-0,302	2,328	0,455
T08nq	64	26,313	17	27,779	1635,9	20150509	20151025	2,716	0,110	2,826	0,490
BORTHNb	64	25,087	17	19,154	1400,7	20150604	20151025	3,367	-0,841	2,526	0,385
Borai	64	24,938	17	20,158	1399,9	20150602	20151025	3,337	-0,937	2,400	0,315
G02k	64	26,845	17	17,748	1560,1	20150602	20151025	2,485	-0,757	1,728	0,315
G03l	64	28,445	17	16,347	1655,3	20150603	20151025	3,153	-0,243	2,910	0,315
G04s	64	30,016	17	15,025	1684,8	20150603	20151025	3,151	0,251	3,402	0,343
Go1r	64	34,014	17	24,920	1758,1	20150603		3,069		3,069	
Hof01l	64	32,327	15	35,844	1141,1	20150512	20151023	2,758	-0,952	1,806	0,175
Fl01e	64	26,161	15	55,628	1347,3	20150513	20151022	3,237	-0,369	2,868	0,238
Skf01e	64	17,989	16	5,003	1283,2	20150513	20151022	3,499	-0,513	2,986	0,140
Bafk01	64	37,000	17	30,000	1917	20150604		3,190			
Bafk02	64	37,243	17	25,995	1875,0	20150610	20151026	3,200	0,322	3,522	0,462
Bafk03	64	38,000	17	23,982	1842,8	20150610	20151026	2,340	0,540	2,880	0,315
Bafk04	64	39,400	17	26,000	1892,0	20150610		2,390			
Barc	64	38,410	17	26,764	1874,9	20150607	20151026	3,960			0,455
K06u	64	38,358	17	31,364	1967,5	20150604	20151026	3,185	0,513	3,698	0,385
D02	64	42,511	16	45,595	1056,4	20150323		0,763			
D01	64	45,649	16	59,045	1123,7	20150323		1,486			

Appendix B: Balance distribution by elevation in 2014_15.

ΔS : area in elevation range, $\sum\Delta S$: cumulative area above given elevation, b_w: specific winter balance, b_s: specific summer balance. b_n: specific winter balance, ΔB_w : winter balance at a given elevation range, $\sum\Delta B_w$: cumulative winter balance above given elevation, ΔB_s summer balance at a given elevation range, $\sum\Delta B_s$: cumulative summer balance above given elevation, ΔB_n: net annual balance in a given elevation range, $\sum B_n$: cumulative net annual balance above given elevation.

Vatnajökull

Elevation (m a.s.l.)			ΔS (km^2)	$\sum\Delta S$ (km^2)	b_w (mm)	b_s (mm)	b_n (mm)	ΔB_w ($10^6 m^3$)	$\sum\Delta B_w$ ($10^6 m^3$)	ΔB_s ($10^6 m^3$)	$\sum\Delta B_s$ ($10^6 m^3$)	ΔB_n ($10^6 m^3$)	$\sum B_n$ ($10^6 m^3$)
2000	2050	2025	0,4	0,4	4322	2047	6369	1,9	2	0,9	1	2,9	3
1950	2000	1975	8,8	9,2	3174	845	4019	27,8	30	7,4	8	35,2	38
1900	1950	1925	36,6	45,8	3103	659	3762	113,4	143	24,1	32	137,6	176
1850	1900	1875	47,4	93,2	3152	743	3896	149,5	293	35,3	68	184,8	360
1800	1850	1825	47,0	140,2	3285	826	4111	154,3	447	38,8	107	193,1	554
1750	1800	1775	54,5	194,7	3160	588	3748	172,4	619	32,1	139	204,5	758
1700	1750	1725	104,3	299,0	3009	388	3398	314,0	933	40,5	179	354,5	1113
1650	1700	1675	222,4	521,4	3001	201	3202	667,5	1601	44,8	224	712,2	1825
1600	1650	1625	373,0	894,4	2854	102	2956	1064,5	2665	38,2	262	1102,7	2927
1550	1600	1575	353,6	1248,0	2755	-67	2688	974,5	3640	-23,9	238	950,7	3878
1500	1550	1525	420,6	1668,6	2664	-155	2509	1120,5	4760	-65,3	173	1055,2	4933
1450	1500	1475	453,2	2121,8	2654	-237	2417	1203,2	5964	-107,4	66	1095,8	6029
1400	1450	1425	503,8	2625,6	2717	-296	2421	1369,4	7333	-149,6	-84	1219,8	7249
1350	1400	1375	548,7	3174,3	2679	-432	2246	1470,0	8803	-237,4	-321	1232,6	8482
1300	1350	1325	540,9	3715,2	2605	-605	1999	1409,3	10212	-327,6	-649	1081,7	9563
1250	1300	1275	512,0	4227,2	2537	-754	1782	1299,3	11512	-386,5	-1036	912,8	10476
1200	1250	1225	453,3	4680,5	2361	-968	1392	1070,6	12582	-439,2	-1475	631,5	11108
1150	1200	1175	403,5	5084,0	2187	-1215	971	882,4	13465	-490,5	-1965	391,8	11499
1100	1150	1125	362,5	5446,5	2052	-1465	587	744,1	14209	-531,1	-2496	213,0	11712
1050	1100	1075	323,6	5770,1	1904	-1712	192	616,4	14825	-554,3	-3051	62,1	11775
1000	1050	1025	301,1	6071,2	1747	-1967	-220	526,1	15351	-592,3	-3643	-66,2	11708
950	1000	975	270,8	6342,0	1597	-2201	-604	432,7	15784	-596,3	-4239	-163,6	11545
900	950	925	238,3	6580,3	1499	-2436	-937	357,3	16141	-580,7	-4820	-223,5	11321
850	900	875	210,2	6790,5	1392	-2672	-1279	292,7	16434	-561,8	-5382	-269,1	11052
800	850	825	192,1	6982,6	1268	-2957	-1689	243,8	16678	-568,4	-5950	-324,6	10728
750	800	775	174,8	7157,4	1125	-3300	-2175	196,7	16874	-576,9	-6527	-380,2	10347
700	750	725	141,2	7298,6	1110	-3492	-2381	156,7	17031	-493,1	-7020	-336,3	10011
650	700	675	121,3	7419,9	1109	-3536	-2427	134,5	17166	-428,9	-7449	-294,4	9717
600	650	625	74,6	7494,5	1147	-3374	-2227	85,6	17251	-251,8	-7701	-166,2	9551
550	600	575	65,8	7560,3	1152	-3384	-2231	75,9	17327	-222,8	-7924	-146,9	9404
500	550	525	48,0	7608,3	1095	-3715	-2619	52,6	17380	-178,2	-8102	-125,6	9278
450	500	475	40,4	7648,7	993	-4047	-3054	40,1	17420	-163,5	-8265	-123,4	9155
400	450	425	44,5	7693,2	844	-4502	-3658	37,6	17457	-200,5	-8466	-162,9	8992
350	400	375	40,0	7733,2	580	-5150	-4570	23,2	17481	-206,1	-8672	-182,9	8809
300	350	325	38,1	7771,3	232	-5772	-5540	8,9	17490	-219,8	-8892	-211,0	8598
250	300	275	36,6	7807,9	-68	-6320	-6388	-2,5	17487	-231,5	-9123	-234,0	8364
200	250	225	37,5	7845,4	-374	-6846	-7221	-14,0	17473	-256,5	-9380	-270,6	8093
150	200	175	32,5	7877,9	-698	-7443	-8142	-22,7	17450	-241,5	-9621	-264,2	7829
100	150	125	28,3	7906,2	-906	-7980	-8886	-25,7	17425	-225,9	-9847	-251,6	7578
50	100	75	25,9	7932,1	-1076	-8537	-9614	-27,9	17397	-221,1	-10068	-248,9	7329
0	50	25	18,3	7950,4	-1281	-8745	-10027	-23,5	17373	-160,1	-10228	-183,6	7145

Tungnaárjökull

Elevation (m a.s.l.)			ΔS (km^2)	∑ΔS (km^2)	b_w (mm)	b_s (mm)	b_n (mm)	ΔB_w ($10^6 m^3$)	$\sum\Delta B_w$ ($10^6 m^3$)	ΔB_s ($10^6 m^3$)	$\sum\Delta B_s$ ($10^6 m^3$)	ΔB_n ($10^6 m^3$)	$\sum B_n$ ($10^6 m^3$)
1650	1700	1675	2,4	2,4	2781	91	2872	6,6	7	0,2	0	6,8	7
1600	1650	1625	13,2	15,6	2687	71	2759	35,4	42	0,9	1	36,3	43
1550	1600	1575	15,3	30,9	2643	-61	2582	40,3	82	-0,9	0	39,4	83
1500	1550	1525	15,3	46,2	2579	-199	2379	39,4	122	-3,1	-3	36,4	119
1450	1500	1475	18,5	64,7	2496	-330	2165	46,1	168	-6,1	-9	40,0	159
1400	1450	1425	23,3	88,0	2425	-504	1920	56,5	224	-11,8	-21	44,8	204
1350	1400	1375	21,7	109,7	2372	-698	1674	51,4	276	-15,1	-36	36,3	240
1300	1350	1325	28,1	137,8	2315	-922	1393	65,0	341	-25,9	-62	39,1	279
1250	1300	1275	21,8	159,6	2254	-1185	1069	49,2	390	-25,9	-88	23,3	302
1200	1250	1225	24,0	183,6	2160	-1464	696	51,9	442	-35,2	-123	16,7	319
1150	1200	1175	21,0	204,6	2047	-1729	318	42,9	485	-36,2	-159	6,7	326
1100	1150	1125	19,2	223,8	1900	-2007	-107	36,6	521	-38,6	-198	-2,1	324
1050	1100	1075	20,0	243,8	1759	-2285	-526	35,2	557	-45,7	-243	-10,5	313
1000	1050	1025	18,2	262,0	1592	-2541	-949	29,0	586	-46,2	-290	-17,3	296
950	1000	975	18,9	280,9	1414	-2823	-1408	26,7	612	-53,3	-343	-26,6	269
900	950	925	15,2	296,1	1233	-3262	-2028	18,7	631	-49,5	-392	-30,8	239
850	900	875	15,1	311,2	1048	-3837	-2789	15,8	647	-57,8	-450	-42,0	197
800	850	825	13,4	324,6	860	-4669	-3808	11,5	658	-62,3	-512	-50,8	146
750	800	775	10,0	334,6	711	-5410	-4699	7,1	665	-54,0	-566	-46,9	99
700	750	725	5,7	340,3	615	-5899	-5283	3,5	669	-33,7	-600	-30,2	69
650	700	675	0,3	340,6	606	-6040	-5434	0,2	669	-2,1	-602	-1,9	67

Sylgjujökull

Elevation (m a.s.l.)			ΔS (km^2)	∑ΔS (km^2)	b_w (mm)	b_s (mm)	b_n (mm)	ΔB_w ($10^6 m^3$)	$\sum\Delta B_w$ ($10^6 m^3$)	ΔB_s ($10^6 m^3$)	$\sum\Delta B_s$ ($10^6 m^3$)	ΔB_n ($10^6 m^3$)	$\sum B_n$ ($10^6 m^3$)
1600	1650	1625	2,0	2,0	2667	22	2689	5,4	5	0,0	0	5,4	5
1550	1600	1575	6,8	8,8	2630	-119	2511	17,8	23	-0,8	-1	17,0	22
1500	1550	1525	18,9	27,7	2556	-309	2246	48,2	71	-5,8	-7	42,4	65
1450	1500	1475	12,3	40,0	2466	-442	2023	30,3	102	-5,4	-12	24,9	90
1400	1450	1425	8,2	48,2	2409	-555	1854	19,8	121	-4,6	-17	15,2	105
1350	1400	1375	5,1	53,3	2363	-691	1672	12,0	134	-3,5	-20	8,5	113
1300	1350	1325	5,3	58,6	2294	-947	1347	12,1	146	-5,0	-25	7,1	120
1250	1300	1275	10,4	69,0	2219	-1219	1000	23,0	169	-12,6	-38	10,4	131
1200	1250	1225	12,6	81,6	2127	-1489	637	26,7	195	-18,7	-57	8,0	139
1150	1200	1175	14,4	96,0	2020	-1732	288	29,0	224	-24,9	-81	4,1	143
1100	1150	1125	13,2	109,2	1868	-2031	-163	24,6	249	-26,8	-108	-2,2	141
1050	1100	1075	13,4	122,6	1735	-2483	-747	23,3	272	-33,3	-141	-10,0	131
1000	1050	1025	8,9	131,5	1594	-2837	-1243	14,2	286	-25,2	-167	-11,0	120
950	1000	975	2,8	134,3	1475	-2982	-1507	4,2	291	-8,4	-175	-4,3	116
900	950	925	1,2	135,5	1407	-3103	-1696	1,7	292	-3,8	-179	-2,1	113
850	900	875	0,0	135,5	1412	-3273	-1861	0,0	292	0,0	-179	0,0	113

Köldukvíslarjökul

Elevation (m a.s.l.)			ΔS (km^2)	∑ΔS (km^2)	b_w (mm)	b_s (mm)	b_n (mm)	ΔB_w ($10^6 m^3$)	$\sum\Delta B_w$ ($10^6 m^3$)	ΔB_s ($10^6 m^3$)	$\sum\Delta B_s$ ($10^6 m^3$)	ΔB_n ($10^6 m^3$)	$\sum B_n$ ($10^6 m^3$)
1950	2000	1975	3,6	3,6	3032	563	3595	10,9	11	2,0	2	12,9	13
1900	1950	1925	12,4	16,0	2964	542	3506	36,7	48	6,7	9	43,5	56
1850	1900	1875	5,9	21,9	2812	490	3303	16,5	64	2,9	12	19,4	76
1800	1850	1825	6,0	27,9	2733	449	3183	16,3	80	2,7	14	19,0	95
1750	1800	1775	10,5	38,4	2769	434	3204	29,2	110	4,6	19	33,7	129
1700	1750	1725	17,9	56,3	2600	372	2972	46,5	156	6,7	26	53,1	182
1650	1700	1675	15,6	71,9	2451	241	2692	38,2	194	3,8	29	42,0	224
1600	1650	1625	13,8	85,7	2365	65	2430	32,7	227	0,9	30	33,6	257
1550	1600	1575	19,2	104,9	2330	-196	2133	44,8	272	-3,8	26	41,0	298
1500	1550	1525	20,9	125,8	2366	-458	1907	49,5	321	-9,6	17	39,9	338
1450	1500	1475	19,3	145,1	2294	-678	1616	44,3	366	-13,1	4	31,2	369
1400	1450	1425	14,2	159,3	2192	-890	1301	31,2	397	-12,7	-9	18,5	388
1350	1400	1375	15,2	174,5	2157	-1088	1069	32,9	430	-16,6	-26	16,3	404
1300	1350	1325	17,5	192,0	2114	-1316	797	37,0	467	-23,0	-49	14,0	418
1250	1300	1275	18,1	210,1	2053	-1603	449	37,2	504	-29,0	-78	8,1	426
1200	1250	1225	18,3	228,4	1944	-1896	48	35,5	539	-34,7	-112	0,9	427
1150	1200	1175	16,4	244,8	1692	-2166	-474	27,7	567	-35,5	-148	-7,8	419
1100	1150	1125	14,9	259,7	1290	-2416	-1125	19,2	586	-36,0	-184	-16,8	403
1050	1100	1075	13,1	272,8	928	-2667	-1739	12,2	598	-35,1	-219	-22,9	380
1000	1050	1025	11,1	283,9	693	-2892	-2199	7,7	606	-32,0	-251	-24,3	355
950	1000	975	10,0	293,9	574	-3058	-2483	5,7	612	-30,5	-281	-24,8	331
900	950	925	3,9	297,8	519	-3169	-2650	2,0	614	-12,2	-294	-10,2	320
850	900	875	0,1	297,9	480	-3278	-2797	0,0	614	-0,4	-294	-0,3	320

Dyngjujökull

Elevation (m a.s.l.)			ΔS (km^2)	∑ΔS (km^2)	b_w (mm)	b_s (mm)	b_n (mm)	ΔB_w ($10^6 m^3$)	$\sum\Delta B_w$ ($10^6 m^3$)	ΔB_s ($10^6 m^3$)	$\sum\Delta B_s$ ($10^6 m^3$)	ΔB_n ($10^6 m^3$)	$\sum B_n$ ($10^6 m^3$)
1950	2000	1975	7,4	7,4	3060	543	3604	22,7	23	4,0	4	26,7	27
1900	1950	1925	23,2	30,6	3154	546	3700	73,0	96	12,6	17	85,7	113
1850	1900	1875	15,9	46,5	2579	531	3111	41,1	137	8,5	25	49,5	162
1800	1850	1825	9,7	56,2	2866	489	3355	27,9	165	4,8	30	32,7	195
1750	1800	1775	16,0	72,2	2969	427	3396	47,5	212	6,8	37	54,3	249
1700	1750	1725	27,3	99,5	3028	325	3354	82,5	295	8,9	46	91,4	340
1650	1700	1675	71,6	171,1	3029	232	3261	216,9	512	16,6	62	233,5	574
1600	1650	1625	114,0	285,1	2864	136	3000	326,6	838	15,6	78	342,2	916
1550	1600	1575	94,7	379,8	2735	-60	2674	259,1	1097	-5,7	72	253,4	1170
1500	1550	1525	89,6	469,4	2637	-150	2486	236,2	1334	-13,5	59	222,7	1392
1450	1500	1475	75,0	544,4	2534	-233	2301	190,1	1524	-17,5	41	172,6	1565
1400	1450	1425	61,3	605,7	2429	-309	2120	149,0	1673	-19,0	22	130,0	1695
1350	1400	1375	49,3	655,0	2305	-410	1895	113,7	1786	-20,2	2	93,4	1788
1300	1350	1325	37,9	692,9	2182	-547	1634	82,6	1869	-20,7	-19	61,9	1850
1250	1300	1275	41,3	734,2	2046	-740	1306	84,5	1954	-30,6	-49	54,0	1904
1200	1250	1225	48,7	782,9	1881	-1025	855	91,7	2045	-50,0	-99	41,7	1946
1150	1200	1175	48,1	831,0	1692	-1395	297	81,4	2127	-67,1	-167	14,3	1960
1100	1150	1125	43,7	874,7	1545	-1750	-205	67,6	2194	-76,6	-243	-9,0	1951
1050	1100	1075	33,1	907,8	1344	-2078	-734	44,5	2239	-68,8	-312	-24,3	1927
1000	1050	1025	35,6	943,4	1120	-2422	-1301	39,9	2279	-86,2	-398	-46,3	1881
950	1000	975	30,8	974,2	919	-2834	-1915	28,3	2307	-87,3	-486	-59,0	1822
900	950	925	25,8	1000,0	745	-3234	-2488	19,2	2326	-83,3	-569	-64,1	1757
850	900	875	25,0	1025,0	592	-3601	-3008	14,8	2341	-89,9	-659	-75,1	1682
800	850	825	18,9	1043,9	457	-3939	-3481	8,7	2350	-74,6	-733	-65,9	1616
750	800	775	13,8	1057,7	335	-4267	-3931	4,6	2354	-58,9	-792	-54,3	1562
700	750	725	1,6	1059,3	279	-4429	-4150	0,4	2355	-7,0	-799	-6,6	1556

Brúarjökull

Elevation (m a.s.l.)			ΔS (km^2)	∑ΔS (km^2)	b_w (mm)	b_s (mm)	b_n (mm)	ΔB_w ($10^6 m^3$)	$\sum\Delta B_w$ ($10^6 m^3$)	ΔB_s ($10^6 m^3$)	$\sum\Delta B_s$ ($10^6 m^3$)	ΔB_n ($10^6 m^3$)	$\sum B_n$ ($10^6 m^3$)
1850	1900	1875	0,9	0,9	3593	569	4163	3,1	3	0,5	1	3,6	4
1800	1850	1825	4,2	5,1	3577	523	4100	14,8	18	2,2	3	17,0	21
1750	1800	1775	3,0	8,1	3373	397	3770	10,0	28	1,2	4	11,2	32
1700	1750	1725	3,7	11,8	3058	270	3328	11,4	39	1,0	5	12,5	44
1650	1700	1675	5,3	17,1	2917	218	3135	15,4	55	1,2	6	16,6	61
1600	1650	1625	44,4	61,5	2791	189	2981	124,0	179	8,4	14	132,5	193
1550	1600	1575	47,6	109,1	2744	-14	2729	130,7	310	-0,7	14	130,0	323
1500	1550	1525	69,9	179,0	2600	-64	2536	181,7	491	-4,5	9	177,2	501
1450	1500	1475	73,9	252,9	2611	-101	2509	193,1	684	-7,5	2	185,6	686
1400	1450	1425	108,1	361,0	2792	-92	2700	301,9	986	-10,0	-8	292,0	978
1350	1400	1375	148,3	509,3	2751	-272	2478	408,1	1394	-40,5	-49	367,6	1346
1300	1350	1325	151,3	660,6	2605	-495	2109	394,3	1789	-75,0	-124	319,3	1665
1250	1300	1275	144,8	805,4	2465	-642	1823	357,0	2146	-93,0	-217	264,0	1929
1200	1250	1225	121,8	927,2	2210	-797	1412	269,3	2415	-97,2	-314	172,1	2101
1150	1200	1175	105,8	1033,0	1971	-1030	940	208,6	2624	-109,0	-423	99,6	2201
1100	1150	1125	86,8	1119,8	1768	-1292	475	153,4	2777	-112,2	-535	41,2	2242
1050	1100	1075	73,3	1193,1	1565	-1510	54	114,8	2892	-110,8	-646	4,0	2246
1000	1050	1025	65,6	1258,7	1331	-1752	-421	87,4	2979	-115,0	-761	-27,7	2218
950	1000	975	59,3	1318,0	1107	-2063	-956	65,7	3045	-122,4	-884	-56,7	2161
900	950	925	48,9	1366,9	922	-2428	-1505	45,1	3090	-118,8	-1002	-73,6	2088
850	900	875	44,7	1411,6	763	-2815	-2051	34,2	3124	-125,9	-1128	-91,7	1996
800	850	825	41,2	1452,8	622	-3328	-2705	25,7	3150	-137,1	-1265	-111,5	1885
750	800	775	35,9	1488,7	496	-4121	-3625	17,8	3168	-148,0	-1413	-130,2	1754
700	750	725	23,5	1512,2	424	-4803	-4378	10,0	3178	-112,8	-1526	-102,8	1652
650	700	675	11,8	1524,0	360	-5275	-4914	4,3	3182	-62,3	-1588	-58,0	1594
600	650	625	0,3	1524,3	370	-5549	-5179	0,1	3182	-1,6	-1590	-1,5	1592

Eyjabakkajökull

Elevation (m a.s.l.)			ΔS (km^2)	∑ΔS (km^2)	b_w (mm)	b_s (mm)	b_n (mm)	ΔB_w ($10^6 m^3$)	$\sum\Delta B_w$ ($10^6 m^3$)	ΔB_s ($10^6 m^3$)	$\sum\Delta B_s$ ($10^6 m^3$)	ΔB_n ($10^6 m^3$)	$\sum B_n$ ($10^6 m^3$)
1550	1600	1575	0,0	0,0	3529	38	3567	0,0	0	0,0	0	0,0	0
1500	1550	1525	0,0	0,0	3537	53	3590	0,3	0	0,0	0	0,3	0
1450	1500	1475	1,0	1,0	3530	22	3553	3,4	4	0,0	0	3,4	4
1400	1450	1425	1,8	2,8	3496	-13	3483	6,4	10	0,0	0	6,4	10
1350	1400	1375	2,5	5,3	3391	-109	3281	8,6	19	-0,3	0	8,3	19
1300	1350	1325	3,9	9,2	3292	-199	3092	12,9	32	-0,8	-1	12,1	31
1250	1300	1275	13,4	22,6	3135	-394	2741	41,9	74	-5,3	-6	36,6	67
1200	1250	1225	13,3	35,9	2852	-631	2221	38,0	112	-8,4	-15	29,6	97
1150	1200	1175	14,7	50,6	2564	-970	1594	37,7	149	-14,3	-29	23,4	120
1100	1150	1125	12,3	62,9	2285	-1366	919	28,0	177	-16,7	-46	11,3	132
1050	1100	1075	10,6	73,5	2001	-1792	209	21,2	198	-19,0	-65	2,2	134
1000	1050	1025	10,1	83,6	1782	-2148	-365	18,0	217	-21,7	-86	-3,7	130
950	1000	975	7,7	91,3	1592	-2447	-855	12,3	229	-18,9	-105	-6,6	123
900	950	925	5,2	96,5	1415	-2725	-1309	7,3	236	-14,1	-120	-6,8	117
850	900	875	3,9	100,4	1304	-2888	-1584	5,1	241	-11,3	-131	-6,2	110
800	850	825	3,2	103,6	1218	-3004	-1785	3,9	245	-9,5	-140	-5,6	105
750	800	775	3,4	107,0	1101	-3287	-2185	3,7	249	-11,1	-151	-7,4	97
700	750	725	3,3	110,3	956	-3803	-2847	3,2	252	-12,6	-164	-9,4	88
650	700	675	1,7	112,0	849	-4249	-3399	1,4	253	-7,2	-171	-5,8	82

Hoffellsjökull

Elevation (m a.s.l.)			ΔS (km^2)	∑ΔS (km^2)	b_w (mm)	b_s (mm)	b_n (mm)	ΔB_w ($10^6 m^3$)	$\sum\Delta B_w$ ($10^6 m^3$)	ΔB_s ($10^6 m^3$)	$\sum\Delta B_s$ ($10^6 m^3$)	ΔB_n ($10^6 m^3$)	$\sum B_n$ ($10^6 m^3$)
1450	1500	1475	0,9	0,9	3536	28	3564	3,3	3	0,0	0	3,3	3
1400	1450	1425	6,7	7,6	3442	7	3450	23,1	26	0,0	0	23,1	26
1350	1400	1375	10,0	17,6	3386	-102	3284	33,8	60	-1,0	-1	32,7	59
1300	1350	1325	15,4	33,0	3331	-269	3062	51,2	111	-4,1	-5	47,0	106
1250	1300	1275	33,6	66,6	3203	-461	2742	107,5	219	-15,5	-21	92,0	198
1200	1250	1225	26,8	93,4	3130	-649	2480	83,9	303	-17,4	-38	66,5	265
1150	1200	1175	18,2	111,6	2950	-863	2086	53,7	356	-15,7	-54	38,0	303
1100	1150	1125	17,5	129,1	2749	-1029	1719	48,1	405	-18,0	-72	30,1	333
1050	1100	1075	13,6	142,7	2545	-1215	1330	34,5	439	-16,5	-88	18,0	351
1000	1050	1025	10,0	152,7	2367	-1398	969	23,6	463	-14,0	-102	9,7	361
950	1000	975	9,0	161,7	2164	-1585	578	19,5	482	-14,3	-117	5,2	366
900	950	925	6,4	168,1	1956	-1749	207	12,6	495	-11,3	-128	1,3	367
850	900	875	4,3	172,4	1793	-1895	-102	7,8	503	-8,2	-136	-0,4	367
800	850	825	3,6	176,0	1763	-2004	-240	6,3	509	-7,2	-143	-0,9	366
750	800	775	3,9	179,9	1663	-2135	-471	6,5	515	-8,3	-151	-1,8	364
700	750	725	3,8	183,7	1544	-2256	-711	5,9	521	-8,6	-160	-2,7	361
650	700	675	3,4	187,1	1400	-2411	-1010	4,7	526	-8,1	-168	-3,4	358
600	650	625	2,5	189,6	1251	-2622	-1371	3,1	529	-6,5	-175	-3,4	354
550	600	575	1,8	191,4	1137	-2889	-1751	2,1	531	-5,3	-180	-3,2	351
500	550	525	1,5	192,9	1040	-3328	-2287	1,5	533	-4,9	-185	-3,4	348
450	500	475	0,9	193,8	938	-3826	-2888	0,9	534	-3,6	-188	-2,7	345
400	450	425	0,9	194,7	749	-4487	-3737	0,7	534	-4,3	-193	-3,6	342
350	400	375	0,6	195,3	462	-5146	-4683	0,3	535	-3,0	-196	-2,8	339
300	350	325	0,9	196,2	166	-5711	-5545	0,2	535	-5,2	-201	-5,0	334
250	300	275	2,2	198,4	-211	-6363	-6574	-0,5	534	-13,8	-215	-14,3	320
200	250	225	3,3	201,7	-639	-7092	-7732	-2,1	532	-23,2	-238	-25,3	294
150	200	175	2,6	204,3	-898	-7710	-8608	-2,3	530	-20,0	-258	-22,4	272
100	150	125	2,1	206,4	-1031	-8144	-9175	-2,2	528	-17,3	-275	-19,5	252
50	100	75	2,8	209,2	-1267	-8836	-10103	-3,5	524	-24,7	-300	-28,3	224
0	50	25	0,6	209,8	-1397	-9099	-10497	-0,8	523	-5,1	-305	-5,9	218

Breiðamerkurjökull

Elevation (m a.s.l.)			ΔS (km^2)	∑ΔS (km^2)	b_w (mm)	b_s (mm)	b_n (mm)	ΔB_w ($10^6 m^3$)	$\sum\Delta B_w$ ($10^6 m^3$)	ΔB_s ($10^6 m^3$)	$\sum\Delta B_s$ ($10^6 m^3$)	ΔB_n ($10^6 m^3$)	$\sum B_n$ ($10^6 m^3$)
1900	1950	1925	0,0	0,0	4264	2051	6315	0,2	0	0,0	0	0,3	0
1850	1900	1875	0,4	0,4	4257	2018	6276	1,5	2	0,7	1	2,3	3
1800	1850	1825	0,4	0,8	4223	1877	6100	1,9	4	0,8	2	2,7	5
1750	1800	1775	0,8	1,6	4169	1589	5759	3,4	7	1,3	3	4,7	10
1700	1750	1725	2,5	4,1	3689	698	4388	9,1	16	1,7	5	10,8	21
1650	1700	1675	5,8	9,9	3209	205	3414	18,5	35	1,2	6	19,7	41
1600	1650	1625	15,8	25,7	2955	52	3008	46,7	81	0,8	7	47,5	88
1550	1600	1575	25,7	51,4	2826	-17	2808	72,7	154	-0,5	6	72,2	160
1500	1550	1525	32,2	83,6	2801	-97	2703	90,1	244	-3,1	3	87,0	247
1450	1500	1475	44,3	127,9	2857	-106	2750	126,5	371	-4,7	-2	121,7	369
1400	1450	1425	58,3	186,2	2816	-194	2622	164,3	535	-11,3	-13	153,0	522
1350	1400	1375	88,7	274,9	2794	-353	2441	247,9	783	-31,4	-44	216,5	739
1300	1350	1325	96,9	371,8	2773	-525	2247	268,8	1052	-51,0	-95	217,8	956
1250	1300	1275	59,4	431,2	2751	-674	2077	163,5	1215	-40,1	-135	123,4	1080
1200	1250	1225	39,7	470,9	2700	-788	1911	107,1	1322	-31,3	-167	75,8	1156
1150	1200	1175	32,6	503,5	2606	-916	1690	85,1	1407	-29,9	-197	55,2	1211
1100	1150	1125	27,7	531,2	2483	-1075	1408	68,9	1476	-29,8	-226	39,0	1250
1050	1100	1075	24,1	555,3	2390	-1237	1152	57,5	1534	-29,8	-256	27,8	1278
1000	1050	1025	22,1	577,4	2316	-1402	914	51,3	1585	-31,0	-287	20,2	1298
950	1000	975	24,5	601,9	2227	-1571	656	54,6	1640	-38,5	-326	16,1	1314
900	950	925	27,4	629,3	2125	-1672	453	58,2	1698	-45,8	-372	12,4	1326
850	900	875	26,2	655,5	1974	-1823	150	51,7	1750	-47,8	-419	3,9	1330
800	850	825	26,1	681,6	1812	-1977	-164	47,3	1797	-51,5	-471	-4,3	1326
750	800	775	25,3	706,9	1633	-2144	-511	41,3	1838	-54,2	-525	-12,9	1313
700	750	725	23,9	730,8	1524	-2301	-776	36,5	1875	-55,0	-580	-18,6	1294
650	700	675	30,8	761,6	1417	-2433	-1016	43,7	1918	-75,1	-655	-31,3	1263
600	650	625	26,2	787,8	1257	-2596	-1339	32,9	1951	-68,0	-723	-35,1	1228
550	600	575	27,0	814,8	1134	-2868	-1734	30,6	1982	-77,4	-801	-46,8	1181
500	550	525	15,7	830,5	1069	-3232	-2162	16,8	1999	-50,9	-852	-34,0	1147
450	500	475	16,3	846,8	938	-3749	-2810	15,3	2014	-60,9	-912	-45,7	1102
400	450	425	15,9	862,7	777	-4341	-3563	12,3	2026	-68,9	-981	-56,6	1045
350	400	375	13,0	875,7	580	-4964	-4383	7,6	2034	-64,7	-1046	-57,2	988
300	350	325	13,1	888,8	311	-5636	-5325	4,1	2038	-73,6	-1120	-69,5	918
250	300	275	12,1	900,9	-55	-6356	-6412	-0,7	2037	-76,6	-1196	-77,3	841
200	250	225	11,5	912,4	-494	-7055	-7550	-5,7	2032	-81,1	-1277	-86,8	754
150	200	175	8,6	921,0	-841	-7724	-8565	-7,2	2024	-66,3	-1344	-73,5	681
100	150	125	7,9	928,9	-1045	-8346	-9391	-8,2	2016	-65,7	-1409	-73,9	607
50	100	75	6,1	935,0	-1179	-8929	-10109	-7,2	2009	-54,2	-1464	-61,4	545
0	50	25	3,0	938,0	-1263	-9254	-10518	-3,8	2005	-27,7	-1491	-31,5	514

Síðujökull

Elevation (m a.s.l.)			ΔS (km^2)	∑ΔS (km^2)	b_w (mm)	b_s (mm)	b_n (mm)	ΔB_w ($10^6 m^3$)	$\sum\Delta B_w$ ($10^6 m^3$)	ΔB_s ($10^6 m^3$)	$\sum\Delta B_s$ ($10^6 m^3$)	ΔB_n ($10^6 m^3$)	$\sum B_n$ ($10^6 m^3$)
1700	1750	1725	0,7	0,7	3286	402	3688	2,5	3	0,3	0	2,8	3
1650	1700	1675	5,2	5,9	3118	266	3384	16,1	19	1,4	2	17,4	20
1600	1650	1625	11,1	17,0	2869	176	3045	31,9	51	2,0	4	33,9	54
1550	1600	1575	10,1	27,1	2798	58	2857	28,3	79	0,6	4	28,9	83
1500	1550	1525	20,1	47,2	2719	-63	2656	54,8	134	-1,3	3	53,5	137
1450	1500	1475	40,1	87,3	2607	-344	2262	104,5	238	-13,8	-11	90,7	227
1400	1450	1425	26,9	114,2	2491	-525	1965	66,9	305	-14,1	-25	52,8	280
1350	1400	1375	21,3	135,5	2443	-677	1765	52,1	357	-14,4	-39	37,7	318
1300	1350	1325	17,4	152,9	2411	-868	1543	42,0	399	-15,1	-55	26,9	345
1250	1300	1275	16,6	169,5	2366	-1089	1276	39,2	438	-18,0	-73	21,1	366
1200	1250	1225	21,2	190,7	2329	-1262	1066	49,3	488	-26,7	-99	22,6	388
1150	1200	1175	18,1	208,8	2253	-1500	753	40,8	528	-27,2	-127	13,6	402
1100	1150	1125	17,0	225,8	2175	-1915	260	37,0	566	-32,6	-159	4,4	406
1050	1100	1075	18,0	243,8	2066	-2170	-103	37,1	603	-39,0	-198	-1,9	405
1000	1050	1025	21,7	265,5	1890	-2399	-508	40,9	644	-51,9	-250	-11,0	394
950	1000	975	21,8	287,3	1686	-2805	-1119	36,7	680	-61,1	-311	-24,4	369
900	950	925	22,0	309,3	1537	-3122	-1585	33,9	714	-68,8	-380	-35,0	334
850	900	875	20,8	330,1	1434	-3299	-1865	29,8	744	-68,6	-449	-38,8	295
800	850	825	24,6	354,7	1343	-3465	-2122	33,1	777	-85,3	-534	-52,2	243
750	800	775	24,5	379,2	1250	-3660	-2410	30,6	808	-89,5	-623	-59,0	184
700	750	725	25,4	404,6	1140	-3964	-2824	29,0	837	-100,9	-724	-71,8	112
650	700	675	14,7	419,3	1048	-4254	-3205	15,4	852	-62,6	-787	-47,2	65
600	650	625	4,2	423,5	1010	-4424	-3414	4,2	856	-18,4	-805	-14,2	51

Skaftárjökull

Elevation (m a.s.l.)			ΔS (km^2)	∑ΔS (km^2)	b_w (mm)	b_s (mm)	b_n (mm)	ΔB_w ($10^6 m^3$)	$\sum\Delta B_w$ ($10^6 m^3$)	ΔB_s ($10^6 m^3$)	$\sum\Delta B_s$ ($10^6 m^3$)	ΔB_n ($10^6 m^3$)	$\sum B_n$ ($10^6 m^3$)
1350	1400	1375	2,4	2,4	2377	-684	1692	5,8	6	-1,7	-2	4,1	4
1300	1350	1325	5,5	7,9	2343	-871	1472	12,8	19	-4,8	-6	8,0	12
1250	1300	1275	4,5	12,4	2300	-1138	1161	10,4	29	-5,1	-12	5,2	17
1200	1250	1225	6,5	18,9	2247	-1364	882	14,5	43	-8,8	-20	5,7	23
1150	1200	1175	9,3	28,2	2171	-1657	514	20,1	64	-15,3	-36	4,8	28
1100	1150	1125	12,3	40,5	2073	-1995	77	25,4	89	-24,4	-60	1,0	29
1050	1100	1075	14,2	54,7	1939	-2240	-300	27,5	116	-31,7	-92	-4,3	25
1000	1050	1025	12,1	66,8	1757	-2508	-750	21,3	138	-30,3	-122	-9,1	15
950	1000	975	7,6	74,4	1577	-2858	-1281	12,0	150	-21,7	-144	-9,7	6
900	950	925	5,3	79,7	1419	-3190	-1771	7,5	157	-17,0	-161	-9,4	-4
850	900	875	5,6	85,3	1259	-3522	-2263	7,0	164	-19,6	-181	-12,6	-16
800	850	825	5,5	90,8	1098	-3756	-2657	6,0	170	-20,5	-201	-14,5	-31
750	800	775	5,0	95,8	951	-3878	-2927	4,8	175	-19,5	-221	-14,7	-46
700	750	725	3,3	99,1	790	-4039	-3248	2,6	178	-13,5	-234	-10,9	-56
650	700	675	1,2	100,3	675	-4203	-3527	0,8	178	-5,0	-239	-4,2	-61

Vestari Skaftárketill

Elevation (m a.s.l.)			ΔS (km^2)	∑ΔS (km^2)	b_w (mm)	b_s (mm)	b_n (mm)	ΔB_w ($10^6 m^3$)	$\sum\Delta B_w$ ($10^6 m^3$)	ΔB_s ($10^6 m^3$)	$\sum\Delta B_s$ ($10^6 m^3$)	ΔB_n ($10^6 m^3$)	$\sum B_n$ ($10^6 m^3$)
1900	1950	1925	0,7	0,7	2969	525	3494	2,0	2	0,4	0	2,4	2
1850	1900	1875	0,6	1,3	2930	514	3445	1,7	4	0,3	1	2,0	4
1800	1850	1825	0,7	2,0	3006	500	3506	2,3	6	0,4	1	2,6	7
1750	1800	1775	2,7	4,7	2972	458	3430	8,0	14	1,2	2	9,2	16
1700	1750	1725	5,9	10,6	2761	379	3140	16,2	30	2,2	5	18,4	35
1650	1700	1675	6,7	17,3	2627	234	2861	17,5	48	1,6	6	19,0	54
1600	1650	1625	7,4	24,7	2605	83	2688	19,3	67	0,6	7	20,0	74
1550	1600	1575	5,2	29,9	2573	-71	2501	13,3	80	-0,4	6	12,9	87
1500	1550	1525	1,5	31,4	2569	-119	2450	3,8	84	-0,2	6	3,6	90

Eystri Skaftárketill

Elevation (m a.s.l.)			ΔS (km^2)	∑ΔS (km^2)	b_w (mm)	b_s (mm)	b_n (mm)	ΔB_w ($10^6 m^3$)	$\sum\Delta B_w$ ($10^6 m^3$)	ΔB_s ($10^6 m^3$)	$\sum\Delta B_s$ ($10^6 m^3$)	ΔB_n ($10^6 m^3$)	$\sum B_n$ ($10^6 m^3$)
1750	1800	1775	1,1	1,1	2995	446	3442	3,3	3	0,5	1	3,8	4
1700	1750	1725	11,1	12,2	2859	346	3205	31,9	35	3,9	4	35,7	40
1650	1700	1675	16,2	28,4	2812	209	3021	45,5	81	3,4	8	48,9	88
1600	1650	1625	9,2	37,6	2706	140	2847	25,0	106	1,3	9	26,3	115
1550	1600	1575	2,2	39,8	2697	126	2823	6,0	112	0,3	9	6,2	121

Gjálp

Elevation (m a.s.l.)			ΔS (km^2)	∑ΔS (km^2)	b_w (mm)	b_s (mm)	b_n (mm)	ΔB_w ($10^6 m^3$)	$\sum\Delta B_w$ ($10^6 m^3$)	ΔB_s ($10^6 m^3$)	$\sum\Delta B_s$ ($10^6 m^3$)	ΔB_n ($10^6 m^3$)	$\sum B_n$ ($10^6 m^3$)
1900	1950	1925	0,5	0,5	2919	529	3449	1,6	2	0,3	0	1,9	2
1850	1900	1875	0,6	1,1	2822	514	3336	1,7	3	0,3	1	2,1	4
1800	1850	1825	1,2	2,3	3002	496	3498	3,5	7	0,6	1	4,1	8
1750	1800	1775	4,5	6,8	3043	456	3500	13,8	21	2,1	3	15,9	24
1700	1750	1725	15,9	22,7	3027	362	3390	48,3	69	5,8	9	54,0	78
1650	1700	1675	16,5	39,2	3079	273	3353	50,9	120	4,5	14	55,4	133
1600	1650	1625	0,0	39,2	3081	272	3353	0,0	120	0,0	14	0,0	134

Grímsvötn

Elevation (m a.s.l.)			ΔS (km^2)	∑ΔS (km^2)	b_w (mm)	b_s (mm)	b_n (mm)	ΔB_w ($10^6 m^3$)	$\sum\Delta B_w$ ($10^6 m^3$)	ΔB_s ($10^6 m^3$)	$\sum\Delta B_s$ ($10^6 m^3$)	ΔB_n ($10^6 m^3$)	$\sum B_n$ ($10^6 m^3$)
1700	1750	1725	0,8	0,8	3139	211	3351	2,6	3	0,2	0	2,7	3
1650	1700	1675	40,8	41,6	3111	37	3149	127,1	130	1,5	2	128,6	131
1600	1650	1625	30,6	72,2	3114	-186	2928	95,4	225	-5,7	-4	89,7	221
1550	1600	1575	18,6	90,8	3201	-470	2730	59,6	285	-8,8	-13	50,9	272
1500	1550	1525	16,9	107,7	3244	-686	2558	54,7	339	-11,6	-24	43,1	315
1450	1500	1475	11,6	119,3	3279	-820	2458	38,0	377	-9,5	-34	28,5	344
1400	1450	1425	15,1	134,4	3307	-920	2387	49,8	427	-13,9	-48	36,0	380
1350	1400	1375	0,6	135,0	3249	-614	2634	2,1	429	-0,4	-48	1,7	381

Appendix C: Coordinates at velocity measurement stakes in 2015.

Position of velocity measurement stakes determined by GPS sub-metre differential (I), fast static (FS) and kinematic (K).
(Accuracy of horizontal position 0.5 – 1.0 m, and vertical accuracy 1-2 m for DGPS, about 1cm for fast static, and 3 cm for kinematic).
The station Hofn in Höfn í Hornafirði is used as a stationary reference for all measurements, ÍSN93 datum, h_l is elevation above ellipsoid, dL antenna height, N estimated difference between ellipsoid and sea-level, H elevation in metres above sea level ($H= h_l+N+dL$). X and Y are ÍSN93 Lambert conformal conic projected coordinates. M is a quality marker.

Site	time	Date	Calender Day #	Year	Latitude	Longitude	h_l (m a. e.)	dL (m)	N (m)	H (m a. s. l.)	X	Y	M
B07u	11,159	13	5	133	2015	64 25,79416	16 17,44836	1425,9	0,0	-67,1	1358,9	630480,45	439241,53	K
B07u	18,741	22	10	295	2015	64 25,79338	16 17,44745	1423,1	0,0	-67,1	1356,0	630481,24	439240,10	K
B09v	16,404	11	5	131	2015	64 45,03855	16 5,47332	810,1	0,0	-66,7	743,4	638441,64	475386,82	K
B09v	12,423	24	10	297	2015	64 45,03856	16 5,47367	804,3	0,0	-66,7	737,7	638441,36	475386,83	K
B10u	15,961	11	5	131	2015	64 43,68705	16 6,69773	866,1	0,0	-66,7	799,4	637585,75	472833,83	K
B10u	15,953	24	10	297	2015	64 43,68706	16 6,69786	861,4	0,0	-66,7	794,7	637585,65	472833,84	K
B11e	13,250	11	5	131	2015	64 40,94122	16 10,48847	1027,0	0,0	-66,8	960,2	634806,21	467601,16	K
B11e	10,805	24	10	297	2015	64 40,94355	16 10,48683	1023,5	0,0	-66,8	956,7	634807,32	467605,54	K
B12u	11,989	11	5	131	2015	64 38,26539	16 14,13168	1145,2	0,0	-66,9	1078,4	632128,11	462506,13	K
B12u	10,257	24	10	297	2015	64 38,27267	16 14,12485	1142,9	0,0	-66,9	1076,0	632132,95	462519,87	K
B13u	10,439	11	5	131	2015	64 34,53442	16 19,71437	1283,5	0,0	-67,0	1216,5	627976,57	455389,00	K
B13u	18,614	23	10	296	2015	64 34,54379	16 19,70328	1281,2	0,0	-67,0	1214,2	627984,68	455406,76	K
B13rora	10,665	24	10	297	2015	64 34,54197	16 19,71213	1281,5	0,0	-67,0	1214,5	627977,76	455403,07	K
B14x	18,264	10	5	130	2015	64 31,63485	16 24,70572	1384,8	0,0	-67,1	1317,7	624214,11	449840,33	K
B14x	18,505	23	10	296	2015	64 31,64238	16 24,69259	1382,3	0,0	-67,1	1315,2	624224,03	449854,73	K
B15j	17,537	10	5	130	2015	64 28,48609	16 30,01278	1469,0	0,0	-67,2	1401,8	620202,72	443823,70	K
B15j	17,750	23	10	296	2015	64 28,49077	16 30,00102	1466,4	0,0	-67,2	1399,2	620211,79	443832,75	K
B16x	16,326	10	5	130	2015	64 24,12221	16 40,85031	1595,2	0,0	-67,3	1527,8	611818,74	435390,01	K
B16x	10,741	28	10	301	2015	64 24,12251	16 40,84948	1593,5	0,0	-67,3	1526,2	611819,39	435390,60	K
B17u	19,546	10	5	130	2015	64 36,73635	16 28,78873	1281,5	0,0	-67,1	1214,3	620572,25	459179,41	K
B17u	19,593	23	10	296	2015	64 36,74364	16 28,78375	1279,7	0,0	-67,1	1212,5	620575,68	459193,09	K
B18s	10,689	12	5	132	2015	64 31,58477	16 0,12112	1381,2	0,0	-66,9	1314,3	643869,09	450616,16	K
B18s	20,348	22	10	295	2015	64 31,59057	16 0,12564	1379,7	0,0	-66,9	1312,8	643865,00	450626,80	K
B19s	22,097	12	5	132	2015	64 27,93218	15 55,16820	1498,8	0,0	-66,9	1432,0	648157,96	444028,18	K
B19s	20,154	22	10	295	2015	64 27,93177	15 55,16705	1495,8	0,0	-66,9	1428,9	648158,93	444027,46	K
BB0t	10,109	13	5	133	2015	64 22,71816	16 5,04617	1588,1	0,0	-66,9	1521,3	640692,42	433975,29	K
BB0t	18,747	22	10	295	2015	64 22,71822	16 5,04783	1584,1	0,0	-66,9	1517,3	640691,07	433975,34	K
BB10	12,000	27	5	147	1998	64 29,84449	17 39,02107	1643,4	-0,8	-61,8	1580,8	564856,30	444663,10	P
Baf15-02	14,440	10	6	161	2015	64 37,24343	17 25,99534	1942,9	0,0	-67,9	1875,0	574945,90	458646,66	K
Baf15-02	12,739	26	10	299	2015	64 37,24339	17 25,99003	1943,1	0,0	-67,9	1875,2	574950,14	458646,68	K
Baf15-03	15,943	10	6	161	2015	64 38,00043	17 23,98234	1910,7	0,0	-67,9	1842,8	576514,84	460092,91	K
Baf15-03	16,018	26	10	299	2015	64 37,99998	17 23,97721	1912,0	0,0	-67,9	1844,1	576518,94	460092,18	K
Barc-b	12,119	10	5	130	2015	64 38,40957	17 26,76607	1940,0	0,0	-67,9	1872,2	574278,30	460797,53	K
Barc-c	14,264	4	6	155	2015	64 38,40953	17 26,76414	1942,7	0,0	-67,9	1874,9	574279,84	460797,49	K
BBs01a	10,562	10	5	130	2015	64 36,94568	17 26,21274	1956,9	0,0	-67,9	1889,0	574786,28	458089,33	K
BBs01a	12,365	4	6	155	2015	64 36,94561	17 26,21132	1959,2	0,0	-67,9	1891,4	574787,42	458089,21	K
BBs01a	18,482	26	10	299	2015	64 36,94608	17 26,20591	1957,5	0,0	-67,9	1889,6	574791,71	458090,21	K
BBs02a	11,150	10	5	130	2015	64 37,59063	17 26,15623	1936,6	0,0	-67,9	1868,8	574801,70	459288,39	K
BBs02a	19,748	4	6	155	2015	64 37,59050	17 26,15447	1939,3	0,0	-67,9	1871,4	574803,10	459288,17	K
BBs02a	12,847	26	10	299	2015	64 37,59091	17 26,14821	1939,0	0,0	-67,9	1871,1	574808,07	459289,05	K
BBs03a	11,269	10	5	130	2015	64 38,42411	17 26,14777	1931,9	0,0	-67,9	1864,1	574770,13	460836,69	K
BBs03a	19,247	4	6	155	2015	64 38,42375	17 26,14582	1935,0	0,0	-67,9	1867,2	574771,69	460836,06	K
BBs03a	15,502	26	10	299	2015	64 38,42285	17 26,13777	1936,0	0,0	-67,9	1868,2	574778,15	460834,53	K
BBs04a	11,919	10	5	130	2015	64 39,11983	17 26,16193	1942,3	0,0	-67,9	1874,5	574726,87	462128,64	K
BBs04a	19,577	4	6	155	2015	64 39,11942	17 26,16030	1945,1	0,0	-67,9	1877,2	574728,19	462127,93	K
BBs04a	18,054	26	10	299	2015	64 39,11869	17 26,15339	1944,7	0,0	-67,9	1876,8	574733,72	462126,69	K

BBs05a	11,784	10	5	130	2015	64	39,57832	17	26,13510	1969,6	0,0	-67,9	1901,7	574727,15	462980,79	K
BBs05a	19,455	4	6	155	2015	64	39,57789	17	26,13364	1971,6	0,0	-67,9	1903,8	574728,34	462980,03	K
BBs05a	17,865	26	10	299	2015	64	39,57741	17	26,12769	1967,9	0,0	-67,9	1900,0	574733,09	462979,26	K
BBs06a	11,377	10	5	130	2015	64	38,44600	17	24,61173	1913,1	0,0	-67,9	1845,3	575992,57	460907,86	K
BBs06a	19,369	4	6	155	2015	64	38,44562	17	24,61054	1916,0	0,0	-67,9	1848,2	575993,55	460907,19	K
BBs06a	15,683	26	10	299	2015	64	38,44523	17	24,60573	1916,9	0,0	-67,9	1849,1	575997,40	460906,56	K
BBs07a	11,541	10	5	130	2015	64	38,46438	17	23,23316	1928,5	0,0	-67,9	1860,6	577089,73	460969,82	K
BBs07a	18,608	4	6	155	2015	64	38,46401	17	23,23236	1930,8	0,0	-67,9	1863,0	577090,38	460969,15	K
BBs07a	16,241	26	10	299	2015	64	38,46563	17	23,22937	1928,7	0,0	-67,9	1860,9	577092,70	460972,20	K
BBs08a	11,698	10	5	130	2015	64	39,03870	17	23,20620	1942,7	0,0	-67,8	1874,9	577083,97	462037,10	K
BBs08a	18,757	4	6	155	2015	64	39,03850	17	23,20480	1945,0	0,0	-67,8	1877,2	577085,10	462036,76	K
BBs08a	17,639	26	10	299	2015	64	39,03883	17	23,20057	1941,4	0,0	-67,8	1873,6	577088,45	462037,47	K
BBs09a	11,016	10	5	130	2015	64	37,12836	17	23,75551	1918,7	0,0	-67,9	1850,9	576736,67	458477,72	K
BBs09a	19,872	4	6	155	2015	64	37,12758	17	23,75374	1920,1	0,0	-67,9	1852,3	576738,12	458476,30	K
BBs10a	12,219	10	5	130	2015	64	38,46092	17	28,58483	1967,2	0,0	-67,9	1899,3	572827,30	460857,63	K
BBs10a	15,957	4	6	155	2015	64	38,46055	17	28,58287	1969,7	0,0	-67,9	1901,8	572828,88	460856,98	K
BBs10a	14,315	26	10	299	2015	64	38,45956	17	28,57450	1968,6	0,0	-67,9	1900,7	572835,59	460855,30	K
BBs11a	12,333	10	5	130	2015	64	38,87474	17	29,92009	2006,1	0,0	-67,9	1938,2	571745,49	461600,84	K
BBs11a	14,917	4	6	155	2015	64	38,87444	17	29,91885	2005,5	0,0	-67,9	1937,6	571746,49	461600,31	K
BBs11a	14,176	26	10	299	2015	64	38,87323	17	29,91142	2003,3	0,0	-67,9	1935,4	571752,46	461598,21	K
BBs12a	12,543	10	5	130	2015	64	37,55404	17	28,81235	1970,8	0,0	-67,9	1902,9	572686,58	459168,77	K
BBs12a	16,130	4	6	155	2015	64	37,55380	17	28,81097	1973,0	0,0	-67,9	1905,1	572687,70	459168,36	K
BBs12a	13,007	26	10	299	2015	64	37,55350	17	28,80532	1971,3	0,0	-67,9	1903,4	572692,21	459167,92	K
BBs13a	12,819	10	5	130	2015	64	37,26546	17	30,53509	1986,9	0,0	-67,9	1919,0	571326,28	458600,05	K
BBs13a	15,417	4	6	155	2015	64	37,26522	17	30,53492	1986,9	0,0	-67,9	1916,1	571326,42	458599,59	K
BBth01	11,390	7	6	158	2015	64	33,46345	17	16,54235	1713,7	0,0	-67,8	1645,9	582672,12	451822,25	K
BBth02	11,544	7	6	158	2015	64	33,51497	17	18,02698	1739,8	0,0	-67,8	1672,1	581483,48	451885,82	K
BBth03	11,784	7	6	158	2015	64	33,60271	17	20,11217	1768,3	0,0	-67,8	1700,5	579813,37	452004,44	K
BBth04	11,939	7	6	158	2015	64	33,98634	17	21,41481	1785,1	0,0	-67,8	1717,3	578754,23	452689,76	K
BBth05	12,132	7	6	158	2015	64	33,96863	17	24,97401	1827,4	0,0	-67,8	1759,5	575912,41	452584,30	K
BBth06	12,359	7	6	158	2015	64	36,65787	17	27,51429	1978,6	0,0	-67,9	1910,7	573761,67	457529,24	K
BBth07	12,557	7	6	158	2015	64	36,09840	17	27,52397	1981,2	0,0	-67,9	1913,3	573779,29	456489,88	K
BBth08	12,732	7	6	158	2015	64	37,16217	17	29,56078	1981,8	0,0	-67,9	1914,0	572107,48	458426,61	K
BBth09	12,903	7	6	158	2015	64	36,50736	17	30,56144	1980,0	0,0	-67,9	1912,1	571338,48	457191,40	K
BBth10	13,130	7	6	158	2015	64	35,98105	17	30,92354	1961,0	0,0	-67,9	1893,1	571072,68	456206,99	K
BBth11	13,279	7	6	158	2015	64	36,07586	17	31,41549	1963,0	0,0	-67,9	1895,1	570676,12	456373,89	K
BBth12	13,511	7	6	158	2015	64	36,55801	17	34,54302	1964,3	0,0	-67,9	1896,4	568161,10	457212,25	K
BBth13	13,759	7	6	158	2015	64	37,23420	17	32,63153	1996,4	0,0	-67,9	1928,5	569656,52	458503,02	K
BBth14	13,976	7	6	158	2015	64	38,17677	17	32,57030	2025,3	0,0	-67,9	1957,4	569664,96	460254,97	K
BBth15	14,139	7	6	158	2015	64	38,07818	17	30,51753	1995,5	0,0	-67,9	1927,6	571304,65	460109,99	K
BBth16	14,361	7	6	158	2015	64	39,13895	17	30,53941	2016,8	0,0	-67,9	1948,9	571240,73	462079,94	K
BBth17	14,544	7	6	158	2015	64	38,55532	17	28,79938	1974,2	0,0	-67,9	1906,4	572652,20	461028,87	K
BBth18	15,346	7	6	158	2015	64	39,53910	17	26,70679	1971,7	0,0	-67,9	1903,9	574273,90	462896,72	K
BBth19	15,569	7	6	158	2015	64	39,10424	17	22,87798	1936,8	0,0	-67,8	1868,9	577342,18	462165,53	K
BBth20	15,730	7	6	158	2015	64	38,95121	17	23,52102	1940,9	0,0	-67,9	1873,1	576837,45	461868,22	K
BBth21	15,907	7	6	158	2015	64	38,68147	17	24,76945	1918,3	0,0	-67,9	1850,4	575855,97	461342,07	K
BBth22	16,059	7	6	158	2015	64	38,41839	17	25,63790	1926,2	0,0	-67,9	1858,3	575176,51	460836,12	K
BBth23	16,330	7	6	158	2015	64	37,67900	17	27,56746	1953,8	0,0	-67,9	1886,0	573673,05	459424,91	K
BBth24	16,661	7	6	158	2015	64	37,17276	17	24,58148	1937,6	0,0	-67,9	1869,7	576076,18	458543,53	K
BBth25	16,909	7	6	158	2015	64	38,00184	17	21,40752	1883,8	0,0	-67,8	1816,0	578566,14	460148,17	K
BBth26	17,148	7	6	158	2015	64	37,61537	17	20,54231	1848,9	0,0	-67,8	1781,0	579274,28	459448,35	K
BBth27	17,455	7	6	158	2015	64	36,73985	17	17,97559	1728,9	0,0	-67,8	1661,1	581363,39	457876,57	K
BBth28	17,696	7	6	158	2015	64	35,05556	17	16,31729	1678,7	0,0	-67,7	1611,0	582771,07	454784,19	K
BBth29	15,465	10	6	161	2015	64	35,05646	17	20,40528	1787,3	0,0	-67,8	1719,5	579508,30	454698,42	K
BBth30	16,198	10	6	161	2015	64	39,98922	17	14,59806	1565,8	0,0	-67,7	1498,1	583888,50	463985,21	K
BBth31	16,343	10	6	161	2015	64	42,04105	17	15,21536	1529,8	0,0	-67,6	1462,2	583292,02	467782,44	K
BBth32	16,638	10	6	161	2015	64	43,10742	17	19,93544	1570,0	0,0	-67,7	1502,4	579488,71	469661,75	K
BBth33	16,980	10	6	161	2015	64	41,58532	17	24,75406	1721,8	0,0	-67,8	1653,9	575732,76	466736,02	K
BBth34	17,230	10	6	161	2015	64	42,05336	17	21,31144	1625,7	0,0	-67,8	1558,0	578446,85	467675,34	K
BBth35	17,500	10	6	161	2015	64	40,98873	17	18,10609	1605,2	0,0	-67,7	1537,5	581047,30	465765,33	K

BBth36	18,251	10	6	161	2015	64	39,93335	17	20,89302	1770,3	0,0	-67,8	1702,5	578882,29	463746,37	K
BBth37	19,105	10	6	161	2015	64	35,83747	17	23,64279	1898,2	0,0	-67,8	1830,4	576887,44	456082,30	K
BBth38	19,554	10	6	161	2015	64	35,10291	17	23,67624	1849,5	0,0	-67,8	1781,6	576895,41	454717,25	K
BBth39	19,762	10	6	161	2015	64	35,56981	17	27,62782	1901,3	0,0	-67,9	1833,5	573720,37	455506,02	K
BBth40	19,955	10	6	161	2015	64	35,17402	17	27,66372	1863,8	0,0	-67,9	1795,9	573709,63	454770,17	K
BBth41	20,197	10	6	161	2015	64	34,11810	17	27,69594	1827,9	0,0	-67,9	1760,0	573731,65	452808,24	K
BBth42	20,512	10	6	161	2015	64	35,54774	17	31,73646	1922,7	0,0	-67,9	1854,8	570442,91	455386,95	K
BBth43	20,675	10	6	161	2015	64	34,94395	17	32,82432	1826,0	0,0	-67,9	1758,2	569600,63	454245,33	K
BBth44	20,841	10	6	161	2015	64	34,69901	17	34,55456	1789,1	0,0	-67,8	1721,3	568229,70	453758,91	K
BBth45	21,032	10	6	161	2015	64	34,07272	17	36,02425	1742,1	0,0	-67,8	1674,3	567082,08	452569,35	K
BBth46	21,189	10	6	161	2015	64	33,58608	17	38,45586	1685,0	0,0	-67,8	1617,2	565159,39	451623,01	K
BBth47	21,630	10	6	161	2015	64	32,91049	17	27,80362	1801,6	0,0	-67,8	1733,7	573700,19	450563,07	K
BBth48	13,197	12	6	163	2015	64	39,88481	17	30,46323	2035,5	0,0	-67,9	1967,6	571268,68	463466,79	K
BBth49	13,833	12	6	163	2015	64	39,19887	17	32,47800	2067,1	0,0	-67,9	1999,2	569694,68	462155,22	K
BBth50	16,789	12	6	163	2015	64	39,43393	17	35,27352	1616,9	0,0	-67,9	1549,1	567459,19	462541,30	K
Boraj	18,907	2	6	153	2015	64	24,94475	17	20,15923	1472,8	0,0	-67,7	1405,1	580199,15	435922,56	K
Boraj	14,615	25	10	298	2015	64	24,94347	17	20,15991	1471,0	0,0	-67,7	1403,3	580198,67	435920,18	K
BORTHNb	11,857	5	2	36	2015	64	25,07689	17	19,15644	1497,1	-2,7	-67,7	1426,7	580997,94	436189,29	K
BORTHNb	13,880	25	10	298	2015	64	25,07165	17	19,16093	1474,9	0,0	-67,7	1407,2	580994,61	436179,47	K
Br1j	16,083	15	4	105	2015	64	5,55587	16	19,49749	157,4	-1,7	-65,8	89,9	630427,30	401601,97	K
Br1k	17,679	15	4	105	2015	64	5,73743	16	19,69708	198,0	-1,7	-65,9	130,5	630250,96	401932,17	K
Br2k	15,326	15	4	105	2015	64	6,38482	16	22,54074	291,8	-1,7	-66,0	224,1	627891,82	403037,21	K
Br3q	14,523	15	4	105	2015	64	8,48956	16	24,07430	463,9	-1,7	-66,3	395,9	626486,21	406893,17	K
Br4d	13,514	15	4	105	2015	64	10,57340	16	20,24785	574,7	-1,7	-66,3	506,7	629425,37	410890,75	K
Br4e	13,699	15	4	105	2015	64	10,56907	16	20,24269	574,4	-1,7	-66,3	506,4	629429,89	410882,89	K
Br7s	11,991	13	5	133	2015	64	22,14325	16	16,93905	1314,7	0,0	-67,0	1247,7	631180,54	432481,94	K
Br7s	18,315	22	10	295	2015	64	22,11632	16	16,93210	1310,7	0,0	-67,0	1243,7	631188,28	432432,19	K
Brut	18,540	11	5	131	2015	64	41,00406	15	55,22618	833,9	0,0	-66,7	767,2	646928,85	468284,60	K
Brut	16,153	23	10	296	2015	64	41,00414	15	55,22590	827,7	0,0	-66,7	761,0	646929,07	468284,77	K
Budt	8,821	12	5	132	2015	64	35,98889	15	59,87549	1204,4	0,0	-66,9	1137,5	643676,95	458799,10	K
Budt	16,639	23	10	296	2015	64	35,99967	15	59,87293	1201,1	0,0	-66,9	1134,2	643678,04	458819,20	K
D05s	11,941	10	5	130	2015	64	42,24929	16	54,65341	1270,2	0,0	-67,4	1202,9	599618,22	468664,95	K
D05s	15,871	24	10	297	2015	64	42,25558	16	54,64422	1267,8	0,0	-67,3	1200,4	599625,13	468676,88	K
D07s	10,832	10	5	130	2015	64	38,29460	16	59,23677	1440,5	0,0	-67,5	1373,0	596210,78	461202,68	K
D07s	15,284	24	10	297	2015	64	38,30513	16	59,22726	1438,2	0,0	-67,5	1370,7	596217,73	461222,48	K
D09r	9,675	10	5	130	2015	64	31,81257	17	0,55283	1650,8	0,0	-67,6	1583,2	595541,85	449131,88	K
D09r	14,662	24	10	297	2015	64	31,81592	17	0,55411	1649,1	0,0	-67,6	1581,6	595540,63	449138,07	K
D12s	20,250	9	5	129	2015	64	28,97246	17	0,16611	1717,2	0,0	-67,6	1649,7	596017,75	443867,36	K
D12s	13,941	24	10	297	2015	64	28,97288	17	0,16598	1714,8	0,0	-67,6	1647,2	596017,83	443868,14	K
E01t	14,683	12	5	132	2015	64	41,05450	15	34,11475	775,0	0,0	-66,7	708,3	663695,56	469242,64	K
E01t	13,973	23	10	296	2015	64	41,05424	15	34,11538	769,1	0,0	-66,7	702,4	663695,08	469242,14	K
E02t	15,389	12	5	132	2015	64	39,13767	15	35,97370	1020,9	0,0	-66,8	954,1	662410,45	465606,46	K
E02t	10,683	23	10	296	2015	64	39,14695	15	35,97032	1017,3	0,0	-66,8	950,5	662412,21	465623,82	K
E03u	16,339	12	5	132	2015	64	36,66391	15	36,91831	1256,0	0,0	-66,9	1189,2	661905,20	460976,45	K
E03u	10,221	23	10	296	2015	64	36,66930	15	36,92098	1252,1	0,0	-66,9	1185,2	661902,54	460986,34	K
E04t	17,111	12	5	132	2015	64	34,95203	15	37,09281	1357,3	0,0	-66,8	1290,5	661936,28	457792,90	K
E04t	9,865	23	10	296	2015	64	34,95296	15	37,09244	1353,2	0,0	-66,8	1286,4	661936,48	457794,63	K
Fl01f	9,105	13	5	133	2015	64	26,16841	15	55,63035	1415,3	0,0	-66,8	1348,5	647947,04	440736,93	K
Fl01f	19,668	22	10	295	2015	64	26,16191	15	55,61507	1410,9	0,0	-66,8	1344,1	647959,87	440725,47	K
G02l	11,294	4	6	155	2015	64	26,84971	17	17,72319	1633,2	0,0	-67,7	1565,5	582060,06	439512,83	K
G02l	15,087	25	10	298	2015	64	26,84689	17	17,72624	1628,9	0,0	-67,7	1561,2	582057,76	439507,53	K
G03m	11,475	4	6	155	2015	64	28,44310	17	16,33972	1727,6	0,0	-67,7	1659,8	583088,89	442502,36	K
G03m	15,626	25	10	298	2015	64	28,44162	17	16,34095	1723,5	0,0	-67,7	1655,7	583087,98	442499,59	K
G04t	11,677	4	6	155	2015	64	30,00217	17	15,00141	1757,1	0,0	-67,7	1689,4	584081,16	445427,52	K
G04t	13,301	25	10	298	2015	64	30,00291	17	15,00100	1753,6	0,0	-67,7	1685,9	584081,45	445428,89	K
gb2e	9,812	12	5	132	2015	64	34,10379	16	0,01906	1270,2	0,0	-66,9	1203,3	643728,65	455295,10	K
gb2e	9,558	23	10	296	2015	64	34,11227	16	0,02085	1267,2	0,0	-66,9	1200,3	643726,48	455310,78	K
Go1s	12,130	4	6	155	2015	64	33,98681	17	24,98493	1827,7	0,0	-67,8	1759,9	575902,85	452617,84	K
HAABo	11,418	5	6	156	2015	64	20,96587	17	24,11268	1801,1	0,0	-67,5	1733,5	577211,02	428450,21	K
HAABo	18,893	25	10	298	2015	64	20,96622	17	24,11319	1796,4	0,0	-67,5	1728,9	577210,60	428450,85	K

Hof01m	18,647	12	5	132	2015	64	32,31340	15	35,83751	1208,6	0,0	-66,7	1141,9	663200,91	452951,20	K
Hof01m	10,968	23	10	296	2015	64	32,30599	15	35,83764	1204,3	0,0	-66,7	1137,7	663201,54	452937,43	K
K01v	14,769	9	5	129	2015	64	35,16528	17	51,79174	1127,7	0,0	-67,6	1060,1	554451,60	454346,31	K
K01v	11,069	26	10	299	2015	64	35,16639	17	51,79694	1123,9	0,0	-67,6	1056,3	554447,41	454348,30	K
K02x	15,589	9	5	129	2015	64	34,81078	17	49,67676	1245,9	0,0	-67,6	1178,3	556152,04	453718,59	K
K02x	10,532	26	10	299	2015	64	34,81329	17	49,68103	1242,3	0,0	-67,6	1174,7	556148,54	453723,20	K
K03v	16,326	9	5	129	2015	64	34,24783	17	46,39480	1364,5	0,0	-67,7	1296,9	558792,61	452722,55	K
K03v	10,412	26	10	299	2015	64	34,24975	17	46,40777	1361,6	0,0	-67,7	1294,0	558782,18	452725,91	K
K04x	17,259	9	5	129	2015	64	33,20902	17	42,25921	1555,8	0,0	-67,7	1488,1	562135,04	450858,76	K
K04x	11,458	26	10	299	2015	64	33,21230	17	42,28113	1552,6	0,0	-67,7	1484,9	562117,40	450864,49	K
K05x	18,165	9	5	129	2015	64	33,44931	17	35,42628	1749,6	0,0	-67,8	1681,8	567585,50	451421,95	K
K05x	11,665	26	10	299	2015	64	33,44673	17	35,44077	1747,3	0,0	-67,8	1679,5	567574,03	451416,90	K
K06v	17,725	4	6	155	2015	64	38,35627	17	31,36516	2021,8	0,0	-67,9	1953,9	570617,26	460610,67	K
K06v	13,536	26	10	299	2015	64	38,35558	17	31,35953	2016,7	0,0	-67,9	1948,8	570621,77	460609,50	K
K07r	12,826	9	5	129	2015	64	29,12145	17	42,03744	1602,3	0,0	-67,7	1534,6	562468,36	443269,31	K
K07r	10,111	26	10	299	2015	64	29,12162	17	42,04007	1599,3	0,0	-67,7	1531,6	562466,24	443269,58	K
Ln1-1c	15,222	5	6	156	2015	64	24,49850	17	13,00252	1571,7	0,0	-67,6	1504,0	585969,84	435250,50	K
Ln1-1c	12,389	25	10	298	2015	64	24,49729	17	13,00404	1568,2	-1,0	-67,6	1499,6	585968,69	435248,22	K
Ln1-2c	15,116	5	6	156	2015	64	24,74378	17	12,01857	1595,1	0,0	-67,6	1527,4	586747,23	435728,46	K
Ln1-2c	12,653	25	10	298	2015	64	24,74115	17	12,01931	1591,0	-1,0	-67,6	1522,4	586746,78	435723,55	K
Ln1-3c	15,021	5	6	156	2015	64	24,99311	17	11,00078	1600,7	0,0	-67,6	1533,1	587551,34	436214,91	K
Ln1-3c	12,741	25	10	298	2015	64	24,99074	17	11,00238	1597,1	-1,0	-67,6	1528,5	587550,19	436210,47	K
Ln1-4c	14,914	5	6	156	2015	64	25,24086	17	10,01627	1627,0	0,0	-67,6	1559,3	588328,56	436697,86	K
Ln1-4c	12,858	25	10	298	2015	64	25,23825	17	10,01868	1623,2	-1,0	-67,6	1554,6	588326,77	436692,95	K
Ln1-5c	14,769	5	6	156	2015	64	25,74291	17	8,00462	1667,0	0,0	-67,6	1599,4	589916,13	437677,54	K
Ln1-5c	12,987	25	10	298	2015	64	25,73997	17	8,00456	1663,7	-1,0	-67,6	1595,1	589916,34	437672,07	K
S01k	18,364	7	5	127	2015	64	6,99873	17	49,96156	802,9	0,0	-66,8	736,0	556878,78	402048,09	K
S01k	16,051	26	10	299	2015	64	6,99848	17	49,96097	797,7	0,0	-66,8	730,8	556879,27	402047,64	K
S02n	19,294	7	5	127	2015	64	12,16639	17	48,95431	1076,7	0,0	-67,1	1009,6	557516,85	411663,32	K
S02n	15,669	26	10	299	2015	64	12,15794	17	48,95786	1072,1	0,0	-67,1	1005,0	557514,27	411647,58	K
S04o	17,159	7	5	127	2015	64	16,18013	17	48,20573	1227,2	0,0	-67,2	1160,0	557981,66	419131,01	K
S04o	15,339	26	10	299	2015	64	16,16828	17	48,21802	1223,9	0,0	-67,2	1156,7	557972,15	419108,82	K
Skf01f	13,425	13	5	133	2015	64	17,99550	16	5,00522	1351,2	0,0	-66,6	1284,6	641130,01	425211,41	K
Skf01f	17,715	22	10	295	2015	64	17,99295	16	4,98861	1346,7	0,0	-66,6	1280,0	641143,61	425207,29	K
T01np	9,165	7	5	127	2015	64	19,48657	18	8,22771	805,8	0,0	-67,3	738,5	541729,09	425010,47	K
T01np	17,284	26	10	299	2015	64	19,48633	18	8,22699	799,2	0,0	-67,3	731,9	541729,67	425010,03	K
T02nr	10,500	7	5	127	2015	64	19,59837	18	3,96214	1006,5	0,0	-67,3	939,3	545163,88	425267,03	K
T02nr	17,672	26	10	299	2015	64	19,59854	18	3,96698	1001,2	0,0	-67,3	933,9	545159,97	425267,29	K
T03nr	13,487	7	5	127	2015	64	20,20657	17	58,58444	1143,4	0,0	-67,3	1076,1	549479,39	426464,02	K
T03nr	16,312	27	10	300	2015	64	20,20534	17	58,59194	1139,7	0,0	-67,3	1072,4	549473,39	426461,63	K
T04nr	14,519	7	5	127	2015	64	21,33168	17	51,48294	1290,6	0,0	-67,4	1223,3	555162,36	428652,14	K
T04nr	15,551	27	10	300	2015	64	21,32824	17	51,49477	1287,2	0,0	-67,4	1219,9	555152,95	428645,57	K
T05nr	20,219	7	5	127	2015	64	22,28122	17	42,98271	1412,6	0,0	-67,5	1345,1	561969,09	430547,31	K
T05nr	14,773	27	10	300	2015	64	22,27808	17	42,99423	1409,8	0,0	-67,5	1342,4	561959,95	430541,30	K
T05rorf	14,848	27	10	300	2015	64	22,27825	17	43,04498	1409,2	2,9	-67,5	1344,6	561919,11	430540,77	K
T05rorg	14,848	27	10	300	2015	64	22,27825	17	43,04498	1409,2	3,5	-67,5	1345,2	561919,11	430540,77	K
T06nr	20,952	8	5	128	2015	64	24,27015	17	36,52696	1534,6	0,0	-67,6	1467,0	567081,35	434351,74	K
T06nr	12,709	27	10	300	2015	64	24,26624	17	36,53849	1532,7	0,0	-67,6	1465,1	567072,25	434344,28	K
T07nq	10,172	9	5	129	2015	64	25,28995	17	31,19993	1631,6	0,0	-67,7	1563,9	571317,19	436343,24	K
T07nq	17,440	25	10	298	2015	64	25,28778	17	31,20874	1628,7	0,0	-67,7	1561,0	571310,21	436339,03	K
T08nr	11,107	9	5	129	2015	64	26,29155	17	27,75127	1705,3	0,0	-67,8	1637,5	574041,09	438269,75	K
T08nr	16,609	25	10	298	2015	64	26,29114	17	27,75271	1702,7	0,0	-67,8	1634,9	574039,95	438268,96	K

Appendix D: Measured surface velocity on Vatnajökull in 2015.

Site	Calendar day date	#	Calendar day date	#	# of days	translation (m)	(°)	velocity (cm/day)	(m/annum)
B07u	150513	133	151022	295	162	1,62	153	1,00	3,65
B09v	150511	131	151024	297	166	0,28	274	0,17	0,61
B10u	141012	285	150511	131	211	0,74	109	0,35	1,28
B10u	150511	131	151024	297	166	0,10	280	0,06	0,23
B11e	150511	131	151024	297	166	4,51	17	2,72	9,91
B12u	150511	131	151024	297	166	14,54	22	8,76	31,97
B13u	150511	131	151023	296	165	19,48	27	11,81	43,09
B13rora	131003	276	151024	297	751	49,87	27	6,64	24,24
B14x	150510	130	151023	296	166	17,46	37	10,52	38,38
B15j	150510	130	151023	296	166	12,80	47	7,71	28,15
B16x	150510	130	151028	301	171	0,87	50	0,51	1,85
B17u	150510	130	151023	296	166	14,07	16	8,48	30,94
B18s	150512	132	151022	295	163	11,33	341	6,95	25,38
B19s	150512	132	151022	295	163	1,19	129	0,73	2,67
BB0t	150513	133	151022	295	162	1,34	275	0,83	3,02
Baf15-02	150610	161	151026	299	138	4,23	91	3,07	11,19
Baf15-03	150610	161	151026	299	138	4,17	102	3,02	11,03
BBs01a	150510	130	150604	155	25	1,14	97	4,56	16,63
BBs01a	150604	155	151026	299	144	4,40	79	3,06	11,15
BBs02a	150510	130	150604	155	25	1,42	100	5,69	20,77
BBs02a	150604	155	151026	299	144	5,05	81	3,50	12,79
BBs03a	150510	130	150604	155	25	1,69	113	6,76	24,67
BBs03a	150604	155	151026	299	144	6,62	105	4,60	16,79
BBs04a	150510	130	150604	155	25	1,50	120	6,01	21,95
BBs04a	150604	155	151026	299	144	5,66	104	3,93	14,36
BBs05a	150510	130	150604	155	25	1,41	124	5,63	20,57
BBs05a	150604	155	151026	299	144	4,82	101	3,35	12,21
BBs06a	150510	130	150604	155	25	1,18	127	4,72	17,23
BBs06a	150604	155	151026	299	144	3,90	101	2,71	9,88
BBs07a	150510	130	150604	155	25	0,94	137	3,74	13,66
BBs07a	150604	155	151026	299	144	3,83	38	2,66	9,71
BBs08a	150510	130	150604	155	25	1,17	108	4,70	17,15
BBs08a	150604	155	151026	299	144	3,42	80	2,38	8,68
BBs09a	150510	130	150604	155	25	2,02	136	8,08	29,48
BBs10a	150510	130	150604	155	25	1,70	114	6,82	24,89
BBs10a	150604	155	151026	299	144	6,91	105	4,80	17,52
BBs11a	150510	130	150604	155	25	1,13	119	4,53	16,54
BBs11a	150604	155	151026	299	144	6,33	111	4,39	16,03
BBs12a	150510	130	150604	155	25	1,19	112	4,74	17,32
BBs12a	150604	155	151026	299	144	4,54	97	3,15	11,50
BBs13a	150510	130	150604	155	25	0,46	163	1,86	6,78
Boraj	150602	153	151025	298	145	2,43	193	1,68	6,12
BORTHNb	141015	288	150205	36	113	10,76	187	9,52	34,75
BORTHNb	150205	36	151025	298	262	10,35	200	3,95	14,42

Br1j	140906	249	150415	105	221	2,75	139	1,25	4,55
Br2k	140906	249	150415	105	221	6,90	177	3,12	11,39
Br4d	140507	127	150415	105	343	296,10	182	86,33	315,09
Br7s	150513	133	151022	295	162	50,19	174	30,98	113,08
Brut	150511	131	151023	296	165	0,27	56	0,16	0,59
Budt	150512	132	151023	296	164	20,07	6	12,24	44,67
D05s	150510	130	151024	297	167	13,75	32	8,23	30,05
D07s	150510	130	151024	297	167	20,92	21	12,53	45,73
D09r	150510	130	151024	297	167	6,29	351	3,77	13,74
D12s	150509	129	151024	297	168	0,78	8	0,47	1,71
E01t	150512	132	151023	296	164	0,69	226	0,42	1,55
E02t	150512	132	151023	296	164	17,40	9	10,61	38,72
E03u	150512	132	151023	296	164	10,21	348	6,22	22,72
E04t	150512	132	151023	296	164	1,75	10	1,07	3,89
Fl01f	150513	133	151022	295	162	17,18	134	10,61	38,71
G02l	150604	155	151025	298	143	5,77	205	4,03	14,72
G03m	150604	155	151025	298	143	2,91	200	2,04	7,43
G04t	150604	155	151025	298	143	1,41	13	0,99	3,60
gb2e	150512	132	151023	296	164	15,77	355	9,62	35,10
HAABo	150605	156	151025	298	142	0,77	328	0,54	1,97
Hof01m	150512	132	151023	296	164	13,72	180	8,37	30,54
K01v	150509	129	151026	299	170	4,63	296	2,72	9,94
K02x	150509	129	151026	299	170	5,76	324	3,39	12,38
K03v	150509	129	151026	299	170	10,95	289	6,44	23,51
K04x	150509	129	151026	299	170	18,54	289	10,90	39,80
K05x	150509	129	151026	299	170	12,52	248	7,37	26,89
K06v	150604	155	151026	299	144	4,66	106	3,24	11,82
K07r	150509	129	151026	299	170	2,13	278	1,25	4,57
Ln1-1c	150605	156	151025	298	142	2,55	209	1,80	6,56
Ln1-2c	150605	156	151025	298	142	4,91	187	3,46	12,61
Ln1-3c	150605	156	151025	298	142	4,57	196	3,22	11,76
Ln1-4c	150605	156	151025	298	142	5,21	202	3,67	13,38
Ln1-5c	150605	156	151025	298	142	5,45	179	3,83	14,00
S01k	150507	127	151026	299	172	0,67	134	0,39	1,41
S02n	150507	127	151026	299	172	15,91	190	9,25	33,76
S04o	150507	127	151026	299	172	24,08	204	14,00	51,11
Skf01f	150513	133	151022	295	162	14,20	109	8,77	32,00
T01np	150507	127	151026	299	172	0,73	127	0,42	1,55
T02nr	150507	127	151026	299	172	3,91	275	2,27	8,30
T03nr	150507	127	151027	300	173	6,46	249	3,73	13,62
T04nr	150507	127	151027	300	173	11,46	236	6,62	24,17
T05nr	150507	127	151027	300	173	10,94	238	6,32	23,08
T05rorf	141014	287	151027	300	378	21,07	239	5,58	20,35
T06nr	150508	128	151027	300	172	11,76	232	6,84	24,95
T07nq	150509	129	151025	298	169	8,14	240	4,81	17,57
T08nr	150509	129	151025	298	169	1,38	237	0,82	2,99

Appendix E: Melt water runoff to selected rivers in summer 2015, derived from summer balance.

ΔS: area in a given elevation range where summer balance is negative, **∑ΔS**: cumulative area above a given elevation, **ΔQ_s**: melt water runoff from a given elevation range, **$\sum\Delta Q_s$** : cumulative melt water runoff from an area above given elevation.

Tungnaá water drainage basin

Elevation (m a. s. l.)		ΔS km^2	∑ΔS km^2	ΔQ_s ($10^6 m^3$)	$\sum\Delta Q_s$ ($10^6 m^3$)
1350	1400	0,6	0,6	0,5	0,5
1300	1350	6,2	6,8	6	6,4
1250	1300	10,7	17,4	13,5	19,9
1200	1250	11,4	28,9	17,5	37,4
1150	1200	10,8	39,6	19,1	56,5
1100	1150	12,8	52,4	26	82,5
1050	1100	11,9	64,3	27,8	110,3
1000	1050	9,7	74	24,8	135,1
950	1000	10,8	84,8	30,3	165,4
900	950	9	93,7	29,3	194,8
850	900	8,3	102	32,4	227,2
800	850	8,6	110,6	39	266,3
750	800	6,3	116,9	33,4	299,7
700	750	4,2	121	23,1	322,7
650	700	0,5	121,6	2,3	325,1

Sylgja water drainage basin

Elevation (m a. s. l.)		ΔS km^2	∑ΔS km^2	ΔQ_s ($10^6 m^3$)	$\sum\Delta Q_s$ ($10^6 m^3$)
1300	1350	1,3	1,3	1,4	1,4
1250	1300	3,6	5	4,6	6
1200	1250	6,4	11,4	9,7	15,7
1150	1200	8,3	19,7	14,2	29,9
1100	1150	6,6	26,3	13,2	43,1
1050	1100	7,6	33,9	18,9	62
1000	1050	3,8	37,7	10,9	72,9
950	1000	1,5	39,2	4,6	77,4
900	950	0,6	39,8	1,8	79,2
850	900	0	39,8	0	79,3

Western Skaftá cauldron water drainage basin

Elevation (m a. s. l.)		ΔS km^2	∑ΔS km^2	ΔQ_s ($10^6 m^3$)	$\sum\Delta Q_s$ ($10^6 m^3$)
1600	1650	0,4	0,4	0	0
1550	1600	4,4	4,8	0,3	0,4
1500	1550	1,5	6,3	0,2	0,5

Eastern Skaftár cauldoron water drainage basin

Elevation (m a. s. l.)		ΔS km^2	∑ΔS km^2	ΔQ_s ($10^6 m^3$)	$\sum\Delta Q_s$ ($10^6 m^3$)
1600	1650	0,4	0,4	0	0
1550	1600	4,4	4,8	0,3	0,4
1500	1550	1,5	6,3	0,2	0,5

Grímsvötn water drainage basin

Elevation (m a. s. l.)		ΔS km^2	∑ΔS km^2	ΔQ_s ($10^6 m^3$)	$\sum\Delta Q_s$ ($10^6 m^3$)
1700	1750	0	0	0	0
1650	1700	13,3	13,3	1,4	1,4
1600	1650	23	36,3	6,7	8,1
1550	1600	18,4	54,6	8,8	16,9
1500	1550	16,7	71,3	11,5	28,4
1450	1500	11,6	82,9	9,5	37,9
1400	1450	15,1	97,9	13,9	51,8
1350	1400	0,6	98,6	0,4	52,2

Kaldakvísl water drainage basin

Elevation (m a. s. l.)		ΔS km^2	∑ΔS km^2	ΔQ_s ($10^6 m^3$)	$\sum\Delta Q_s$ ($10^6 m^3$)
1650	1700	0,1	0,1	0	0
1600	1650	2,5	2,6	0	0
1550	1600	19,2	21,8	3,7	3,8
1500	1550	27,2	49,1	12	15,8
1450	1500	28,5	77,5	17,4	33,2
1400	1450	23,1	100,6	18	51,2
1350	1400	21,6	122,2	21,3	72,5
1300	1350	21,3	143,5	26,6	99,1
1250	1300	22,6	166,1	34,1	133,2
1200	1250	22,6	188,7	40,9	174,2
1150	1200	20,2	208,9	42,2	216,4
1100	1150	18,3	227,2	42,8	259,2
1050	1100	17,2	244,4	45,2	304,4
1000	1050	14,9	259,3	42,9	347,4
950	1000	10,7	269,9	32,4	379,7
900	950	5,6	275,6	17,3	397
850	900	0,5	276,1	1,7	398,7

Jökulsá á Fjöllum water drainage basin

Elevation (m a. s. l.)		ΔS km^2	$\sum\Delta S$ km^2	ΔQ_s $(10^6 m^3)$	$\sum\Delta Q_s$ $(10^6 m^3)$
1650	1700	0	0	0	0
1600	1650	4	4	0	0
1550	1600	90,4	94,5	6,2	6,3
1500	1550	96,9	191,3	14,5	20,8
1450	1500	84,9	276,2	19,7	40,5
1400	1450	73,6	349,9	22,8	63,3
1350	1400	59,8	409,6	24,7	88
1300	1350	49,1	458,7	27,3	115,3
1250	1300	52,5	511,2	40	155,4
1200	1250	57,4	568,6	59,4	214,8
1150	1200	54,5	623,1	76,2	291
1100	1150	45,9	669,1	80,5	371,5
1050	1100	34,1	703,2	70,8	442,3
1000	1050	36,4	739,5	88	530,3
950	1000	31,5	771	89,1	619,4
900	950	26,2	797,2	84,7	704,2
850	900	25,4	822,6	91,3	795,5
800	850	20,2	842,9	79	874,5
750	800	15,2	858	63,8	938,3
700	750	1,7	859,8	7,6	945,9

Kreppa and Kverká water drainage basin

Elevation (m a. s. l.)		ΔS km^2	∑ΔS km^2	ΔQ_s ($10^6 m^3$)	$\sum\Delta Q_s$ ($10^6 m^3$)
1600	1650	0	0	0	0
1550	1600	15,7	15,7	0,7	0,7
1500	1550	14,3	29,9	1,2	1,9
1450	1500	15,4	45,4	1,8	3,6
1400	1450	19,3	64,7	3,1	6,8
1350	1400	25,2	89,9	8,2	15
1300	1350	20,5	110,4	12,8	27,8
1250	1300	16,4	126,8	15	42,8
1200	1250	18,1	144,8	21,6	64,5
1150	1200	18,2	163	24,1	88,5
1100	1150	17,5	180,5	23,7	112,2
1050	1100	11,6	192,1	16,4	128,7
1000	1050	14,1	206,2	22,6	151,2
950	1000	16,1	222,3	31,7	182,9
900	950	14,4	236,6	35	217,9
850	900	14,5	251,1	41,8	259,7
800	850	11,5	262,6	38,1	297,8
750	800	9,3	272	37,8	335,6
700	750	4,2	276,1	20	355,6
650	700	0,4	276,6	2,2	357,8

Hálslón water drainage basin

Elevation (m a. s. l.)		ΔS km^2	∑ΔS km^2	ΔQ_s ($10^6 m^3$)	$\sum\Delta Q_s$ ($10^6 m^3$)
1600	1650	0,1	0,1	0	0
1550	1600	23,5	23,7	0,6	0,6
1500	1550	60,6	84,3	3,7	4,3
1450	1500	63,5	147,8	6,4	10,8
1400	1450	72,2	219,9	9	19,7
1350	1400	122	342	32,7	52,4
1300	1350	133	475,2	63,1	115,5
1250	1300	128	603,5	77,9	193,5
1200	1250	103	706,3	75	268,5
1150	1200	87,3	793,6	84,6	353,1
1100	1150	69,3	862,8	88,4	441,5
1050	1100	61,8	924,6	94,6	536,1
1000	1050	51,8	976,4	93	629,1
950	1000	43,4	1019,8	91,1	720,2
900	950	34,6	1054,5	84,1	804,2
850	900	30,4	1084,8	84,7	888,9
800	850	29,9	1114,7	99,6	988,5
750	800	26,8	1141,5	110,9	1099,4
700	750	19,6	1161,1	93,8	1193,3
650	700	12,3	1173,4	64	1257,3
600	650	0,3	1173,8	1,8	1259,1

Jökulsá á Fljótsdal water drainage basin

Elevation (m a. s. l.)		ΔS km^2	ΣΔS km^2	ΔQ_s ($10^6 m^3$)	$\Sigma\Delta Q_s$ ($10^6 m^3$)
1450	1500	0	0	0	0
1400	1450	0,6	0,6	0	0
1350	1400	1,7	2,4	0,5	0,6
1300	1350	4	6,4	1,7	2,3
1250	1300	15,8	22,2	6,8	9,1
1200	1250	15,9	38,1	10,3	19,4
1150	1200	17,6	55,7	16,9	36,4
1100	1150	15,1	70,9	20,3	56,7
1050	1100	12,7	83,6	22,4	79
1000	1050	11,9	95,5	25,2	104,2
950	1000	9	104,5	21,7	125,9
900	950	5,8	110,2	15,5	141,4
850	900	4,3	114,5	12,3	153,8
800	850	3,3	117,8	9,9	163,6
750	800	3,4	121,2	11,1	174,7
700	750	3,3	124,5	12,6	187,3
650	700	1,7	126,2	7,2	194,5

Hornafjarðarfljót water drainage basin

Elevation (m a. s. l.)		ΔS km^2	∑ΔS km^2	ΔQ_s ($10^6 m^3$)	$\sum\Delta Q_s$ ($10^6 m^3$)
1400	1450	2,2	2,2	0,1	0,1
1350	1400	10,4	12,6	1,4	1,5
1300	1350	17,6	30,2	5	6,5
1250	1300	36,6	66,8	17	23,5
1200	1250	30,2	97	19,7	43,2
1150	1200	20,8	117,8	18,1	61,3
1100	1150	19,8	137,6	20,6	81,8
1050	1100	15,3	152,9	18,8	100,6
1000	1050	11,7	164,5	16,4	117
950	1000	11,1	175,6	17,6	134,6
900	950	8,2	183,8	14,4	149
850	900	5,5	189,3	10,6	159,6
800	850	4,4	193,7	8,9	168,6
750	800	4,1	197,8	8,8	177,4
700	750	4	201,8	9	186,4
650	700	3,5	205,3	8,3	194,7
600	650	2,6	207,8	6,8	201,5
550	600	2	209,9	5,8	207,3
500	550	1,8	211,7	6	213,3
450	500	1,4	213,1	5,4	218,7
400	450	1,3	214,4	5,7	224,3
350	400	0,8	215,2	4	228,4
300	350	1,1	216,3	6,4	234,8
250	300	2,3	218,6	14,9	249,7
200	250	3,5	222,1	24,7	274,4
150	200	2,7	224,8	20,7	295,1
100	150	2,1	227	17,5	312,6
50	100	2,8	229,8	24,7	337,4
0	50	0,6	230,3	5,1	342,5

Jökulsá á Breiðamerkursandi water drainage basin

Elevation (m a. s. l.)		ΔS km^2	∑ΔS km^2	ΔQ_s ($10^6 m^3$)	$\sum\Delta Q_s$ ($10^6 m^3$)
1650	1700	0,2	0,2	0	0
1600	1650	3	3,2	0	0,1
1550	1600	11,6	14,8	0,4	0,5
1500	1550	21,9	36,7	1,7	2,2
1450	1500	25,5	62,2	3,6	5,8
1400	1450	44,3	106,5	8,9	14,7
1350	1400	83,3	189,8	27,7	42,4
1300	1350	85,4	275,1	42,3	84,7
1250	1300	53,1	328,3	35,2	119,9
1200	1250	35,1	363,4	27,3	147,2
1150	1200	28,9	392,2	26,1	173,4
1100	1150	24,6	416,8	26,2	199,6
1050	1100	20,7	437,5	25,5	225,1
1000	1050	17,8	455,3	25,2	250,2
950	1000	19	474,3	29,9	280,1
900	950	20,2	494,5	33,8	313,9
850	900	20,5	515,1	37,4	351,3
800	850	20,2	535,2	39,4	390,8
750	800	19,5	554,8	41,7	432,5
700	750	21,1	575,9	48,4	480,9
650	700	26,7	602,5	64,8	545,7
600	650	18,5	621	48,2	593,8
550	600	18,5	639,6	52,7	646,5
500	550	7	646,6	22,3	668,8
450	500	7,7	654,2	29,3	698,1
400	450	5,8	660,1	25,9	724
350	400	5,5	665,5	27,4	751,4
300	350	6,5	672,1	37,1	788,5
250	300	6	678	38,3	826,9
200	250	6,3	684,4	44,8	871,6
150	200	5,1	689,5	39,7	911,3
100	150	5,1	694,6	42,5	953,7
50	100	4,1	698,7	36,5	990,2
0	50	2,7	701,4	24,7	1014,9

Breiðárlón/Fjallsárlón water drainage basin

Elevation (m a. s. l.)		ΔS km^2	∑ΔS km^2	ΔQ_s ($10^6 m^3$)	$\sum\Delta Q_s$ ($10^6 m^3$)
1700	1750	0	0	0	0
1650	1700	0	0	0	0
1600	1650	0	0	0	0
1550	1600	2,4	2,5	0,3	0,3
1500	1550	6	8,5	1,9	2,2
1450	1500	5	13,5	2,2	4,4
1400	1450	5,3	18,8	2,9	7,3
1350	1400	6,4	25,2	4,4	11,7
1300	1350	12,6	37,8	9,5	21,2
1250	1300	6,7	44,6	5,4	26,6
1200	1250	5,6	50,1	4,8	31,3
1150	1200	5,1	55,2	4,9	36,2
1100	1150	4,5	59,7	5	41,2
1050	1100	5	64,7	6,2	47,5
1000	1050	6	70,7	8,2	55,7
950	1000	7	77,7	10,9	66,5
900	950	8,4	86,1	14	80,5
850	900	6,7	92,8	12,2	92,7
800	850	8,4	101,2	16,6	109,3
750	800	8,8	110	18,9	128,3
700	750	6,1	116,2	13,9	142,2
650	700	7,4	123,6	17,9	160,1
600	650	8,3	131,9	21,5	181,6
550	600	8,8	140,7	25,8	207,4
500	550	9,5	150,2	30,8	238,2
450	500	9,6	159,8	35,5	273,6
400	450	11,1	170,9	47,6	321,2
350	400	8,5	179,4	42,2	363,4
300	350	7,7	187,1	42,8	406,2
250	300	7,4	194,5	46,9	453,1
200	250	6,8	201,3	47,3	500,4
150	200	4,6	205,9	35,4	535,8
100	150	4,3	210,2	35,9	571,7
50	100	3,7	213,9	32,8	604,5
0	50	1,8	215,7	16,8	621,3

Skeiðarársandur (Gígja) water drainage basin (Gígja)

Elevation (m a. s. l.)		ΔS km^2	∑ΔS km^2	ΔQ_s ($10^6 m^3$)	$\sum\Delta Q_s$ ($10^6 m^3$)
1650	1700	0,4	0,4	0	0
1600	1650	2,4	2,8	0,1	0,1
1550	1600	53	55,8	1,7	1,8
1500	1550	103	159,1	7	8,8
1450	1500	97,6	256,7	17,9	26,7
1400	1450	95,1	351,8	35,3	62
1350	1400	83,3	435,1	45,9	108
1300	1350	71,9	507	47,6	155,5
1250	1300	62,8	569,7	50,1	205,6
1200	1250	52,9	622,6	51,5	257,1
1150	1200	44,9	667,5	53,7	310,8
1100	1150	36,1	703,6	50	360,8
1050	1100	29,5	733,1	46,8	407,6
1000	1050	25	758,1	44,2	451,8
950	1000	25	783,1	48	499,8
900	950	24,8	808	53,4	553,2
850	900	27,8	835,8	66,4	619,6
800	850	22,5	858,2	59,2	678,8
750	800	19,6	877,8	55,9	734,6
700	750	19,1	896,9	60	794,7
650	700	11,9	908,8	42,4	837,1
600	650	13,1	921,9	51,8	888,9
550	600	12,4	934,3	51,3	940,2
500	550	8,3	942,6	36,7	976,9
450	500	5,5	948,1	27,2	1004,1
400	450	6,7	954,8	36,4	1040,5
350	400	11,1	965,9	65,8	1106,3
300	350	14,2	980,1	92,8	1199,1
250	300	15,3	995,4	106,6	1305,7
200	250	12,4	1007,8	93	1398,7
150	200	11,3	1019,1	91,5	1490,2
100	150	13,5	1032,6	107,9	1598,1
50	100	5	1037,6	36,2	1634,3

Súla water drainage basin

Elevation (m a. s. l.)		ΔS km^2	∑ΔS km^2	ΔQ_s ($10^6 m^3$)	$\sum\Delta Q_s$ ($10^6 m^3$)
1600	1650	0,3	0,3	0	0
1550	1600	3,3	3,5	0,3	0,3
1500	1550	5,9	9,4	1,2	1,5
1450	1500	11,4	20,8	4,7	6,2
1400	1450	11,1	31,9	5,9	12,1
1350	1400	9,3	41,2	5,9	18
1300	1350	8,2	49,4	5,9	23,9
1250	1300	6,7	56,1	5,5	29,4
1200	1250	8,1	64,2	7,7	37,2
1150	1200	9,2	73,3	10,6	47,8
1100	1150	15,6	89	20,8	68,6
1050	1100	15,9	104,9	25,4	94
1000	1050	16,5	121,4	30,3	124,3
950	1000	18,7	140,1	38,4	162,7
900	950	15,3	155,4	34,4	197,1
850	900	12,1	167,5	29,5	226,6
800	850	11,7	179,2	31	257,6
750	800	7	186,2	20,4	278
700	750	6	192,2	19,6	297,6
650	700	4,9	197,1	17,9	315,5
600	650	9	206,1	36,5	352
550	600	11,7	217,9	50,8	402,7
500	550	8,9	226,8	40,6	443,3
450	500	7,2	233,9	35,3	478,6
400	450	6,3	240,2	34,1	512,7
350	400	4,8	245	28,6	541,3
300	350	1,8	246,8	11,9	553,2
250	300	0,9	247,8	6,6	559,8
200	250	0,8	248,6	5,8	565,6
150	200	0,8	249,4	6,4	572
100	150	0,8	250,2	6,8	578,8
50	100	0,6	250,8	5,2	584

Djúpá water drainage basin

Elevation (m a. s. l.)		ΔS km^2	∑ΔS km^2	ΔQ_s ($10^6 m^3$)	$\sum\Delta Q_s$ ($10^6 m^3$)
1450	1500	0,1	0,1	0	0
1400	1450	0,3	0,5	0,2	0,3
1350	1400	0,9	1,4	0,8	1,1
1300	1350	3,8	5,1	3,5	4,6
1250	1300	3,3	8,5	3,6	8,2
1200	1250	2,9	11,4	3,7	11,9
1150	1200	3,5	14,9	5,2	17,1
1100	1150	5,3	20,3	9,9	26,9
1050	1100	7	27,3	15,2	42,2
1000	1050	9,8	37,1	23,5	65,6
950	1000	8	45,1	23,1	88,7
900	950	8,1	53,2	25,8	114,5
850	900	7,5	60,7	25,1	139,5
800	850	9,1	69,8	31,9	171,4
750	800	6,7	76,5	24,5	195,9
700	750	4	80,6	15,9	211,8
650	700	3	83,5	12,5	224,3
600	650	0,4	84	1,8	226,1

Brunná water drainage basin

Elevation (m a. s. l.)		ΔS km^2	∑ΔS km^2	ΔQ_s ($10^6 m^3$)	$\sum\Delta Q_s$ ($10^6 m^3$)
1050	1100	0	0	0,2	0,2
1000	1050	1,1	1,2	2,7	2,9
950	1000	3,3	4,5	9,2	12,1
900	950	4,2	8,6	12,8	24,9
850	900	4,3	13	13,9	38,8
800	850	4,9	17,8	16,4	55,2
750	800	5,4	23,3	19,6	74,8
700	750	6,4	29,6	25,3	100
650	700	3,9	33,5	16,7	116,7
600	650	2,3	35,9	10,4	127,2
550	600	0	35,9	0,1	127,3

Hverfisfljót water drainage basin

Elevation (m a. s. l.)		ΔS km^2	$\sum\Delta S$ km^2	ΔQ_s $(10^6 m^3)$	$\sum\Delta Q_s$ $(10^6 m^3)$
1600	1650	0	0	0	0
1550	1600	1,2	1,2	0	0
1500	1550	15,6	16,9	1,4	1,4
1450	1500	42	58,9	15	16,4
1400	1450	28,5	87,5	15	31,4
1350	1400	24,5	111,9	16,5	47,9
1300	1350	22,9	134,8	19,8	67,7
1250	1300	18,6	153,3	20,2	87,9
1200	1250	20,2	173,5	25,5	113,5
1150	1200	14,1	187,7	21,1	134,6
1100	1150	10,9	198,6	21,2	155,8
1050	1100	10,2	208,7	22,1	177,9
1000	1050	9,3	218	22,3	200,2
950	1000	9,4	227,4	26	226,2
900	950	8,9	236,3	27,4	253,6
850	900	7,4	243,7	24,1	277,7
800	850	9,3	253	31,8	309,5
750	800	11,5	264,5	41,9	351,3
700	750	13,7	278,1	54	405,4
650	700	7,8	285,9	33,2	438,6
600	650	4,6	290,5	20,1	458,7
550	600	0,2	290,7	0,8	459,5

Skaftá water drainage basin

Elevation (m a. s. l.)		ΔS km^2	$\sum\Delta S$ km^2	ΔQ_s $(10^6 m^3)$	$\sum\Delta Q_s$ $(10^6 m^3)$
1600	1650	0,6	0,6	0	0
1550	1600	21,4	22	2	2
1500	1550	29,5	51,4	6,8	8,8
1450	1500	24,1	75,5	8,1	16,9
1400	1450	22,4	97,9	11,4	28,3
1350	1400	20,7	118,6	14,5	42,8
1300	1350	22,9	141,5	20,9	63,7
1250	1300	16,4	158	19,1	82,7
1200	1250	21,5	179,5	30,3	113
1150	1200	23,9	203,4	40,2	153,3
1100	1150	24,5	227,9	48,8	202,1
1050	1100	26,8	254,7	60,1	262,1
1000	1050	26,3	281	65,8	328
950	1000	20,3	301,3	57,4	385,3
900	950	15,8	317,1	50,2	435,5
850	900	16,2	333,3	58	493,5
800	850	14,7	348	59,5	553,1
750	800	11,6	359,6	51,1	604,1
700	750	8,5	368,1	38,4	642,5
650	700	5,1	373,2	21,8	664,3
600	650	0,9	374,1	3,9	668,2

Appendix F: MODIS satellite images of Vatnajökull and vicinity 2014-2015.

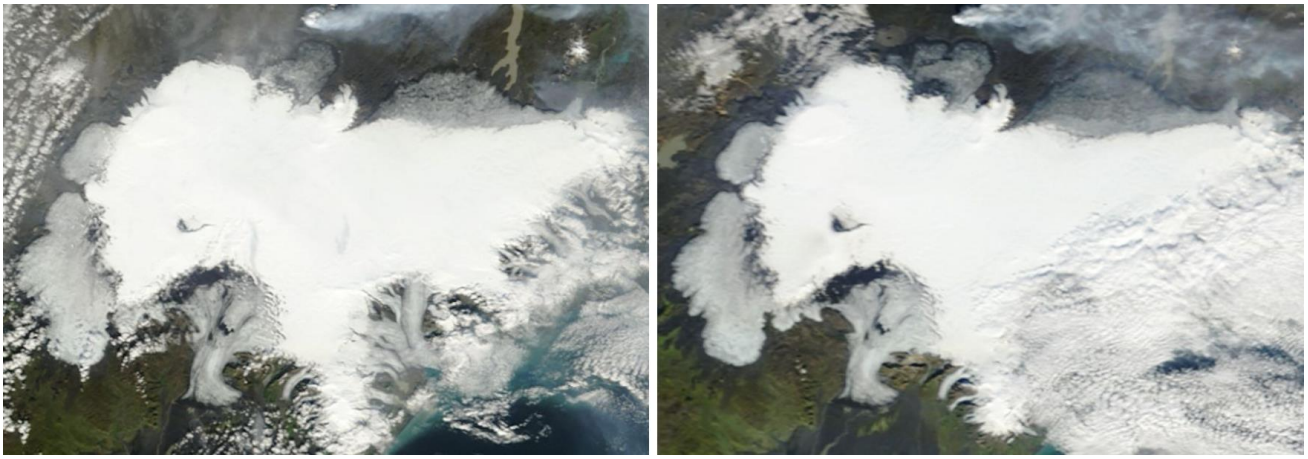

Left: September 5th 2014, the snowline has moved significantly upwards on the N outlets, less so on the W and S outlets; there may be some fresh snow in the highest regions. The Holuhraun eruption north of Dyngjujökull is clearly visible. Right: September 20th, still summer conditions on the glacier, the snowline of the N outlets is still migrating upwards in a warm September. The thick 2011 tephra from Grímsvötn is clearly visible in upper Skeiðarárjökull and Tungnaárjökull.

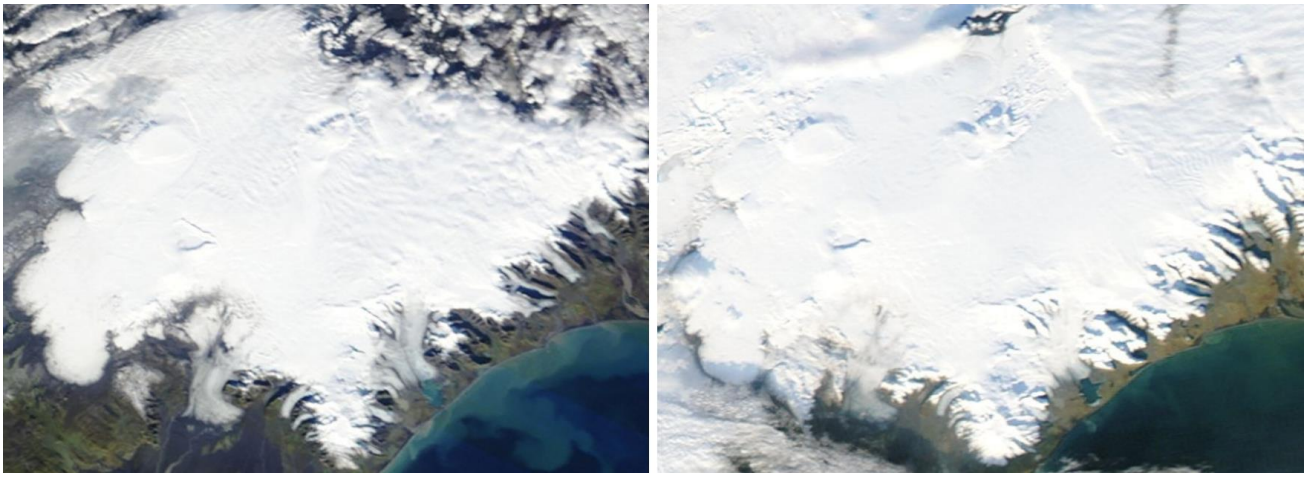

Left: October 10th, winter has arrived; there is now fresh snow on the surface at elevations above ~700m a.s.l..
Right: October 29th; snow cover up to 1.6 m was measured in the autumn mass balance expedition (October 9-17th) in the upper regions, winter has settled in.. The ice free surface of Hálslón is visible through thin cloud cover

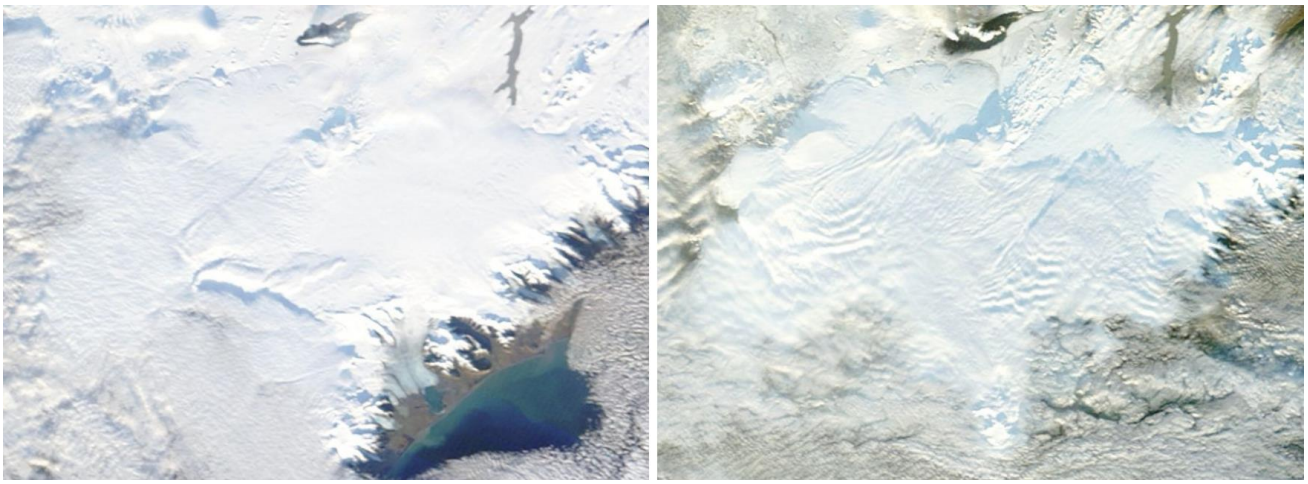

Left: November 4th, Breiðamerkurjökull snow free up to ~600m a.s.l., Right November 17th. The snow cover north of Vatnajökull seems to have thinned; Hálslón still open.

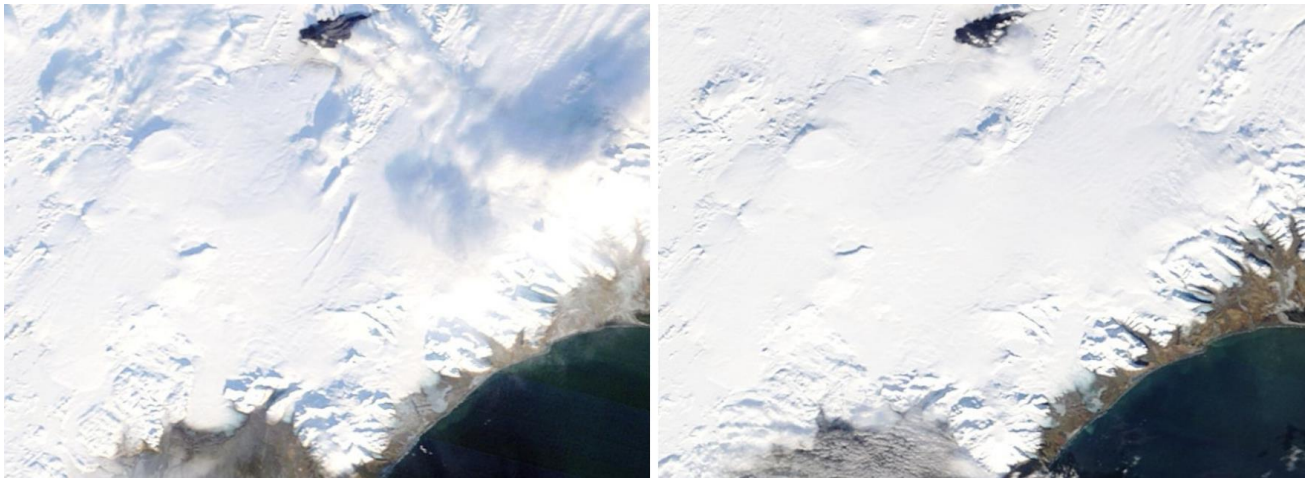

Left: January 31st 2015 and right: February 21st. There is still no snow in the south lowland, but otherwise there is continuous snow cover; Hálslón has frozen over.

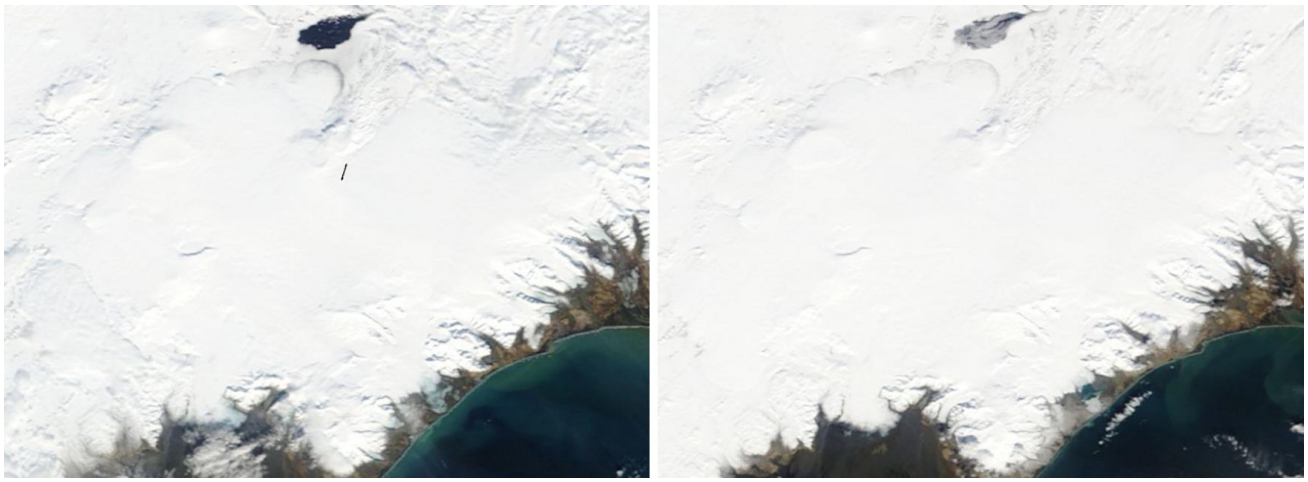

Left: March 20th, in stormy weather every 3 days the whole winter almost no cloud free images were acquired.
Right: April 12th the dark regions on Dyngjujökull snout shows that the thin winter snow has already started to melt.

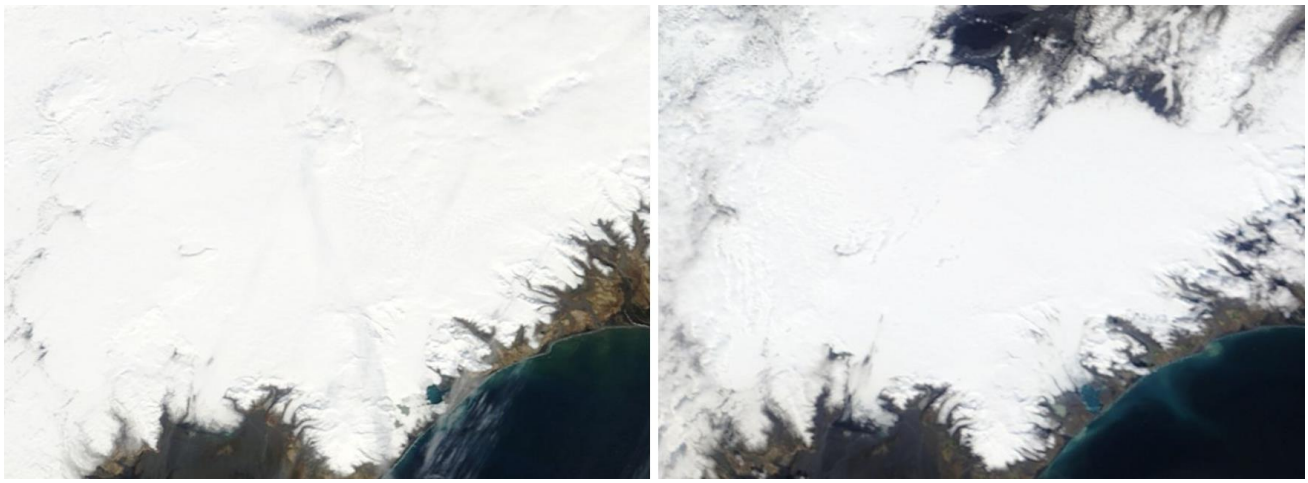

May 5th and June 7th. The spring was cold. Visible changes from early May show that snow has melted in the glacier fore-field but little change is visible on the glacier.

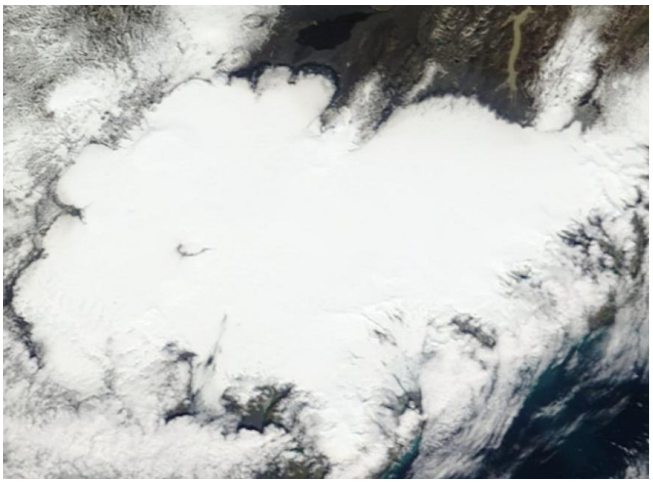
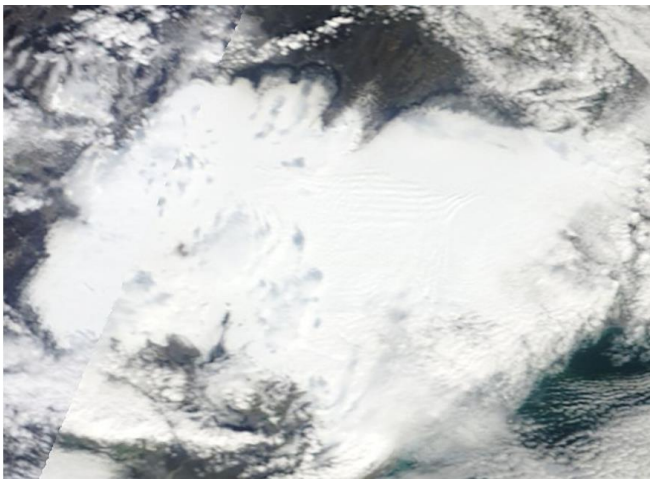

There are no completely cloud-free images in June and July: Left: June 25th, the snowline has only migrated slightly upwards; ablation rates in June are low. Some dirt is now visible on the snow surface from Tungnaárjökull to Brúarjökull that lowers the albedo and enhances melt. Right: July 30nd, the snowline is slowly moving upwards although the summer been cold and wet.

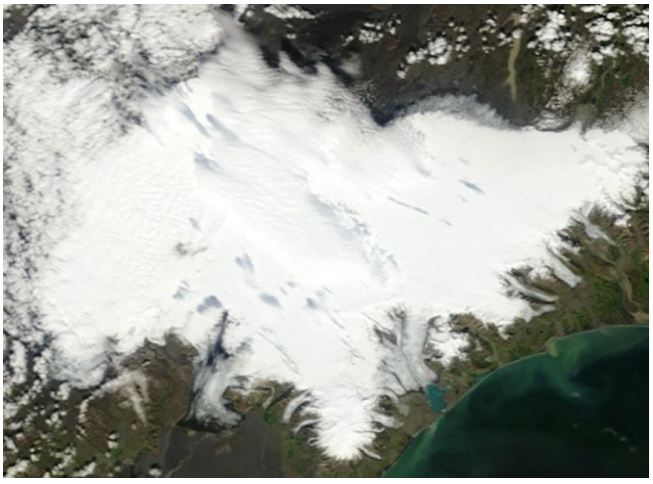
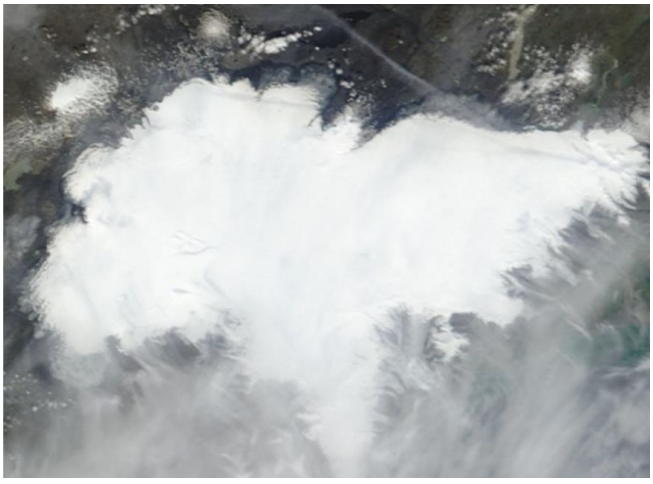

August 11th, and 29nd; The snowline of the N and SE outlets has raised significantly; at last a warm and sunny period in E-Iceland. Note the brownish surface of Brúarjökull and Dyngjujökull that lowers the albedo and enhances melt.

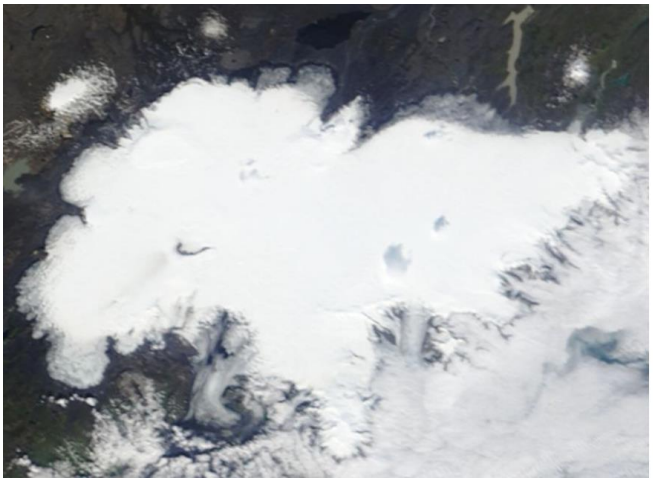
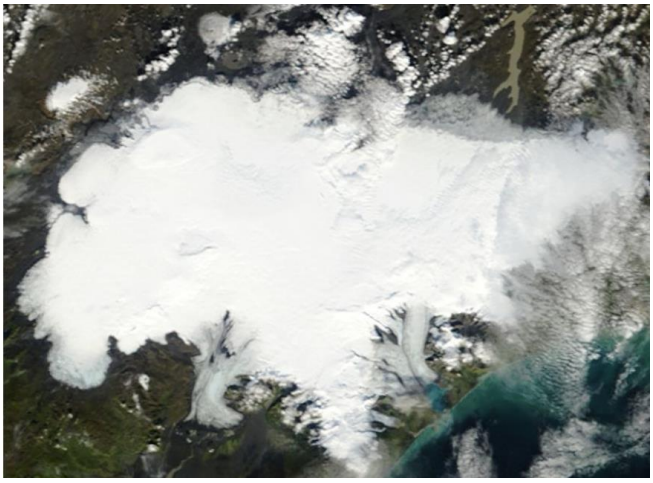

Left: September 5th, the snowline has moved significantly upwards on the N outlets, less so on the W and S outlets; there may be some fresh snow in the highest regions. Note the tephra blown from Grímsvötn to SW onto the upper regions of Síðujökull, this enhanced the melt there.
Right: September 25th, still summer conditions on the glacier, the snowline of the N outlets is still moving upwards in a warm September, but snow has started to cover the W outlets.

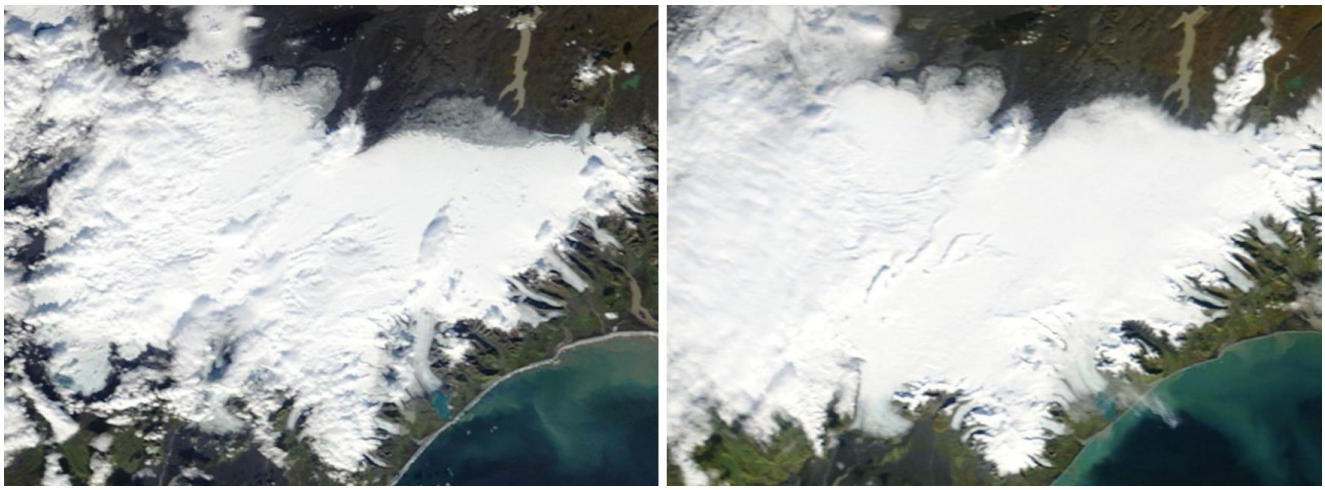

Left: September 10th, still melt and upward migration of the snowline in the north.
Right: October 9th, winter has settled in, fresh snow on most of the glacier.

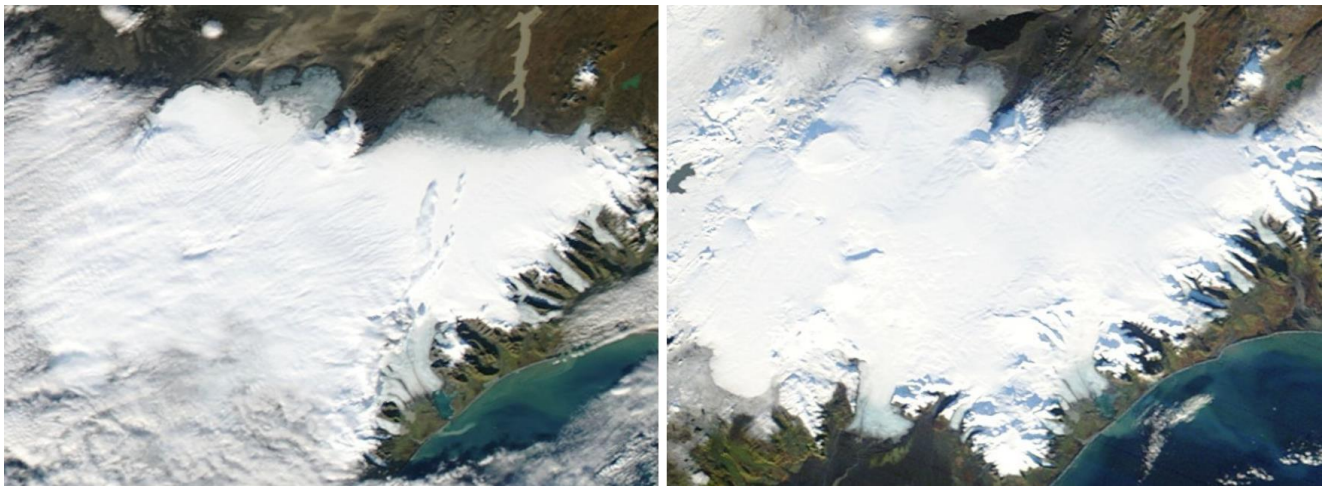

Left: October 17th, the fresh snow on the ablation zone of the N outlets (visible on Oct. 9th) has melted and the snowline has raised slightly. Note the dust storm to the ENE from the region north of Bárðarbunga and Dyngjujökull.
Snow cover up to 1.2 m was measured north of Grímsvötn and on Bárðarbunga in the autumn mass balance expedition (October 22-28th).
Right: November 9th; The ~ 80 km^2 fresh lave field in Holuhraun is clearly visible, and the ice free surface of Hálslón.

The images are either from the MODIS Aqua or MODIS Terra satellites, visible light, 250 m resolution.
http://rapidfire.sci.gsfc.nasa.gov/
The Moderate Resolution Imaging Spectroradiometer (MODIS) flies onboard NASA's Aqua and Terra satellites as part of the NASA-centered international Earth Observing System. Both satellites orbit the Earth from pole to pole, seeing most of the globe every day. Onboard Terra, MODIS sees the Earth during the morning, while Aqua MODIS orbits the Earth in the afternoon.

On the next pages MODIS images for all days of May, June, July, August and September 2015 are shown in 1km resolution.

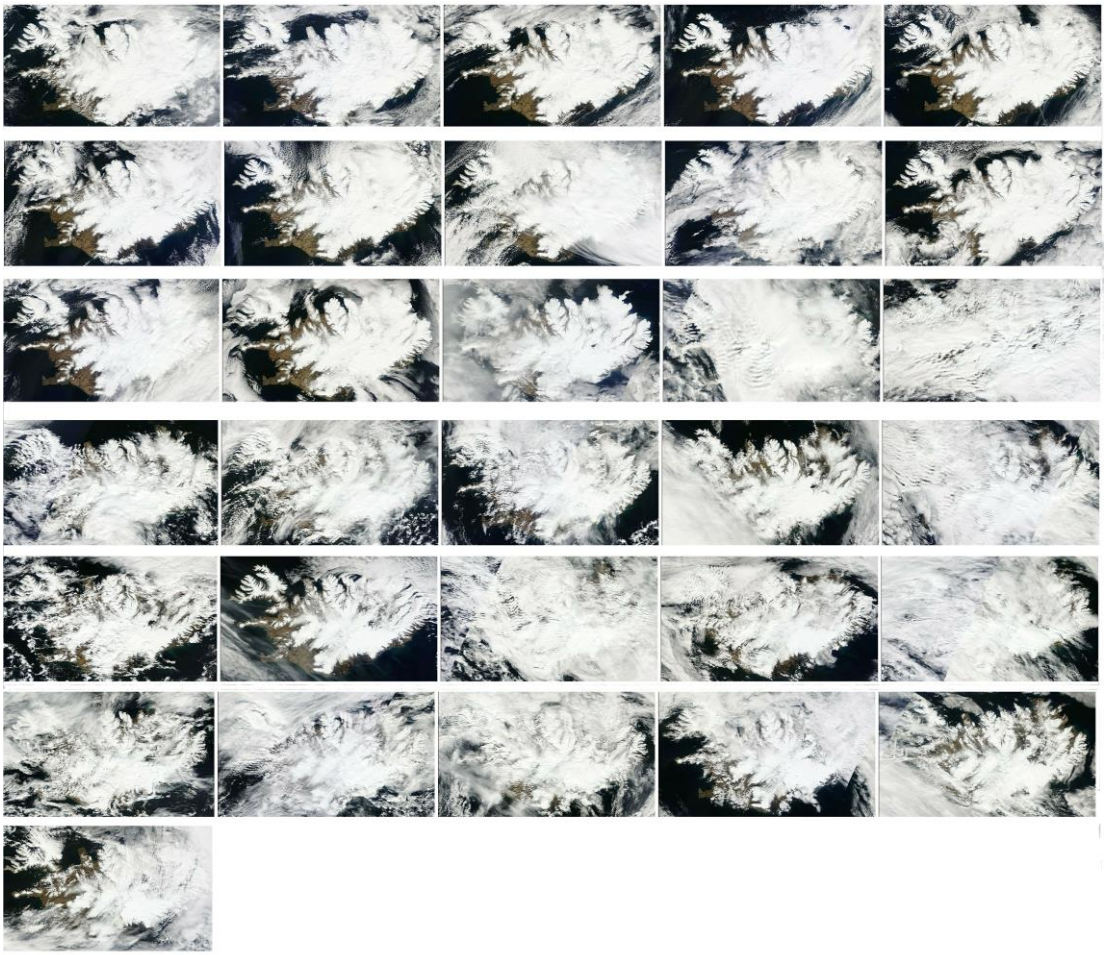

MODIS: May 2015 (read from left to right and downwards).

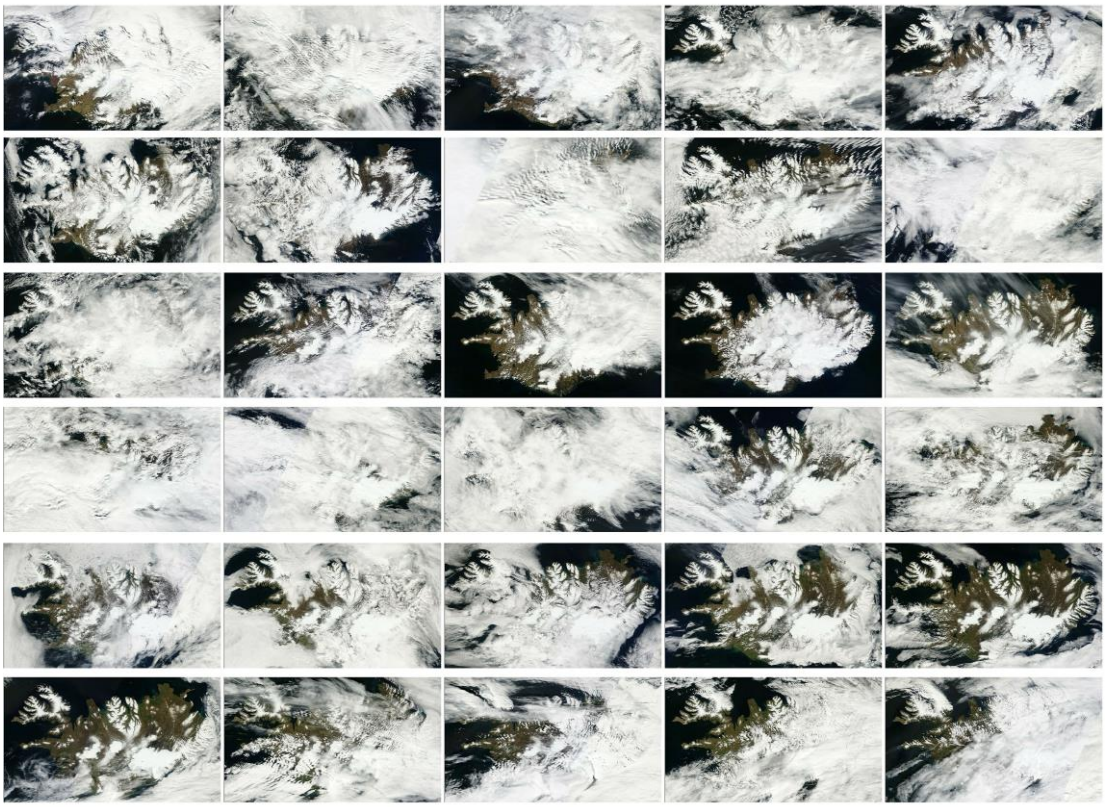

MODIS: June 2015 (read from left to right and downwards).

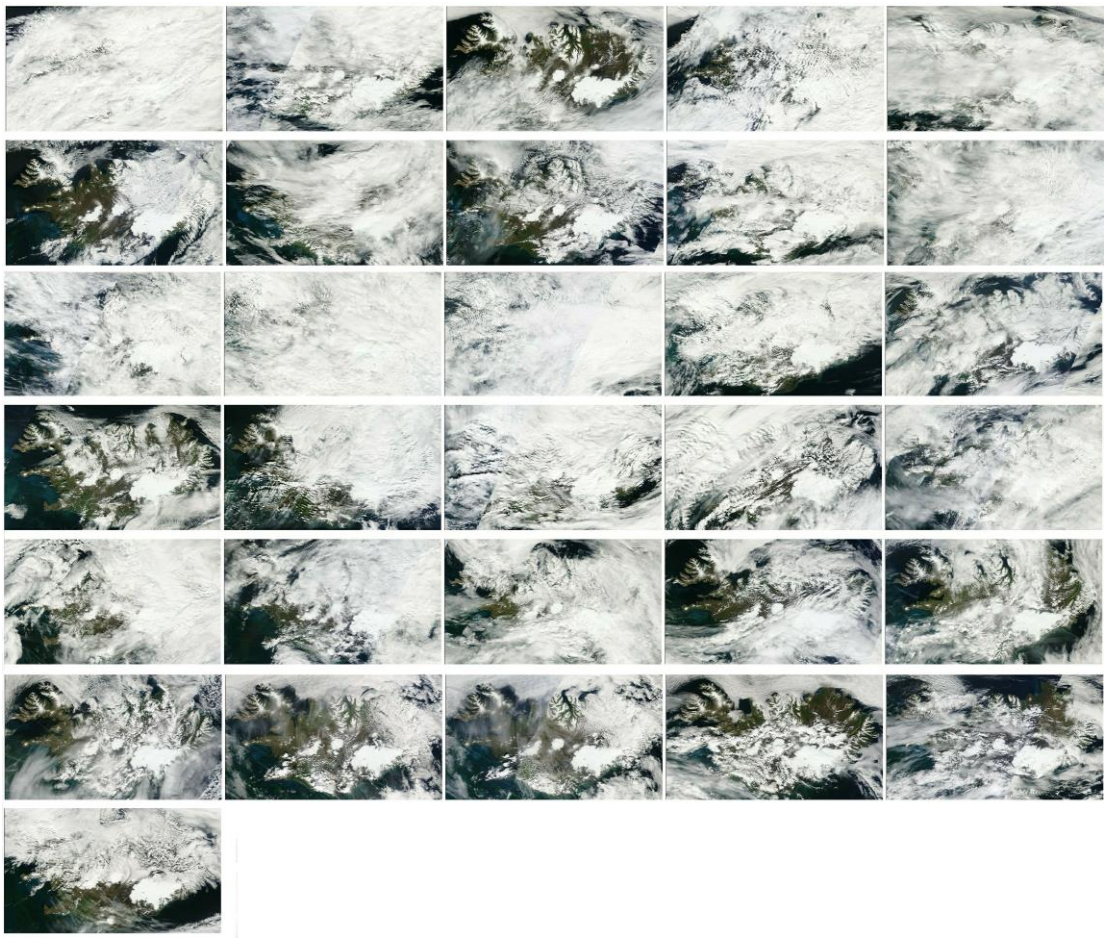

MODIS: July 2014 (read from left to right and downwards).

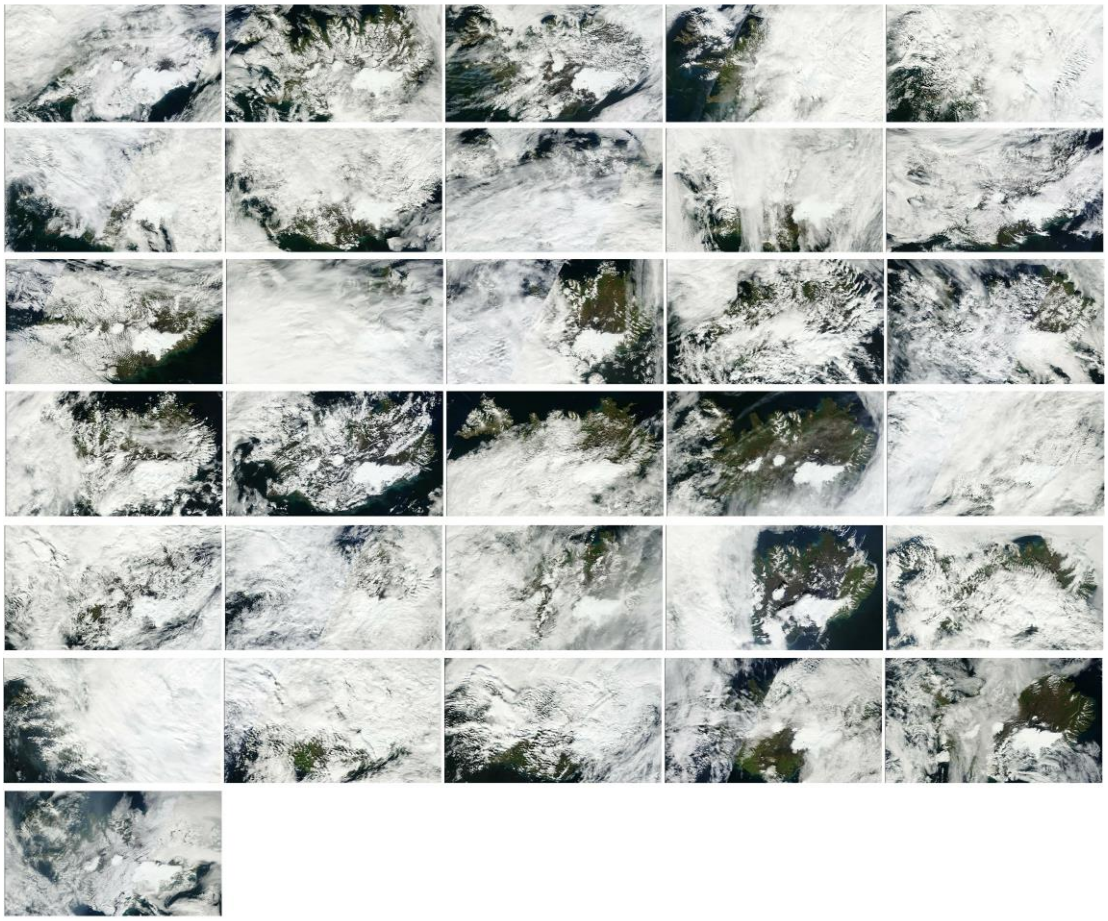

MODIS: August 2015 (read from left to right and downwards).

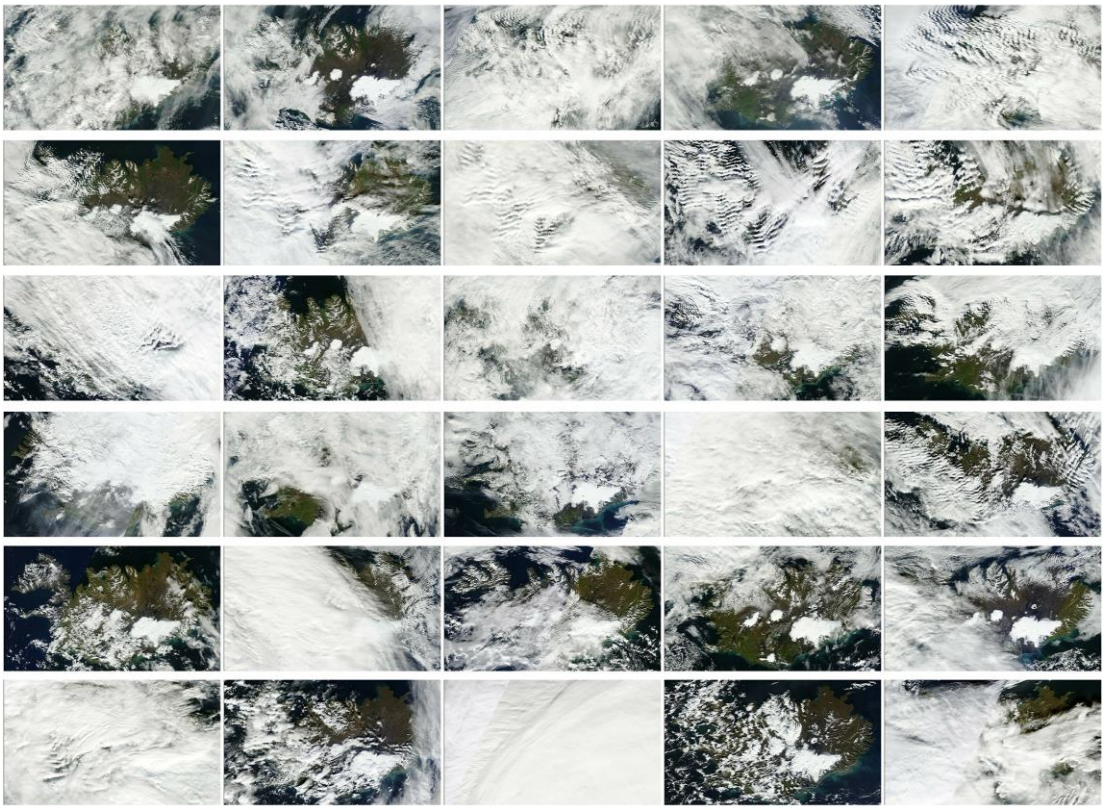

MODIS: September 2015 (read from left to right and downwards).

Landsvirkjun

Háaleitisbraut 68
103 Reykjavik
landsvirkjun.is

landsvirkjun@lv.is
Sími: 515 90 00